

2013

## The effect of gamma radiation on fibre Bragg grating sensors when used as radiation dosimeters

Des Baccini  
*Edith Cowan University*

Follow this and additional works at: [https://ro.ecu.edu.au/theses\\_hons](https://ro.ecu.edu.au/theses_hons)



Part of the [Nuclear Engineering Commons](#), and the [Semiconductor and Optical Materials Commons](#)

---

### Recommended Citation

Baccini, D. (2013). *The effect of gamma radiation on fibre Bragg grating sensors when used as radiation dosimeters*. Edith Cowan University. [https://ro.ecu.edu.au/theses\\_hons/79](https://ro.ecu.edu.au/theses_hons/79)

This Thesis is posted at Research Online.  
[https://ro.ecu.edu.au/theses\\_hons/79](https://ro.ecu.edu.au/theses_hons/79)

2013

# The effect of gamma radiation on fibre Bragg grating sensors when used as radiation dosimeters

Des Baccini  
*Edith Cowan University*

---

## Recommended Citation

Baccini, D. (2013). *The effect of gamma radiation on fibre Bragg grating sensors when used as radiation dosimeters*. Retrieved from [http://ro.ecu.edu.au/theses\\_hons/79](http://ro.ecu.edu.au/theses_hons/79)

This Thesis is posted at Research Online.  
[http://ro.ecu.edu.au/theses\\_hons/79](http://ro.ecu.edu.au/theses_hons/79)

# Edith Cowan University

## Copyright Warning

You may print or download ONE copy of this document for the purpose of your own research or study.

The University does not authorize you to copy, communicate or otherwise make available electronically to any other person any copyright material contained on this site.

You are reminded of the following:

- Copyright owners are entitled to take legal action against persons who infringe their copyright.
- A reproduction of material that is protected by copyright may be a copyright infringement.
- A court may impose penalties and award damages in relation to offences and infringements relating to copyright material. Higher penalties may apply, and higher damages may be awarded, for offences and infringements involving the conversion of material into digital or electronic form.

**THE EFFECT OF GAMMA RADIATION ON FIBRE BRAGG GRATING  
SENSORS WHEN USED AS RADIATION DOSIMETERS**

**Des Baccini**

**Bachelor of Science (Physics and Aviation), ECU, 2012.**

**Bachelor of Science (Physics) Honours Thesis**

**Faculty of Computing, Health and Science**

**School of Engineering**

**Edith Cowan University.**

**February, 2013.**

## **EDITH COWAN UNIVERSITY**

### **USE OF THESIS**

This copy is the property of Edith Cowan University. However the literary rights of the author must also be respected. If any passage from this thesis is quoted or closely paraphrased in a paper or written work prepared by the user, the source of the passage must be acknowledged in the work. If the user desires to publish a paper or written work containing passages copied or closely paraphrased from this thesis, which passages would in total constitute an infringing copy for the purposes of the Copyright Act, he or she must first obtain the written permission of the author to do so.

## ABSTRACT

The effects of Gamma Radiation on Fibre Bragg Gratings (FBGs), when used as a radiation dosimeter, was proposed. The focus of this study centred on the FBG performance, and in particular the Bragg Wavelength Shift (BWS) whilst being exposed to ionizing radiation. Current research suggests that certain types of fibres manufactured by varying methods produce different results. The different responses to exposure from gamma irradiation between Germanium (Ge) doped optical fibres, with and without Hydrogen loading, along with the standard SMF-28 fibre with Hydrogen, were used and results noted and compared to previous work. The FBG's in each fibre were written by Ultraviolet (UV) low energy irradiation. The results indicated that radiation sensitivity is dependent on Ge doping and Hydrogen loading. The increased sensitivity resulted in an overall average BWS of 151.6 pm. Results from the second re-irradiation gave an indication of the effects of pre-irradiation. The BWS average reduced to 88.3pm, showing that possible radiation hardening from pre-irradiation produce insensitive and possibly more stable FBGs.

As FBG sensors are already in use to detect variations in temperature, pressure, stress strain, vibration, electromagnetic fields and virtually any other physical parameter with great success, the progression through to gamma radiation detection is conceivable. One of the main attributes of FBG sensors is their immunity to electromagnetic interference. Gamma rays are a form of electromagnetic radiation. In nuclear environments when FBG's are exposed to gamma irradiation results have shown changes in the Bragg wavelength, although the exact cause or trigger is still unclear.

The main outcome was to achieve results that are compatible with the established data that will help in establishing FBG's as a replacement to current physical and chemical sensors currently being used as radiation dosimeters. Our study has given results that are in keeping with the established data

Throughout my literature review I did not come across any published papers with a similar methodology with regards to the irradiation stages we used i.e. an initial dose of 206kGy over two days followed by one day of relaxation and then repeated. This I feel, reinforces our overall result and paves the way for future irradiation studies with a new generation of FBGs and optical fibre.

## DECLARATION

I certify that this thesis does not, to the best of my knowledge and belief:

- (i) incorporate without acknowledgment any material previously submitted for a degree or diploma in any institution of higher education.
- (ii) contain any material previously published or written by another person except where due reference is made in the text; or
- (iii) contain any defamatory material.

I also grant permission for the Library at Edith Cowan University to make duplicate copies of my thesis as required.

Signature: .....

Date: .....

## **ACKNOWLEDGEMENTS**

I wish to acknowledge the support from my supervisors, Associate Professor Steven Hinckley and Dr.Graham Wild. They have made themselves available when required by me at short notice to assist in queries regarding my project. I thank them for this, and look forward to their continued advice and assistance as I progress further. Also, thanks to Dr.Steven Richardson, who made himself available and for taking time to answer any questions that I put forward. I would also like to acknowledge Daniel Oswald, Gary Allwood and Paul Jansz, fellow post graduate students for their encouragement and advise when needed. Also, I would especially like to thank my wife Vicki, for her ongoing support, guidance and patience throughout the year.

## TABLE OF CONTENTS

<b>Title Page</b>	<b>i</b>
<b>Use of Thesis</b>	<b>ii</b>
<b>Abstract</b>	<b>iii</b>
<b>Declaration</b>	<b>iv</b>
<b>Acknowledgements</b>	<b>v</b>
<b>Table of Contents</b>	<b>vi</b>
<b>List of Figures</b>	<b>viii</b>
<b>List of Tables</b>	<b>x</b>
<b>Chapter 1. Introduction</b>	<b>2</b>
1.1. Aim	2
1.2. Background	2
1.3. Significance	3
1.4. Motivation	4
1.5. Objectives	4
1.5.1. Primary Objectives	4
1.5.2. Secondary Objectives	4
1.6. Research Questions	5
<b>Chapter 2. Theory</b>	<b>6</b>
2.1. Gamma Radiation	6
2.2. Fibre Bragg Grating	7
2.3. Manufacture of FBG's	10
2.4. Radiation Induced Attenuation	12
2.5. Effects of radiation in optical fibres	14
<b>Chapter 3. Literature Review</b>	<b>16</b>
3.1. Significant Journals	16
3.2. Databases	16
3.3. Authors and Research Groups	17
3.4. Literature Summary	17
3.4.1. Advantages of FBG's over traditional sensors	18
3.4.2. FBG's exposed to High dose radiation	19
3.4.3. Germanium doped and Hydrogen loaded fibres	21
3.4.4. FBG's written by UV light and Femtosecond lasers	26
3.4.5. Radiation Induced Attenuation	28
3.4.6. Colour Center Defects ( $E'$ Centers)	29
3.4.7. Latest research and trends	30

3.4.8. New Fibre Technology	31
<b>Chapter 4. Research Methods</b>	<b>34</b>
4.1 FBG samples	34
4.2 Gamma Irradiation facility	35
4.3 Optical Measurements	35
4.4 Gamma Irradiation Protocol	39
4.5 Data Analysis	42
<b>Chapter 5. Results</b>	<b>43</b>
5.1 First Irradiation period	43
5.2 Second irradiation period	44
5.3 Effects of Relaxation	51
5.4 Amplitude variation during First Irradiation	57
5.5 Amplitude variation during second irradiation	58
5.6 FWHM Gaussian change with dose	59
<b>Chapter 6. Discussion and Future Work</b>	<b>66</b>
6.1 Discussion	66
6.2 Future Work	68
<b>Chapter 7. Conclusion</b>	<b>69</b>
7.1 Conclusion	69
<b>Chapter 8. References</b>	<b>70</b>
<b>Chapter 9. Appendices</b>	<b>76</b>
Appendix 1 Experimental research paper	76
Appendix 2 Matlab data for FWHM	80
Appendix 3 ANSTO report	84

## LIST OF FIGURES

Figure 2.1	Penetrating power of Gamma rays	6
Figure 2.2	FBG Sensing Mechanism	7
Figure 2.3	Basic Bragg Sensor set up	9
Figure 2.4	Writing an index grating with UV	10
Figure 2.5	Phase mask set up	11
Figure 2.6	Photo of high quality phase Mask	11
Figure 2.7	Femtosecond laser set up	12
Figure 2.8	Radiation Bragg peak shift with RIA	13
Figure 2.9	Radiation Bragg peak shift without RIA	13
Figure 2.10	Light propagation in optical fibre	14
Figure 2.11	Ge E centre defects	15
Figure 3.1	Shift of Bragg wavelength during gamma irradiation	19
Figure 3.2	Fibre with Ge-content and without Ge-content	20
Figure 3.3	Comparison of BWS, FBGs written without Hydrogen	21
Figure 3.4	Comparison of BWS, FBGs written with Hydrogen	22
Figure 3.5	Comparison of BWS, FBGs written without Hydrogen	22
Figure 3.6	Comparison of BWS, FBGs written with Hydrogen	23
Figure 3.7	Change of refractive index H-loaded UV exposed	24
Figure 3.8	Various Hydrogen pressure loadings	26
Figure 3.9	Photoexcitation and energy levels in Germanosilicate	27
Figure 3.10(a)	Fringe pattern close to mask	28
Figure 3.10(b)	Fringe pattern at distance to phase mask	28
Figure 3.11	Comparison of radiation induced loss	29
Figure 3.12	Increase of E' center with increase dose	30
Figure 3.13	Hollow core Photonic Crystal Fibre	31
Figure 3.14	Solid core Photonic Crystal Fibre	32
Figure 3.15	Random Hole Optic Fibre under irradiation	33
Figure 3.16	Random Hole Optic Fibre during recovery	33
Figure 4.1	GATRI's cobalt 60 radioactive source	35
Figure 4.2	FBG set up in experiment	37

<b>Figure 4.3</b>	<b>Experimental Equipment set up</b>	<b>38</b>
<b>Figure 4.4</b>	<b>Loss and gain of three peaks line three</b>	<b>41</b>
<b>Figure 5.1(a)</b>	<b>First complete irradiation period for line one</b>	<b>45</b>
<b>Figure 5.1(b)</b>	<b>Expanded graph SMF28 line one</b>	<b>46</b>
<b>Figure 5.2</b>	<b>Second complete irradiation period for line one</b>	<b>46</b>
<b>Figure 5.3</b>	<b>First Complete Irradiation period for line two</b>	<b>47</b>
<b>Figure 5.4</b>	<b>Second Complete irradiation for line two</b>	<b>47</b>
<b>Figure 5.5</b>	<b>Line One FBG(SMF 28+ H) 1545nm,First irradiation</b>	<b>48</b>
<b>Figure 5.6</b>	<b>Line One FBG (SMF28+H), 1545nm second irradiation</b>	<b>48</b>
<b>Figure 5.7</b>	<b>Line two FBG, Ge+H, (1555nm) first Irradiation</b>	<b>49</b>
<b>Figure 5.8</b>	<b>Line Two FBG Ge+H, (1555nm), second irradiation</b>	<b>50</b>
<b>Figure 5.9</b>	<b>Line three fbg(SMF 28+H), 1555nm,First relaxation</b>	<b>54</b>
<b>Figure 5.10</b>	<b>Line three fbg(SMF 28+H), 1555nm,Second relaxation</b>	<b>54</b>
<b>Figure 5.11</b>	<b>Line two fbg (Ge), 1545nm, First relaxation</b>	<b>55</b>
<b>Figure 5.12</b>	<b>Line two fbg(Ge), 1545nm, second relaxation</b>	<b>55</b>
<b>Figure 5.13</b>	<b>Line three with outlier removed, first irradiation</b>	<b>56</b>
<b>Figure 5.14</b>	<b>Line two with outlier removed, second irradiation</b>	<b>56</b>
<b>Figure 5.15</b>	<b>Reflection spectra, weaker output Line 3, FBG1&amp;2</b>	<b>58</b>
<b>Figure 5.16</b>	<b>Normal GIF image of Line 2 early stages of irradiation</b>	<b>61</b>
<b>Figure 5.17</b>	<b>Change in GIF image Line 2 final stages second irradiation</b>	<b>62</b>
<b>Figure 5.18(a)</b>	<b>Line one Gaussian fit first irradiation</b>	<b>63</b>
<b>Figure 5.18(b)</b>	<b>Line two Gaussian fit first irradiation</b>	<b>63</b>
<b>Figure 5.19(a)</b>	<b>Line two Gaussian fit first irradiation</b>	<b>64</b>
<b>Figure 5.19(b)</b>	<b>Line two Gaussian fit second irradiation</b>	<b>64</b>
<b>Figure 5.20(a)</b>	<b>Line three Gaussian fit first irradiation</b>	<b>65</b>
<b>Figure 5.20(b)</b>	<b>Line three Gaussian fit second irradiation</b>	<b>65</b>
<b>Figure 6.1</b>	<b>BWS over complete experiment Line two</b>	<b>66</b>

## LIST OF TABLES

<b>Table 3.1</b>	<b>Example of FBG parameters of four manufacturers</b>	<b>23</b>
<b>Table 3.2</b>	<b>Bragg wavelength shift of FBG</b>	<b>25</b>
<b>Table 3.3</b>	<b>E' concentration increase with dose increase</b>	<b>29</b>
<b>Table 4.1</b>	<b>Three lines of FBGs showing series sequence</b>	<b>36</b>
<b>Table 4.2</b>	<b>Copy of actual ANSTO measurements</b>	<b>40</b>
<b>Table 5.1</b>	<b>BWS. Accumulated Dose 206.8 kGy</b>	<b>43</b>
<b>Table 5.2</b>	<b>BWS. Additional dose of 196.4 kGy</b>	<b>44</b>
<b>Table 5.3</b>	<b>BWS. First Relaxation Dose 206.8 kGy</b>	<b>52</b>
<b>Table 5.4</b>	<b>BWS. Second Relaxation Dose 196.4 kGy</b>	<b>53</b>
<b>Table 5.5</b>	<b>Amplitude Variation of first irradiation. 206.8 kGy</b>	<b>57</b>
<b>Table 5.6</b>	<b>Amplitude Variation of second irradiation. 196.4kGy</b>	<b>59</b>
<b>Table 5.7</b>	<b>FWHM first irradiation period</b>	<b>60</b>
<b>Table 5.8</b>	<b>FWHM second irradiation period</b>	<b>60</b>

# CHAPTER 1

## INTRODUCTION

### 1.1 Aim

The main focus of my thesis is to examine the effects of gamma radiation on fibre Bragg gratings (FBGs) when used as radiation dosimeters. The advantages of the FBG in a sensing capacity will be shown when exposed to the ionizing radiation during the experiment. This will be performed using three different types of optical cable, consisting of Germanium (Ge) doped fibres, (with and without hydrogen loading), and a standard SMF-28 with Hydrogen optical fibre. The FBGs used, are written by low energy UV laser irradiation. The experiment will be performed in stages, noting the different Bragg Wavelength Shifts (BWS) as a function of absorbed dose. Particular interest will be looking at the relaxation effect on the FBGs, after the first and second irradiation periods. Pre-irradiation effects will be examined to compare the BWS with results of the first irradiation period. My aim also, is to show any saturation that may occur in both radiation and relaxation stages and examine radiation induced attenuation. Research suggests the narrow wavelength encoding of the sensing information in FBG's helps to avoid attenuation increase [1].

### 1.2 Background

Optical fibre Bragg grating sensors are already in use throughout industry worldwide. The main attributes over mechanical/electrical sensors is they have immunity to electro-magnetic interference, are light weight and small, have greater sensitivity, are mass producible and cost effective, and are able to measure remotely in real time. With radiation dosimetry, the FBG sensors hold a distinct advantage because of their immunity to electro-magnetic interference. With optical fibre dosimeters the radiation levels are relayed by using optical signals not electrical [2]. Current radiation dosimeters in use include film/badge personal dosimeters, thermoluminescent dosimeters (TLDs), electronic and electrical dosimeters and quartz fibre electroscopes (QFE) dosimeters. All have disadvantages such as high cost, short shelf life, fading due to temperature and light effects and sensitivity to rough handling [2]. With older electrical dosimeters, when exposed to radiation over time, degradation occurs to the insulation. This can affect the performance of the dosimeter making it very

unstable. All this leads to a continual monitoring and replacing of the dosimeter, making it less cost effective.

The progression from electrical/mechanical sensors to optical fibre based sensors has taken place in most industries. In radiation environments, however, research is still being performed to try and confirm the accuracy and reliability of optical sensors when they are used as a form of radiation dosimeter. The problem of attenuation increases when exposed to gamma irradiation has been documented previously but now research has turned to FBG's as the basis of a sensing system. The FBG seems to be less susceptible to attenuation, making it a strong candidate for a new form of radiation dosimeter. Studies have shown that when exposed to gamma irradiation, a Bragg wavelength shift (BWS) occurs, although the exact cause or trigger for this is still not known [3].

### **1.3 Significance**

Over the last ten years, the progression of optical fibre sensors through to FBG's, in industry, has evolved to the nuclear environment. Radiation dosimetry is the basis in which FBG's can play a major role. Because researchers are looking at ways to improve the measuring and monitoring of radiation, the FBG's attributes make it the prime candidate as a possible replacement to older dosimeters. The main significance is that the cost factor to the industry will be reduced and real time measurements will be performed with accuracy and safety [2].

An advantage to this new research is that by continuing to experiment, eventually the exact cause for the Bragg Wavelength shift under irradiation may be found. This will lead to a greater understanding of the relationship of how the refractive index changes with regards to the grating period. The more that is understood, the more industry can benefit.

## **1.4 Motivations**

Research in the area of radiation dosimetry in conjunction with FBG's has produced numerous published papers. Most of the results indicate that radiation dosimetry fall into two categories, either low dose or high dose detection. With gamma radiation, which is primarily in the high dose area, FBG's have been shown capable of being used as a new form of a monitoring device in the nuclear environment. I hope my investigations can add credence to the already established data.

## **1.5 Objectives**

### **1.5.1 Primary objectives**

- To use three samples of FBG's in a nuclear environment and whilst under gamma irradiation achieve a radiation induced BWS (Bragg wavelength shift).
- To determine whether FBGs created by UV light, with hydrogen loading and Ge-doping, have greater sensitivity to high dose gamma radiation.
- To determine experimentally, the Bragg wavelength shift as a function of the accumulated dose.

### **1.5.2. Secondary objectives**

- To determine the major cause or trigger for the Bragg wavelength shift.
- To determine if FBGs are compatible and suitable to be used as radiation dosimeters in a nuclear environment.
- Irradiation will be stopped to observe the relaxation effect.
- To examine how the dose rate affects the already irradiated samples and improve on previous experimental results conducted by ECU which were inconclusive.

## **1.6 Research Questions**

- 1.** Under irradiation, what is the effect of the accumulated dose on the BWS?
- 2.** What are the effects of relaxation on FBGs, after two stages of gamma irradiation?
- 3.** Does pre-irradiation affect FBG performance?
- 4.** Is the data consistent with previous research?
- 5.** Are the FBGs suitable to act as a dosimeter for high dose radiation?
- 6.** Is the set up required for the FBG sensor to be highly stable, stress free and at a constant temperature for the best results?
- 7.** Do the results show, radiation sensitivity of the FBGs, to be dependent on the chemical composition (doping) of the optical fibre that they are written in?

## CHAPTER 2 THEORY

In this chapter I will describe the main principles of FBGs, and the various manufacturing techniques used in writing or inscribing the gratings in various optical fibre. I also show the effects of radiation in optical fibre made from the most commonly used core material in optical fibre used today silica or silicate glass

### 2.1 Gamma Radiation

French physicist Paul Villard is credited with discovering gamma rays in 1900. Gamma rays are a form of electromagnetic radiation. He recognized they were different than x-rays in that they had a much larger penetrating depth also they were not affected by electrical or magnetic fields. The major difference however is the way gamma rays are produced. They originate from the nucleus of a radionuclide following radioactive decay. The gamma ray is essentially electromagnetic energy or photons which have the highest energy and shortest wavelength in the electromagnetic radiation spectrum [4]. The high energy of gamma rays allow them to pass through most materials. Lead is the main material used to slow or stop the gamma photons. The gamma ray emitters currently used include Cobalt-60, which I will use for the experiment. Currently it is used for example, to sterilize medical equipment in hospitals and gauge the thickness of metal in steel mills due to its penetrating radiation as shown in Figure 2.1.

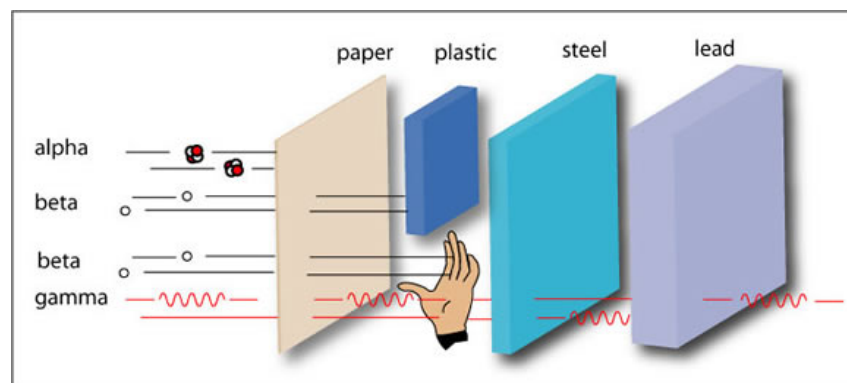


Figure 2.1. penetrating radiation of gamma rays [4].

## 2.2. Fibre Bragg Gratings

The main principle behind the FBG sensor is that when there is a change in temperature, strain due to stress or pressure, the centre of the wavelength reflected from the FBG will alter. It is in a sense, a type of Bragg reflector constructed or written into the optical fibre. The fibre reflects certain wavelengths of light and transmits all others [5]. The Bragg wavelength is related to the refractive index ( $n$ ) of the material and the grating period ( $\Lambda$ ). The grating sensors are therefore based on the reflection and interference of light travelling through the fibre. When a section of fibre is exposed to axial strain, temperature or pressure changes from an external source eg. during gamma irradiation it will change either or both the refractive index and grating period of the FBG[6]. These affect the Bragg wavelength. This enables changes occurring from pressure or expansion to be detected with the FBG from the shift in the Bragg wavelength [7]. It can be measured by recording the actual change in the reflection coefficient as shown in Figure 2.2.

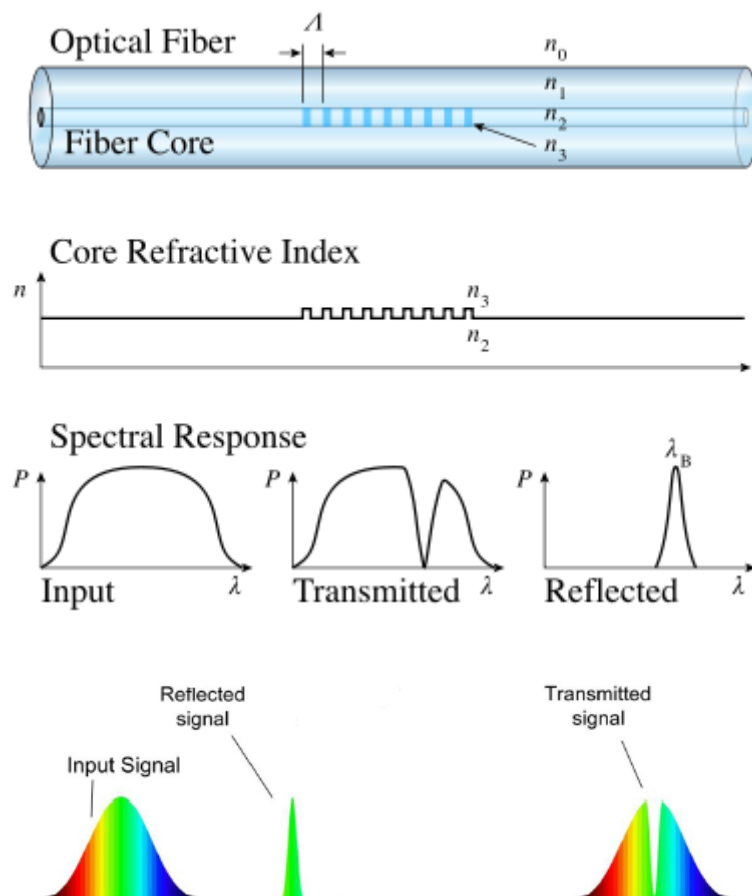


Figure 2.2 FBG Sensing Mechanism [24].

The Bragg wavelength ( $\lambda_B$ ) is given by,

$$\lambda_B = 2n\Lambda \quad (1)$$

where ( $n$ ) is the average refractive index of the grating and ( $\Lambda$ ) is the grating period. Changes in the grating caused by strain associated with pressure or expansion results in a wavelength shift [8]. The change in wavelength caused by strain and temperature is given by,

$$\Delta\lambda_B = \lambda_B \left[ \varepsilon \left( 1 - \frac{n^2}{2} [p_{12} - \nu(p_{12} + p_{11})] \right) + \Delta T \left( \alpha + \frac{1}{n} \frac{dn}{dT} \right) \right], \quad (2)$$

where ( $\nu$ ) is Poisons' ratio,  $p_{12}$  and  $p_{11}$  are the strain optic coefficients, ( $\varepsilon$ ) is the applied strain and ( $\Delta T$ ) is the change in temperature in equation (2), which enables a shift in the wavelength to occur. This will be the new FBG wavelength that will be recorded. A lot of work has been performed investigating the effects of radiation on FBGs. The main area covered for research, is developing radiation resistant FBGs for use in nuclear environments in the areas of temperature and strain measurement applications [2]. Recently however, FBG's have been investigated as possible high dose radiation sensors [9].

The FBG's that were used in the experiment were in fibre that was hydrogen loaded and Ge-doped and written by UV light. When UV light radiates an optical fibre the refractive index of the fibre is changed permanently. Photosensitisation is the process of enhancing the refractive index. To do this, techniques such as hydrogen loading is used. Fibre is put into a high pressure vessel containing hydrogen and pressure of 100-1000 atmospheres are applied. Hydrogen will then diffuse into the silica fibre. Photo-induced refractive index changes up to 100 times greater are obtained by this method [13].

The actual sensing ability of the FBG stems from the sensitivity of the refractive index and the grating period within the fibre when being exposed to external forces. These forces affect the response of the FBG directly through expansion and compression changes caused either by strain or pressure [24]. The strain optic effect or the strain induced change in the glass refractive index, also effects the FBG. To use the FBG as a sensor system, it is usually set up in the configuration shown below in Figure 2.3, showing the transmissive or reflective detection options.

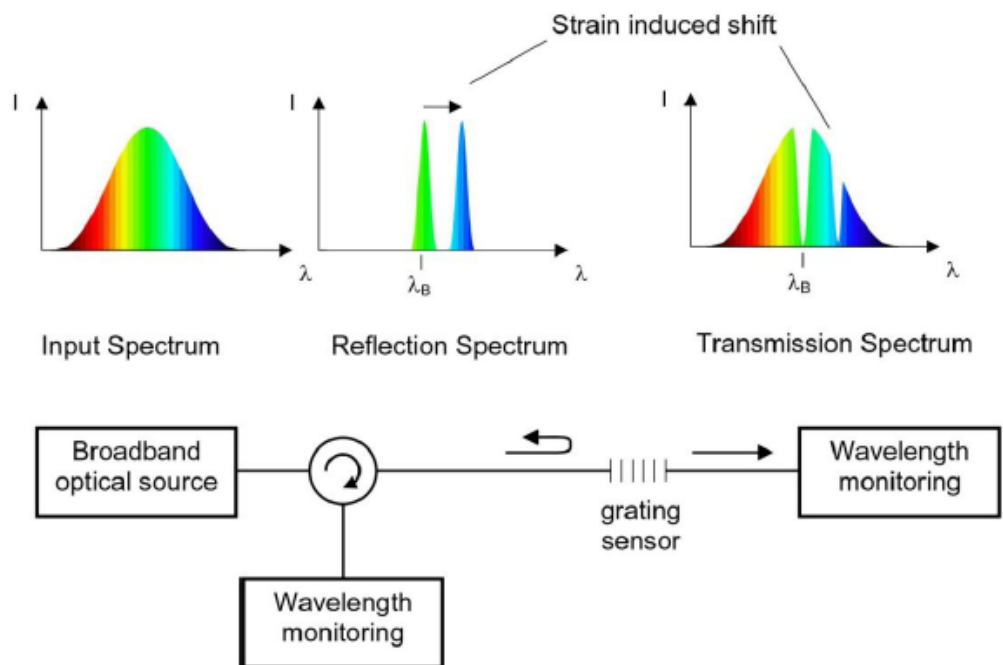


**Figure 2.3. Basic Bragg Sensor set up with transmissive or reflective options [24].**

FBGs can have varying resonant wavelengths by the way they are written. This allows them to be multiplexed into a sensor system where varying stresses and temperatures can be measured along the fibre at different intervals [24]. This makes FBGs very attractive as a possible replacement to conventional radiation dosimeters.

### 2.3 Manufacture of FBG's

The method known as writing or inscribing is used in the fabrication of FBG's. The fibres refractive index is dependent on the density of the dopant it contains. Germanium (Ge) doped silica fibre is the usual form of dopant used. It is used because it is photosensitive, and when it is exposed to intense ultraviolet light, periodic changes to the refractive index of the fibers core occur [10]. This is achieved by a technique known as laser writing, which has the effect of creating areas of either less dense or more dense amounts of dopant in the fibre. To write an index grating directly on to the doped fibre, two UV beams are placed at an angle to produce an interference pattern. This is written on to one side of the fibre that has been stripped bare of external coatings. The interference pattern, consisting of dark and light bands, causes the change in the refractive index by the movement of the dopants in the fibre [11] as seen in Figure 2.4.

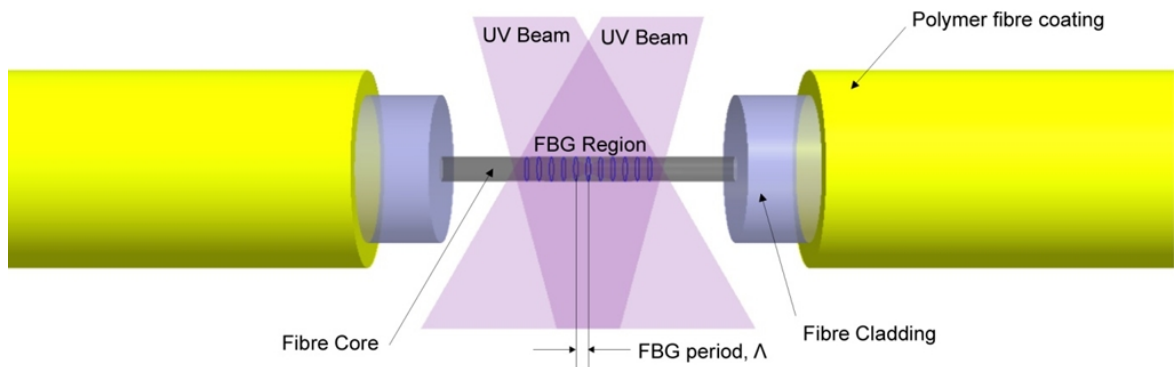


**Figure 2.4. Writing an index grating with UV lasers [12].**

The other method for writing or inscribing an index grating is known as masking. A phase mask is positioned between a UV light source and photosensitive fibre as shown in Figure 2.5. The phase mask pre-determines the wavelength of the reflection grating by the varying light intensity illuminating the fibre, as seen in Figure 2.6 [13]. This method is used to produce FBG's that cannot be made by interference pattern techniques eg. chirped fibre Bragg gratings.

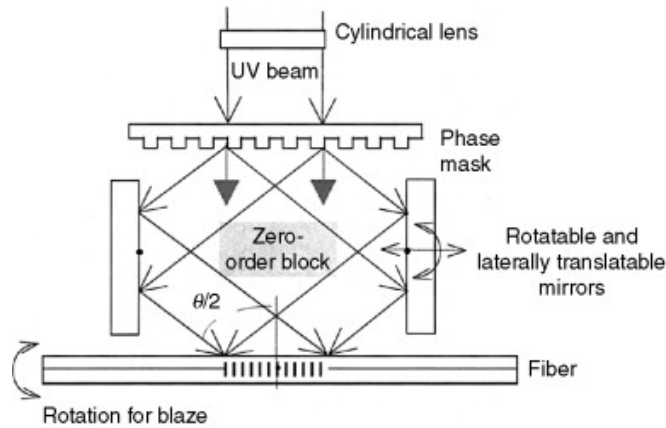


**Figure 2.5. An example of phase mask set up [13].**

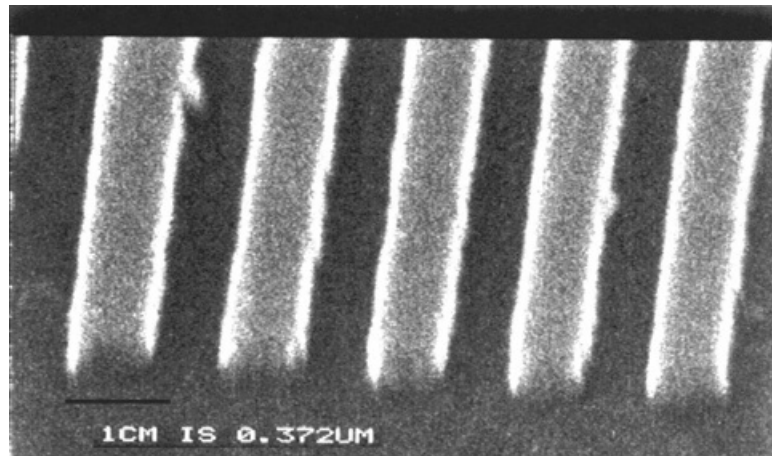


**Figure 2.6. Photograph of high quality phase mask used for grating inscription [13].**

I have mentioned the UV method of writing FBG's. However for future experiments we will also look at FBG's manufactured using high energy femtosecond (fs) lasers. With the normal fabrication method of using UV light, the photons energy of 5eV corresponds to the absorption band of defects in the fibre (usually germano-silicate glass). This fibre is photosensitive due to a high Ge concentration or enhanced by Hydrogen loading [14]. With FBG inscribing commercial femtosecond lasers are used to produce (fs) UV pulses. The pulses are directed by a phase mask onto the fibre by varying the displacement of the lens in relation to the fibre, as seen in Figure 2.7. This allows the variation in UV irradiation intensity. This exposure variation results in the formation of strong FBGs [14].

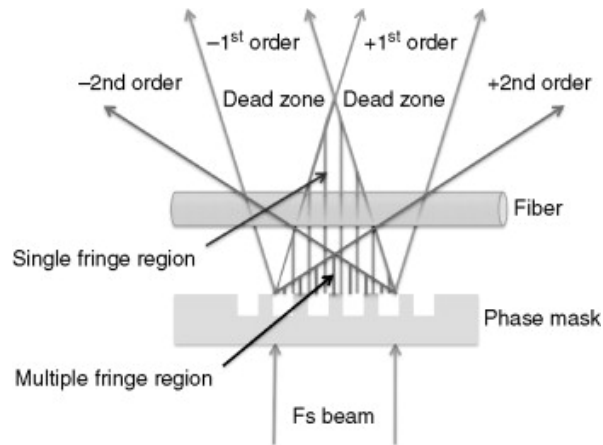


**Figure 2.7. Femtosecond laser set up with phase mask [13].**

## 2.4. Radiation Induced Attenuation (RIA)

Research has shown that exposure to gamma irradiation in nuclear environments causes attenuation of the fibre, due to the change in the refractive index. This is dependent on the fibre composition, including the chemical composition and photosensitization technique used [3]. RIA is mainly caused by the excitation of the Ge atoms in the core of the optical fibre when exposed to gamma radiation. The optical fibres guide light through the core due to the total internal reflection which comes from the difference between the index of refraction between the core and cladding of the fibre. Germanium is a dopant used to increase the index of refraction between the core and cladding, providing enhanced light guiding properties [10]. With attenuation, the power of light traveling through the optical fibre decreases with distance as a result of absorption and scattering [15]. It is defined in units of decibels per kilometer (dB/km). FBG's however, seem to avoid the broadband radiation induced optical power loss because of the narrow wavelength encoding or narrow spectral range of  $< 5\text{nm}$  [3]. With gamma irradiation of Ge-doped fibres, the result is a change in the effective refractive index, which in turn results in a radiation induced Bragg wavelength shift as shown in Figure 2.8 and Figure 2.9. In Figure 2.8. the baseline is lowered due to the RIA of the photosensitive fibre, whilst in Figure 2.9, there is no attenuation. The induced Bragg wavelength shift of the peak position shows that FBG's could be used for dosimetry [14].

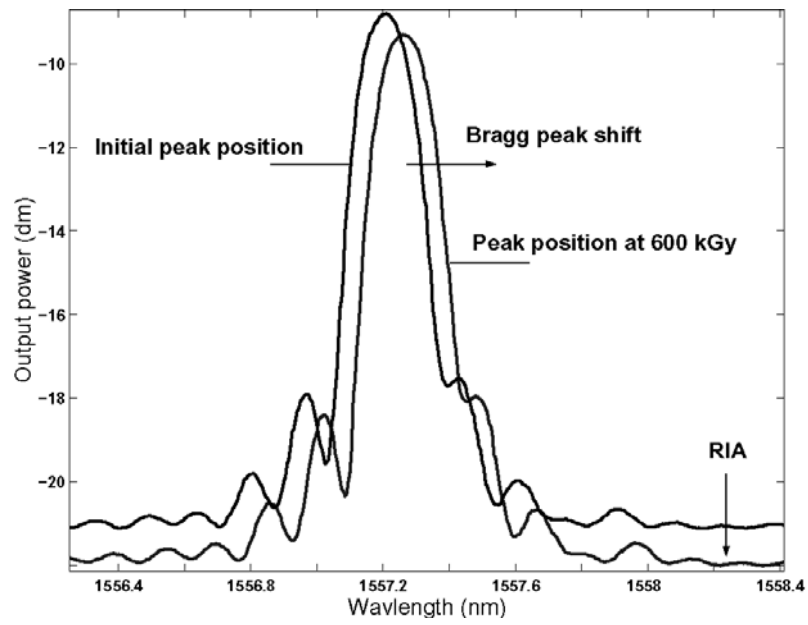


Figure 2.8. Radiation induced Bragg peak shift, with baseline lowered due to RIA [3].

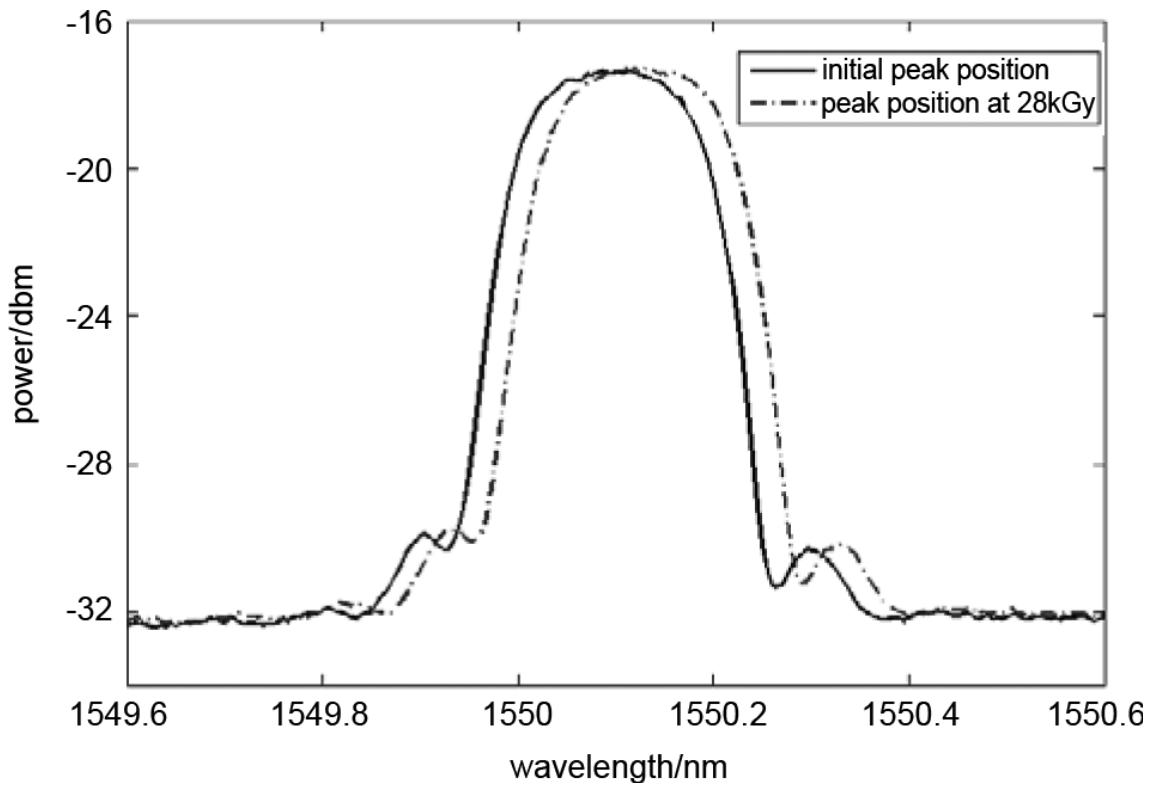
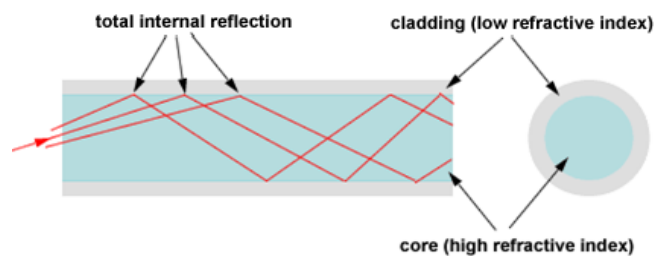


Figure 2.9. Radiation induced Bragg peak shift, with no RIA [13].

## 2.5. Radiation Effects in Optical Fibre

The material used in the fabrication of optical fibre in use today, consist mainly of silicon dioxide ( $\text{SiO}_2$ ) known as pure glass [32]. Plastic fibres and Fluoride based glass are also in use, but have limitations. Plastic optical fibre in particular have high attenuation compared to glass fibres, making them less suitable for optical sensing in radiation environments [32]. Under irradiation, defect centers can form in the silica material of optical fibres. Defect centers or colour centers are the main factor in the cause of attenuation loss [33]. When exposed to radiation, changes of the optical fibre refractive index occur, due to the damage of the fibre matrix structure, increasing the fibre absorption loss [34]. The defects induce new energy levels inside the band gap, with the result being an increase of absorption of the transmitted signal. The increase of absorption is known as Radiation Induced Attenuation (RIA) [35].

With the addition of dopants however, such as Germanium, Fluorine, Boron, Erbium or Phosphorus to the fibre core, it was found that optimization of propagation occurs, along with a reduction of attenuation [36]. The most commonly used core material in optical fibre used today is Germanium(Ge) doped silica or germano-silicate glass [36]. Both germano-silicate and silicate glass show attenuation rates as low as 0.20 dB/km at a wavelength of 1550nm [37]. Germanium is a dopant used to increase the index of refraction between the core and cladding, providing enhanced light guiding properties [10]. Germanium doped silica fibre is also highly photosensitive. With the addition of hydrogen loading and boron co-doping the photosensitivity of the fibre can be enhanced even further[38]. Germanium doping and hydrogen loading in combination increase the radiation sensitivity of the fibre. To achieve light propagation inside the fibre, the core refractive index has to be higher than the cladding, as shown in Figure 2.10.



**Figure 2.10. Light propagation in optical fibre; showing high and low refractive index [38].**

The fabrication of glass fibre with core dopants such as germanium lead to a variety of defects. During the manufacturing process the defects occur because it is not possible for 100% perfection, therefore the deposited chemicals with the core dopant germanium, form suboxides such as  $GeO_x$  ( $x=1$  to  $2$ ) [13]. The best known of the defects are known as paramagnetic  $Ge(n)$  defects, where  $n$  is the amount of neighbour Ge/Si atoms surrounding a Ge ion with an unsatisfied single electron. When exposed to UV light or irradiation, the bond is broken creating what is known as a  $GeE'$  centre as shown in Figure 2.11. A free electron is now free to move within the glass matrix through tunnelling or by two photon excitation into the conduction band [38]. The removal or movement of the electron causes a change in the shape of the molecule which may in turn change the density of the material. This causes the formation of colour centres ( $GeE'$ ) or absorption bands, resulting in the change of the refractive index [38]. The absorption bands are responsible for transmission losses.

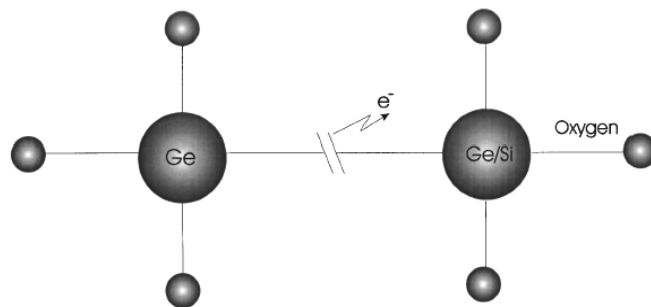


**Figure 2.11.  $GeE'$  centre. Germania defects in Germania doped silica. An electron is released on breaking of the bond [38].**

The concentrations of colour center defects ( $E'$  centers) in silica glass when exposed to irradiation have been shown to vary. To improve the performance of optical fibre in radiation environments the characteristics of these defects must be studied further [33].

## **CHAPTER 3**

### **LITERATURE REVIEW**

#### **3.1 Significant Journals**

A number of Journals can be considered directly related to the topic. These journals are available in full text, and will be used as primary reading sources throughout the candidature. The primary journals include ;

- IEEE Transactions on Nuclear Science.
- IEEE Photonics Technology Letters.
- Journal of Optics, by IOP

#### **3.2 Databases**

There are several major databases that have been used in the sourcing of relevant literature. By doing this it has led to the discovery of other journals where similar subject related material is likely to be found. The most pronounced and significant databases include;

- The International Society for Optical Engineering (SPIE) digital library
- The Institute of Electrical and Electronic Engineers (IEEE) Xplore Digital Library
- The Institute of Physics (IOP) Electronic Journals

Other databases such as Science Direct were also used in assisting the search for relevant material.

### **3.3 Authors and Research Groups**

A number of important authors and research groups have been identified . In the field of developing fiber bragg gratings for radiation environments Henning Henschel, Stefan k. Hoeffgen, A. I . Gusarov, A.Fernandez Fernandez, Udo Weinand and Katerina Krebber are by far the most prominent. Some of the prominent research groups include;

- Communications research Centre, Ottawa, Canada.
- Federal Institute for Materials Research and testing, Berlin, Germany.
- Fraunhofer-INT, Euskirchen, Germany
- SCK-CEN Belgian Nuclear Research Centre, Boeretang,Belgium

### **3.4 Literature Summary**

The literature summary/review will incorporate the areas that are relevant to the thesis topic. These include research that has looked at Fibre Bragg Gratings being used as possible high dose radiation sensors and examination of radiation damage in FBG's. The concepts of different fibres, their behaviour and sensitivity to gamma radiation and the overall advantages compared to traditional physical and chemical sensors will be covered. Photosensitisation methods used to write FBG's either by UV light or fs laser and their relative performance under irradiation will be reviewed. I have also incorporated the Femtosecond laser method as I hope to use this method in future experiments. FBGs created in Ge-doped and Hydrogen loaded fibres, and their sensitivity to gamma radiation, will also be covered. Finally, look at where FBG's stand at this point in time and where the research is expanding as far as radiation dosimetry is concerned.

### **3.4.1 Advantages of Fibre Bragg Grating's over Traditional sensors.**

The main advantages that FBG's have over traditional physical, chemical and gas sensors is that they have immunity against electro-magnetic fields, high voltage, high and low temperatures, and nuclear/ionising radiation environments. They are also lightweight, flexible and non-interfering [16]. Specific attributes include multiplexing capability and are able to be imbedded in composite materials. Economically they are mass producible at a reasonable cost. They are already established in the aerospace, medical, mining, marine, transportation, military, seismology and power fields [17]. Conventional devices used for sensing can be heavy, bulky and spaced at certain distant intervals which can lead to low resolution imaging. This effects the real time measurement and remote sensing capabilities [17]. With FBG's however, processing information at the rate of 100 samples/second is viable. This is a major factor in real time remote sensing allowing for an informed response in the event of emergencies, and also allows for accurate monitoring which is crucial in a nuclear ionising environment [17].

Recently, fibre optic based sensors have been shown to operate in very high temperature and high radiation environments [10]. This is contrary to earlier work which suggested that fibre optic based sensors would not function in harsh environments including high radiation areas [10]. Research and engineering solutions have now been applied to overcome these limitations. Fibre Bragg grating temperature sensors have been shown to survive high gamma radiation doses [10]. Research also shows that FBG's written in fibre that has been hydrogen loaded and Ge-doped are capable of monitoring high gamma radiation doses [2].

Overall, the main advantage of the FBG sensor is that dose information is transmitted using optical signals compared to electrical signals used by physical sensors. As FBG's have immunity to electrical/electromagnetic interference, they do not suffer as many electronic dosimeters do. Electrical dosimetry relies on a high voltage power supply and they must have good insulation. Under irradiation, degradation occurs to the insulation, which affects the operation and stability of the dosimeter. Also, the radiation generates electric noise which can affect the signal transmitting the dose information [18].

### 3.4.2. FBG's exposed to High Dose Radiation.

When FBG's have been exposed to gamma irradiation, a shift of the Bragg wavelength occurs. Results indicate the FBG's sensitivity to radiation increases from 820nm to 1516nm when exposed to gamma radiation as seen in Figure 3.1, up to a total dose of 100kGy. FBG's with a higher wavelength of 1550nm seem to be suited for high dose radiation sensing, as no saturation was observed up to 100kGy [9]. One gray is the SI unit of the absorbed dose which equals 100 rads.

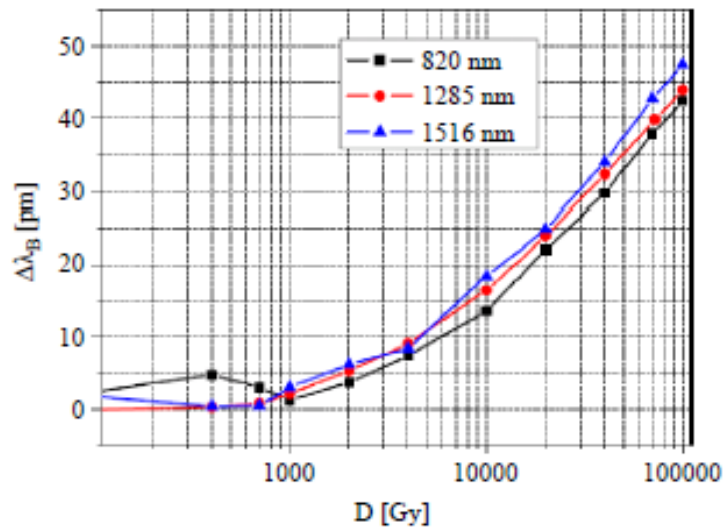
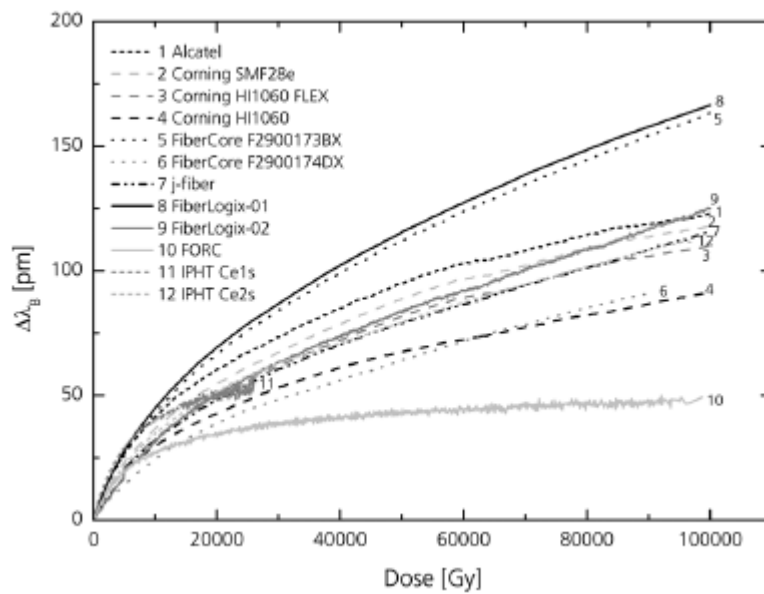


Figure 3.1. Shift of Bragg Wavelength during gamma irradiation [9].

The investigation has shown that temperature, as well as the radiation induced Bragg wavelength shift can be measured with great accuracy. A study was carried out specifically to look at the effects and behaviour of FBGs under high dose gamma radiation. It was reported that the gamma radiation sensitivities written by UV 330nm light in hydrogen loaded, Ge-doped fibre were found to be higher than FBG's written in Ge-doped without hydrogen loading. The radiation induced shift of the Bragg wavelength peak saturated at a higher level for the FBG's written in hydrogen loaded, Ge-doped fibre than FBG's written in Ge-doped with no hydrogen loading [19]

Overall the radiation sensitivity of FBGs is strongly dependent on the photosensitisation method and the chemical composition used for their fabrication. The FBGs that have been written in naturally photosensitive fibre show the best radiation

tolerance, resulting in a minimum Bragg peak wavelength. When the FBG is exposed to gamma radiation the saturation of the radiation induced Bragg peak shift occurs towards the longer wavelengths [25]. The effect of the variation in fabricating methods of FBGs, has shown fibres with medium to high Ge-content and are hydrogen loaded, have produced a Bragg wavelength shift of approximately 160pm after exposure of a dose rate of 100 kGy [26]. A comparison can be made when the fibre had no Ge-content. The result indicated a Bragg wavelength shift of only 50pm as shown in Figure 3.2. This shows fibre with about 10 to 21% Ge-content are well suited to be used for radiation dosimetry [27].



**Figure 3.2 Shows Fibre 8 with Ge-content. Fibre 10 without Ge- content [27].**

The effects of long term exposure to radiation on fibre Bragg gratings in a nuclear reactor have been examined [30]. The gratings were fabricated in photosensitive and standard fibres. The study was conducted over a period of 8 years. They remained in the reactor, during which time it was operational for a total of 4690h. It was found after the eight years of exposure the shape of the gratings spectra and amplitude remained unchanged for fibres without hydrogen loading. The fibres with hydrogen loading showed only slight changes to the grating spectra and amplitude [30]. This suggests that the Bragg gratings can withstand long term exposure without significant degradation of reflectivity and with only a slight shift of the Bragg peak [30]. The test results are important as most experiments previously conducted evaluate the FBGs in

harsh conditions over relatively short time scales of days and weeks. Studies have been conducted similar to the 8 year study. A 50 month study was undertaken to show long term effects on fibre Bragg grating temperature sensors in a low flux nuclear reactor [31]. The results showed that the sensors still operated and demonstrated that Bragg gratings can withstand long-term exposure to at least moderate nuclear radiation. The temperature sensitivity was unaffected by the long term irradiation allowing to perform a temperature measurement change with an accuracy better than 3 degrees C, which is acceptable for measurement applications in nuclear installations [31]. The two studies show the viability of FBGs being used a radiation dosimeters long term.

### 3.4.3 Ge-Doped and Hydrogen loaded FBGs.

When under high dose gamma radiation, FBGs written in Ge-doped and hydrogen loaded fibres showed a greater sensitivity to gamma irradiation than those without hydrogen loading, as shown in Figure 3.3 and Figure 3.4. The width and amplitude of the Bragg peak changed in the FBGs written in Ge-doped and hydrogen loaded fibres. There was no change in the Ge-doped unloaded fibre [19].

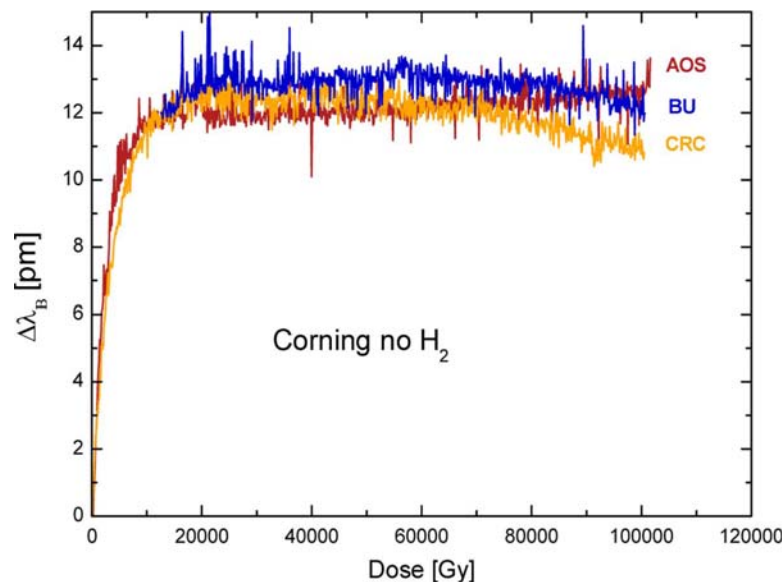
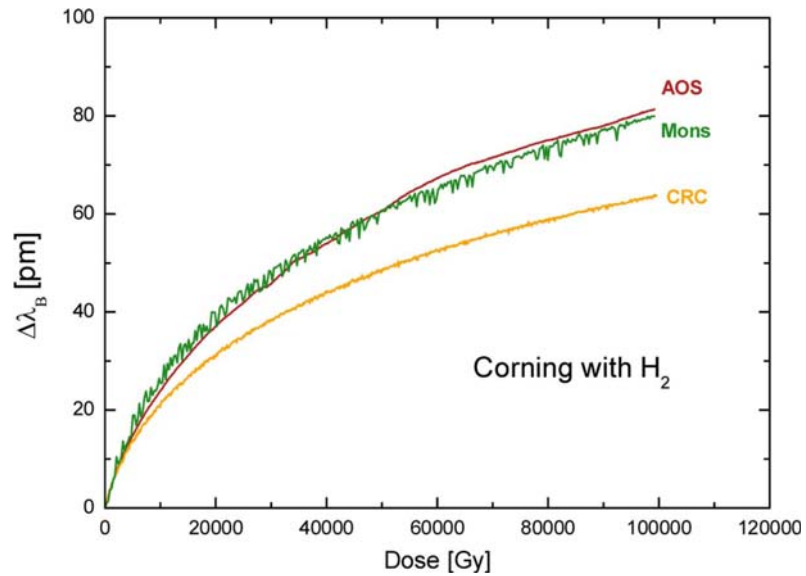
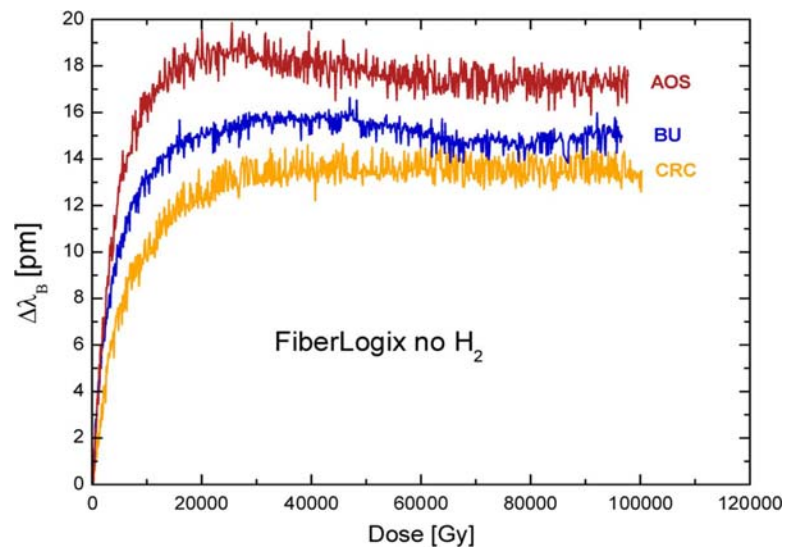


Figure 3.3 Comparison of BWS of fibres without Hydrogen [20].



**Figure 3.4 Comparison of BWS of fibres with Hydrogen [20].**

The Corning fiber type results show a distinct lower Bragg wavelength shift without hydrogen loading than the hydrogen loaded fiber. The Germanium concentration in the Corning SMF-28 was found to be 5 wt%. For a comparison, the FiberLogix HNA-01 had a Ge concentration of 9 wt%. The Bragg wavelength shift of the FiberLogix is higher, as seen in Figures 3.5 and 3.6, than the Corning fibre, which due to the Ge content of the FiberLogix being higher [20].



**Figure 3.5 Comparison of BWS of Fibres without Hydrogen [20].**

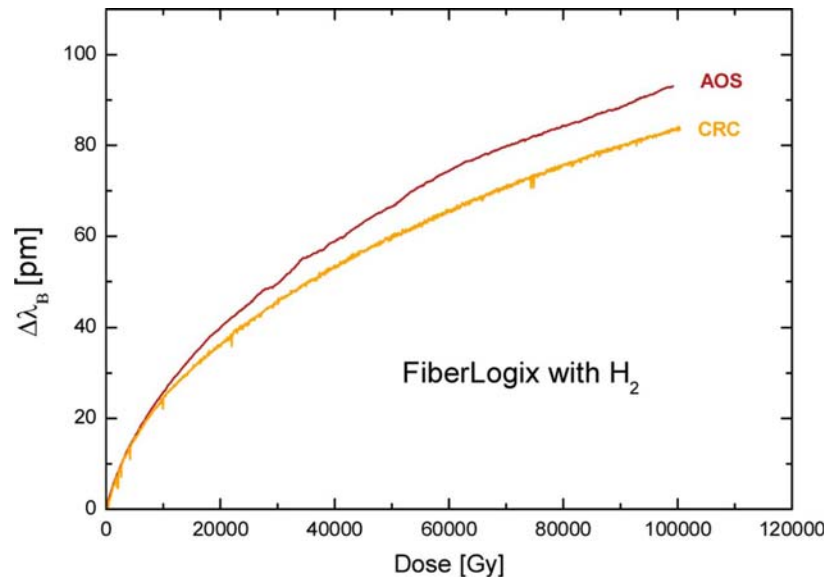


**Figure 3.6 Comparison of BWS of Fibres with hydrogen [20].**

This data is very relevant to the experiment that we will perform as we will use four types of samples; Ge-doped optical fibres with and without hydrogen loading similar to those seen in Table 3.1.

**Table 3.1 Example of FBG parameters [20].**

Manufacturer	Fiber Type	H <sub>2</sub> -Loading	Laser Type	Stabilization
AOS, Germany	Corning SMF-28	yes	UV	3 d at 100 °C
		no	UV	3 d at 100 °C
	FiberLogix HNA-01	yes	UV	3 d at 100 °C
		no	UV	3 d at 100 °C
Business Unitec, Russia	Corning SMF-28	no	UV	none
	FiberLogix HNA-01	no	UV	none
CRC, Canada	Corning SMF-28	yes	fs IR	4 d at 100 °C
		no	fs IR	4 d at 100 °C
	FiberLogix HNA-01	yes	fs IR	4 d at 100 °C
		no	fs IR	4 d at 100 °C
University Mons, Belgium	Corning SMF-28	yes	UV	45 h at 100 °C

When the fibre is hydrogen loaded, the reaction with the Ge ion forms GeH, which changes the band structure in the UV region. The resultant changes cause the refractive

index profile to change. When the fiber is exposed to UV, the refractive index increases, resulting in a greater sensitivity to gamma irradiation, as seen in Figure 3.7 [13].

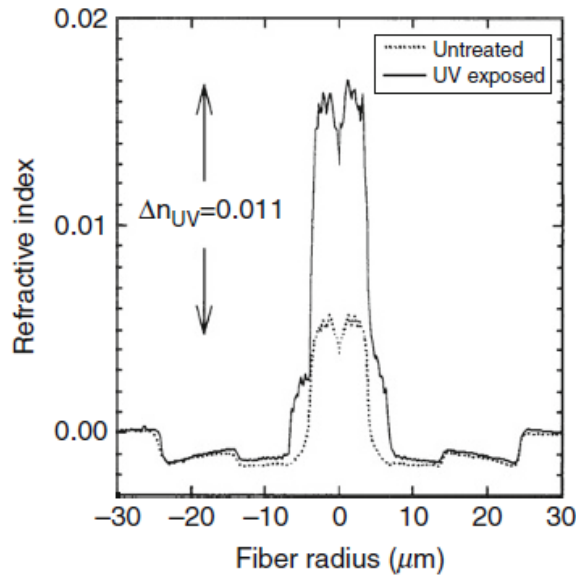


**Figure 3.7. Change of refractive index of hydrogen loaded fibre before and after UV exposure [13].**

The aspect of radiation tolerance of FBGs has also been examined noting the influence of various grating fabrications. Pre-irradiation and hydrogen loading along with Ge-dopants, significantly change the radiation sensitivity of FBGs [26]. Pre-irradiation can increase the radiation hardness of the Bragg gratings, resulting in a decrease of the Bragg wavelength peak shift whilst hydrogen loading and Ge-dopants increase the radiation sensitivity resulting in higher Bragg wavelength shifts [26]. In Table 3.2, the grating labels 3-6 and 4-1 indicate that for a total dose of 50kGy, the Bragg wavelength peak shift are the highest at 46pm and 40pm respectively. Both have hydrogen loading and Ge-dopants with no pre-irradiation. The grating labels 3-1, 3-2 and 3-3 have Ge-dopants without hydrogen loading and no pre-irradiation. The result indicates that they have the lowest Bragg wavelength peak shifts and therefore less sensitive. Overall, the results are a good representation of radiation effects on fibre Bragg gratings.

**Table 3.2 Bragg Wavelength Shift of Fibre Bragg Gratings [26].**

Grating label	Fiber	Core Dopants (mol%)	H <sub>2</sub> -loading	Pre-irradiation	Max peak shift (pm)
1-1	SMF28	GeO <sub>2</sub> (3)	Yes	Yes	30
1-2	PSF-GeB-125	GeO <sub>2</sub> (23), B <sub>2</sub> O <sub>3</sub> (17)	No	Yes	17
2-1	CS 1060	GeO <sub>2</sub> (12.1)	Yes	Yes	29
2-2	CS 1060	GeO <sub>2</sub> (6)	Yes	Yes	25
2-3	PSF-GeB-125	GeO <sub>2</sub> (23), B <sub>2</sub> O <sub>3</sub> (17)	Yes	Yes	37
3-1	PSF-GeB-125	GeO <sub>2</sub> (20.59), B <sub>2</sub> O <sub>3</sub> (17)	No	No	15
3-2	PSF-GeB-125	GeO <sub>2</sub> (20.37), B <sub>2</sub> O <sub>3</sub> (17)	No	No	14
3-3	PSF-GeB-125	GeO <sub>2</sub> (20.2), B <sub>2</sub> O <sub>3</sub> (17)	No	No	13
3-4	CS 1060	GeO <sub>2</sub> (12.1)	Yes	No	36
3-5	CS 1060	GeO <sub>2</sub> (6)	Yes	No	32
3-6	PSF-GeB-125	GeO <sub>2</sub> (23), B <sub>2</sub> O <sub>3</sub> (17)	Yes	No	46
4-1	PSF-GeB-125	GeO <sub>2</sub> (20.59), B <sub>2</sub> O <sub>3</sub> (17)	Yes	No	40
4-2	PSF-GeB-125	GeO <sub>2</sub> (20.37), B <sub>2</sub> O <sub>3</sub> (17)	Yes	No	31
4-3	PSF-GeB-125	GeO <sub>2</sub> (20.2), B <sub>2</sub> O <sub>3</sub> (17)	Yes	No	26
4-4	CS 1060	GeO <sub>2</sub> (0.33)	Yes	No	17
4-5	PSF-GeB-125	GeO <sub>2</sub> (23), B <sub>2</sub> O <sub>3</sub> (17)	No	No	25

Further study has revealed the influence of hydrogen loading pressure on the radiation sensitivity of fibre Bragg gratings. The Bragg wavelength shift as a function of dose rate was measured, with FBGs that were made after loading the fibre at various hydrogen pressures of 100 bar, 200bar and 300 bar [29]. The results indicate that in the pressure range of 100-200 bar, the radiation sensitivity of the FBG is not influenced as compared with pressure of 300 bar. When increased to 300 bar the radiation sensitivity increased by 14%, which increased the Bragg wavelength shift as shown in Figure 3.8. The conclusion is, fibres loaded with 100 bar and 200 bar need no special attention when radiation sensitivity is concerned, however with 300 bar loaded fibres consideration of the increase in sensitivity must be taken into account [29]. It also reveals the range of manufacturing parameters that influence the FBGs sensitivity.

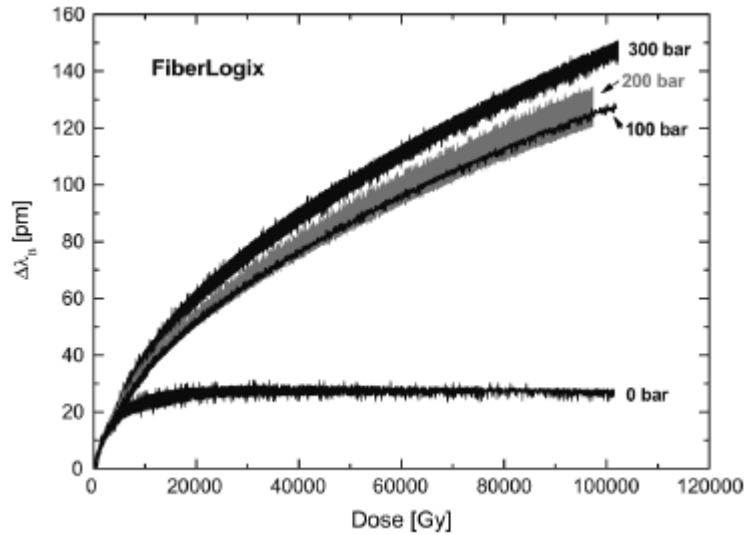


**Figure 3.8 Various hydrogen loading pressures and wavelength shift.**

#### **3.4.4 Gratings Written by UV light and Femtosecond Laser.**

Fibre Bragg gratings can be written by either UV low intensity light or by high intensity UV femtosecond laser. By using a 264nm high intensity femtosecond laser and a phase masking procedure, the fibre Bragg grating inscription was studied to see the effect on different photosensitive and normal fibres. Results indicate that the high intensity fs laser irradiation improved the photosensitivity in comparison with the conventional 248nm low intensity exposure. The factor rose by a factor of 6-128 times, depending on the fibre used and irradiation intensity [21]. For standard excimer lasers at 248nm, the inscription of FBGs is used in conjunction with a continuous UV source at 240nm. The refractive index produced at these wavelengths is linked with the absorption band of defects found in the germanosilicate glass. The other way to reach a high value of excitation energy is to use the high intensity 264nm UV laser irradiation. This results in an increase in the photosensitivity because of the additional excitation from the two-photon excitation process, as seen in Figure 3.9 [21].

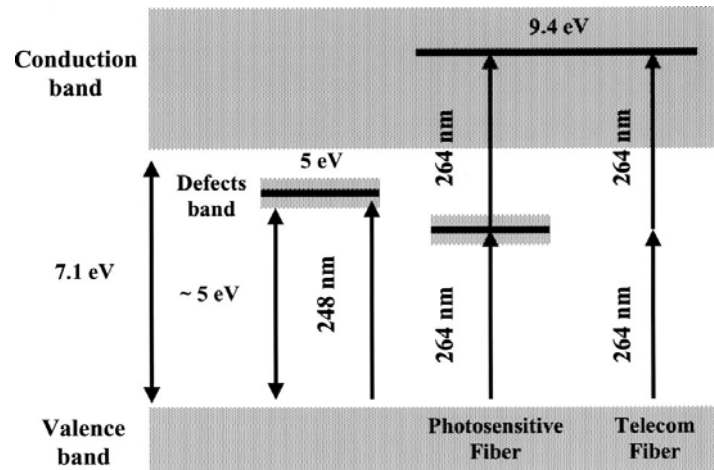


**Figure 3.9 Photoexcitation and energy levels in Germanosilicate glass [21].**

With regards to the effect of gamma radiation (cobalt 60) on FBGs written by a femtosecond UV laser, the gratings written in three different fibres were both photosensitive and hydrogen sensitised. The result showed both had a nearly identical shift of the Bragg reflection wavelength under gamma irradiation [14]. The most common form for FBG inscription is by using low intensity UV light with the photon energy of 5eV. The comparison between the fs and low intensity FBG fabrication show that the femtosecond procedure influences the FBG sensitivity greatly, therefore opening the gate for new possibilities in the field of dosimetry [14].

When actually writing with fs laser pulses with a phase mask, the distance between the lens and the mask should be at a distance where no damage is caused. To produce a clean uniform fringe pattern the fibre should be placed a certain distance from the mask. This is where only single diffraction orders can interfere. In Figures 3.10 (a) and (b) below, we can see the comparison of varied distances and the resultant fringe pattern. When too close to the mask, it requires the use of a wider beam to maintain overlap between the orders. The orders therefore only fully overlap immediately behind the mask. Further away from the mask, the pulses of the different orders cannot overlap as they are too short. The overlap occurs at a distance which has enough high intensity to write the grating, giving a clean sharp fringe pattern, as seen in Figure 3.10 (b) [13]

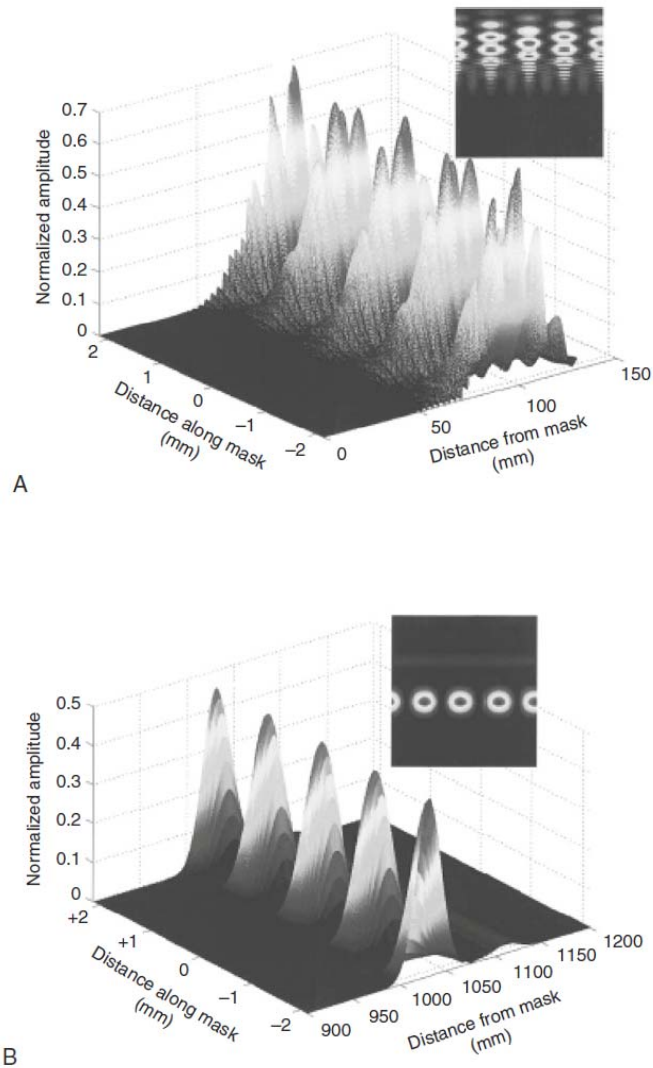


**Figure 3.10 (a) fringe pattern close to mask  
(b) further away from mask(sharp) [13].**

### 3.4.5 Radiation Induced Attenuation (RIA) of Fibres

Early work indicated that fibre optic sensors were not suited to a gamma radiation environment. High attenuation seemed to be the problem after the fibre had been exposed to ionizing radiation, especially in nuclear environments [1]. According to the Kramers-Kronig dispersion relations, an increase of attenuation is accompanied by a change of the refractive index. Since the RIA depends on the wavelength of the transmitted light, with a minimum at 1100nm, FBG's made for 650nm, 820nm, 1300nm and 1520nm were used to show a comparison of attenuation. The RIA shows a strong increase towards shorter wavelengths and moderate increase to the far infrared [9]. The wavelength of 820nm shows a distinctly higher RIA than the 1518nm wavelength, as

seen in Figure 3.11 [9]. This result is relevant to the experiment that we will conduct as we will use a light source with a centre wavelength of 1550nm.

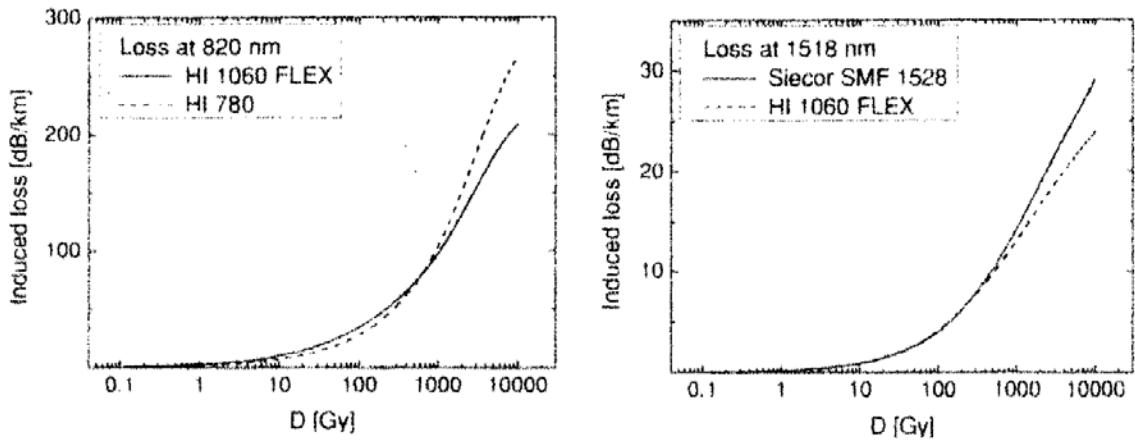


Figure 3.11 Comparison of radiation induced loss at 820nm and 1518nm [9].

### 3.4.6 Colour Center Defects ( $E'$ Centers)

When optical fibres are exposed to radiation (Gamma, Neutron or alpha particle radiation) the main three effects that occur to optical fibre are, (1) there is an increase in optical fibre absorption loss, (2) changes occur to the refractive index of the fibre and (3) optical fibre luminescence occurs [34]. A study has found that, the presence of defect centres can be reduced by pre-irradiation and thermal annealing[40]. In table 3.3 there are three groups, initial (not irradiated or annealed), irradiated at 20kGy, irradiated at 40kGy at room temperature. The irradiated samples ( by gamma rays) were annealed at different temperatures; 300C, 500C, 700C, 900C, 1100C, 1300C for one hour. Table 1 shows when the dose increases from 20 to 40 kGy the  $E'$  centre concentrations increase [40].

Table 3.3  $E'$  Concentration Increased With Dose Increase [40].

samples	initial	irradiated (20kGy)	irradiated (40kGy)
$E'$ concentrations	$1.84 \times 10^{14} \text{ cm}^{-3}$	$1.55 \times 10^{16} \text{ cm}^{-3}$	$3.55 \times 10^{16} \text{ cm}^{-3}$

A comparative study was completed using silica optical fibre showing similar results concerning  $E'$  centre concentration and thermal annealing [33]. It shows that the  $E'$  concentration of optical fibre increases with an increased dose rate, shown in figure 3.12. Samples were irradiated by gamma rays to a dose of 50kGy. The increase shows a near linear trend [33]. The effects of thermal annealing involved samples being irradiated by gamma rays to a dose of 20kGy, then annealed at different temperatures for 10 minutes respectively. When the samples cool to room temperature the  $E'$  concentration was measured by ESR (electron spin resonance and spectrophotometer). The  $E'$  concentration at 25C was  $1.55 \times 10^{16} \text{cm}^{-3}$  and decreased to  $3.45 \times 10^{14} \text{cm}^{-3}$  at 300C [33].

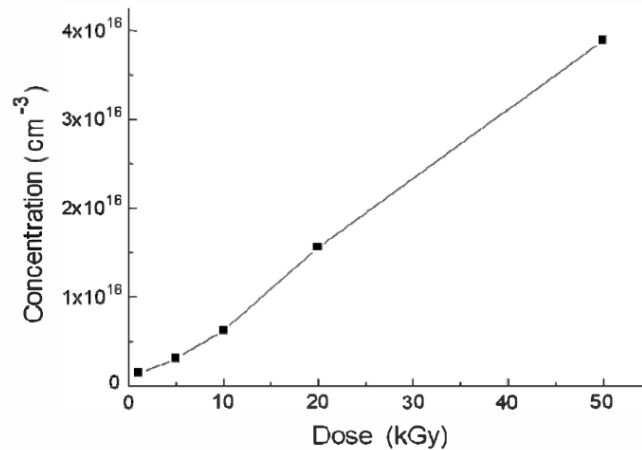


Figure 3.12 Increase of  $E'$  centre with increase of accumulated dose [33].

### 3.4.7 Latest Research and Trend

With the advances in high power fs lasers over recent years, the impact on the technology of writing gratings will be enhanced by reducing factors such as, operating costs and improving the flexibility of systems. Presently, the cost factors compared to using UV sources are high. UV sources currently are easily accessible and the technique that they use is highly controllable [13]. Femtosecond IR lasers have now been shown that they are capable of FBG inscription in non silica and silica based fibres [24]. Writing of FBG's in pure silica fibres is possible but difficult. Therefore fs (IR) lasers

has been investigated into writing FBG's in radiation hardened fibres with a pure or F(fluorine)-doped silica core without hydrogen loading [23]. The advantage of this is that a F-doped silica core produces fibre that has a low radiation induced attenuation (RIA) which therefore produces reliable strain and temperature measurements. The overall results however when compared to gratings written by UV laser show that the radiation induced wavelength in comparison with the IR laser were virtually the same. The aim was to find the method which produces FBG's that are radiation insensitive and radiation sensitive. For the radiation insensitive FBG's the radiation hardened fibres showed a BWS between 3pm-7pm after a dose of 100kGY. The FBG's made of radiation sensitive fibres did not show a higher BWS. The main observation is that the same result was obtained by FBG's written in fibre that was hydrogen loaded by a UV laser. Therefore UV laser and fs-IR lasers produce FBG's capable of measuring high radiation dose values above 100Gy but not sensitive ones for measuring low dose up to 100Gy [23]. In summary at this point in time the UV high intensity laser is the most cost effective method although restrictive, in that the fibre must be enhanced by hydrogen to achieve results. Then we have the main advantage of the fs-IR laser which is that the FBG fabrication is not limited to silica based UV photosensitive fibres [24].

### 3.4.8 New Fibre Technology

New technology has emerged in the form of Photonic Crystal fibre (PCF) also known as micro-structured fibre (MSF) or Holey fibre. The wave guiding properties of this form of optical fibre is obtained from, not varying the glass composition through doping, but from the arrangement of closely spaced tiny holes surrounding a hollow or solid core, which run through the length of the fibre as shown in Figure 3.13 and Figure 3.14.

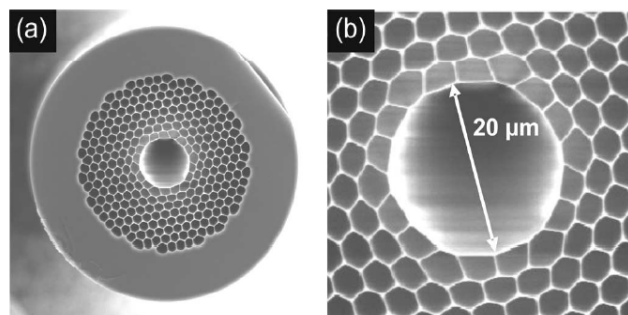
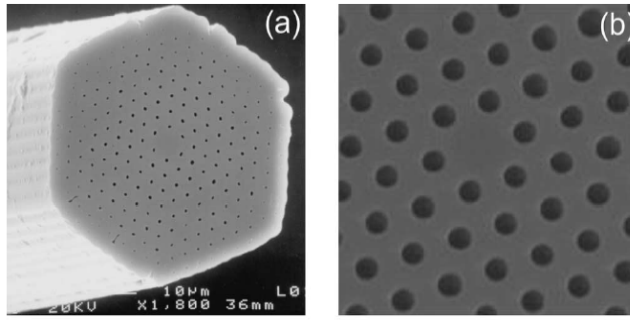


Figure 3.13 (a) Example of hollow core PCF (b) Detail of core region [41].



**Figure 3.14 (a) PCF with solid core surrounded by air channels (b) detail of low loss solid core [41].**

In normal fibre, light is contained in the core by internal reflection. To obtain a higher refractive index, doping of the fibre core is needed. The problem with doping is that it increases attenuation. However, in PCF with a solid or hollow core, results indicate that attenuation loss is feasible to be eventually lower than conventional fibre [41]. Temperature sensitivity is also a governing factor in standard optical fibre in relation to optical fibre sensors. MSFs are made of glass with a uniform composition in the entire cross section. Therefore there is no thermal stress in PCFs induced by the difference in thermal expansion coefficients between the core and the cladding [42]. This eliminates the consideration of discriminating the sensitivity to temperature from other sensitivities, when using PCFs as sensors, compared to standard fibres [42]. The studies and effects of radiation on PCFs is limited, however a new type of MSF known as a random hole optical fibre (RHOF) has been developed. In this fibre, thousands of holes that surround the pure silica core are both random in size and location. A study was completed on the effects of gamma radiation on the RHOFs and their potential use in radiation sensing [43]. The study compared the RHOF with standard SMF(single mode) and MMF(multi mode) and pure silica fibre(PSC). Measurements were taken of the radiation induced absorption (RIA) centred at 1550nm. Under a high intensity gamma ray field ( $4 \times 10^4$  rad/hr). The RIA of the RHOF is much lower than the standard fibres as shown in Figure 3.15. RIA of the fibres for the total duration of the experiment is shown in Figure 3.16 It shows the fibre behaviour under irradiation and post irradiation. The results indicate that the RHOF have a superior recovery time compared to the other fibres tested [43]. The mechanism for this is not fully understood. The negative RIA represents an improvement in the transmission of the optical signal [43].

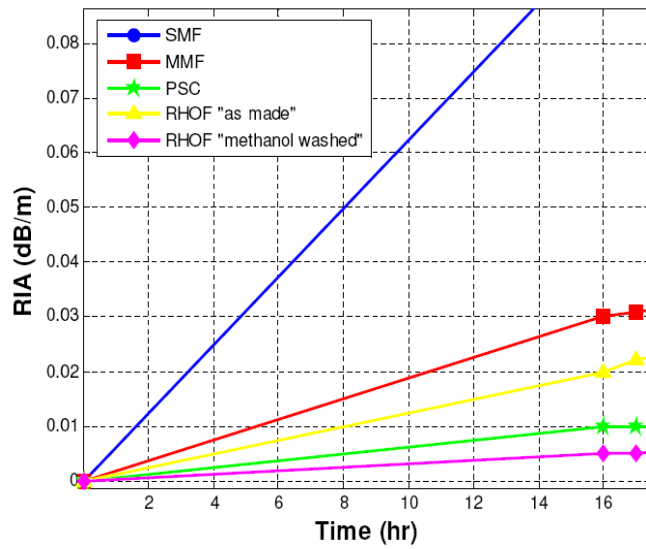


Figure 3.15 RIA of the fibres for first 16 hours of irradiation. RHO is much lower than standard SMF and MMF [43].

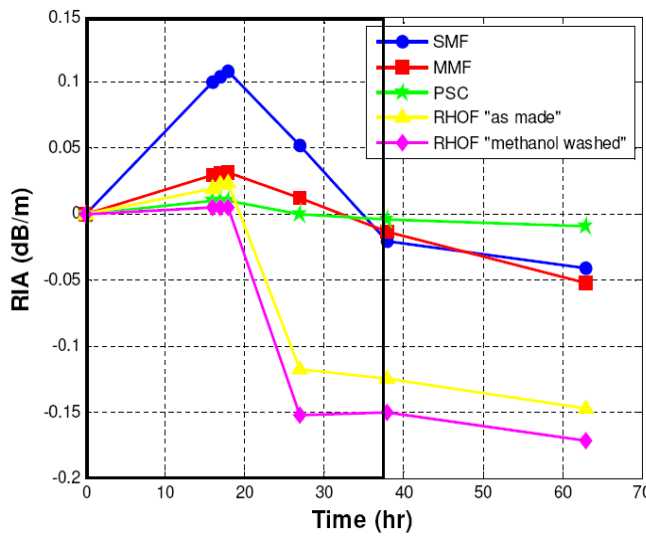


Figure 3.16 RIA of sample fibres for total duration showing behaviour under and post irradiation recovery time [43].

## CHAPTER 4

### RESEARCH METHODS

This chapter highlights the sample set, the irradiation set up at ANSTO, and the equipment that was used for the collection and analysis of data, throughout the four main stages. The stages include; (1) First irradiation, (2) First relaxation, (3) Second irradiation, and (4) Second relaxation.

#### 4.1 FBG Samples

The FBGs were purchased through Alxenses Company Limited (Hongkong). A total of nine FBGs were used. Three of each were manufactured in standard single mode optical fibre with (a) Germanium doping plus Hydrogen loading, (b) Germanium only, and (c) standard SMF-28 optical fibre with Hydrogen loading. Each group of three single FBGs had centre wavelengths of 1545nm, 1550nm and 1555nm for spectral separation. Each FBG had a reflectivity of  $> 90\%$ . The length of each FBG was 10mm with a bandwidth @-3dB:  $< 0.3$  nm. The hydrogen loading for each fibre was completed at 100bar for seven days. When we tried to find the exact germanium content from the manufacturer, we were given an approximation only, which stated that the Ge content was probably in the medium to high range of 18-21 mol.%. We had hoped to perform a composition analysis of the Ge content in the optical fibre through the ICP standard, however due to time restrictions we were unable to complete. The centre wavelength tolerances for each FBG were given as  $\pm 0.5$ nm. The total fibre length for each sample was 30cm, with the FBG centrally located. All the results were extracted from FBGs written by low-energy UV irradiation.

The sample numbers of the FBGs are:

- Ge-doped optical fibre (with hydrogen loading), samples 1, 2 & 3.
- Ge-doped optical fibre (without hydrogen loading), samples 4, 5 & 6.
- Standard SMF-28 optical fibre (with hydrogen loading), samples 8, 9 & 10.

## 4.2 Gamma Irradiation Facility

The experiment was conducted at the Australian Nuclear Science and Technology Organisation (ANSTO), using the GATRI gamma irradiation facility under the AINSE Research Award ALNGRA12029P for 2012. The experiment continues on from a previous study by ECU which included 3 days of irradiation to a total dose of less than 86kGy on FBGs in standard SMF-28 optical fibre. The results on that occasion were unable to establish a definite trend and were inconsistent, due to the experimental method. Measurements were performed at a dose rate of 2.2 kGy/hr up to an absolute dose of 86kGy. A copy of the research paper is attached in the Appendix(1). On this occasion, we used the GATRI gamma irradiation wet storage cobalt-60 facility, as shown in Figure 4.1, over a period of 6 days. The dose rate of approx. 4.0 kGy/hr was set for the initial irradiation and post irradiation stages.



Figure 4.1 GATRI's cobalt-60 radioactive source [28].

## 4.3 Optical Measurements

Optical measurements were performed, to determine the shift of the Bragg wavelength as a function of accumulated dose and relaxation time, compared to the base non-irradiated Bragg wavelength. The four stages of the experiment from which we

obtained data included; 1) Initial irradiation, 2) Initial relaxation, 3) Second irradiation 4) Second relaxation. The total accumulated dose of 206.8 kGy was reached after 51.3hrs for stage (1). The accumulated dose for stage (3) reached 196.4kGy after 48.7 hrs. Overall, the FBGs were subjected to 403.2kGy over a period of 100hrs. The relaxation period for stage (2) was 22hrs, whilst for stage (4) it was 20hrs. In summary, the irradiation periods equated to approximately 2 full days for each of stages (1) and (3), whilst the relaxation periods for both stages (2) and (4) equated to approximately 1 day each. Also, the similarity of each stage of the experiment gave us continuity, which enabled us to compare results.

A superluminescent light emitting diode (SLD) (Dense Light DL-BZ1-SC5403A) was used as the light source with a centre wavelength of 1550nm, bandwidth of 100nm, and 25mW optical power. The reflective spectrum as a function of wavelength was measured using an Optical Spectrum Analyser (Agilent 86142B) shown in Figure 4.3. We used the reflective spectra to determine the Bragg wavelength shift as a function of accumulated dose/time and as a function of post irradiation relaxation time. We used three lines each containing three single FBGs in series, all connected using FC/APC connectors. Each line consisted of a sample of each type of optical fibre i.e. Ge+H, Ge and SMF-28 fibre, as shown in Table 4.1.

**Table 4.1 Three lines of FBGs used showing series sequence.**

<b>LINE</b>	<b>SAMPLE POSITION</b>	<b>FBG TYPE</b>	<b>SAMPLE NO.</b>	<b><math>\lambda_B</math></b>
<b>ONE</b>	<b>1</b>	<b>SMF-28</b>	<b>Sample 8</b>	<b>1545nm</b>
	<b>2</b>	<b>Ge + H</b>	<b>Sample 2</b>	<b>1550nm</b>
	<b>3</b>	<b>Ge</b>	<b>Sample 6</b>	<b>1555nm</b>
<b>TWO</b>	<b>1</b>	<b>Ge</b>	<b>Sample 4</b>	<b>1545nm</b>
	<b>2</b>	<b>SMF-28</b>	<b>Sample 9</b>	<b>1550nm</b>
	<b>3</b>	<b>Ge + H</b>	<b>Sample 3</b>	<b>1555nm</b>
<b>THREE</b>	<b>1</b>	<b>Ge +H</b>	<b>Sample 1</b>	<b>1545nm</b>
	<b>2</b>	<b>Ge</b>	<b>Sample 5</b>	<b>1550nm</b>
	<b>3</b>	<b>SMF-28</b>	<b>Sample 10</b>	<b>1555nm</b>

All three lines were set up in the GATRI chamber, attached to and set in position in a polystyrene box, as shown in Figure 4.2.

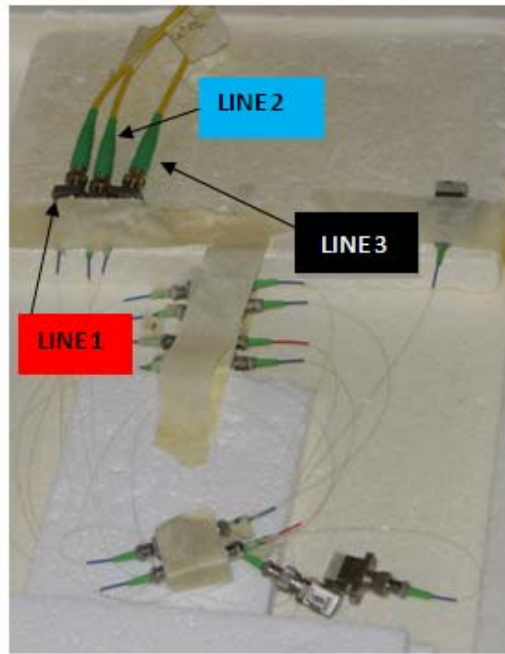


**Figure 4.2 Photograph of the three FBG lines arranged in the polystyrene box.**

The lines were attached to patch cables that were threaded through an access port in the irradiation facility shield. Each cable connector was attached one at a time to the Optical Spectrum Analyser (OSA) via the circulator to establish a baseline (no irradiation). Once the baseline was measured and recorded, the irradiation process commenced. During the irradiation process, at regular time intervals, measurements from each of the three lines were taken. The time periods between measurements were 2 hours through the daylight hours (7.30am to 7.30pm) and every three hours during the night (10.30pm to 7.30am). On average over a 24 hour period, one measurement of each line was taken every 2.5 hours. The measurements continued from the three lines for the allocated two day period or when the 200kGy accumulated dose had been achieved. After the initial irradiation finished, the first relaxation period began. Measurements again were taken every 2 hours daily and every 3 hours nightly. This was performed for 22 hours until no further relaxation occurred, i.e. until the shift in the Bragg wavelength was negligible. The irradiation process commenced again, and the whole process was

repeated. Each line was manually attached to the circulator individually for measurements.

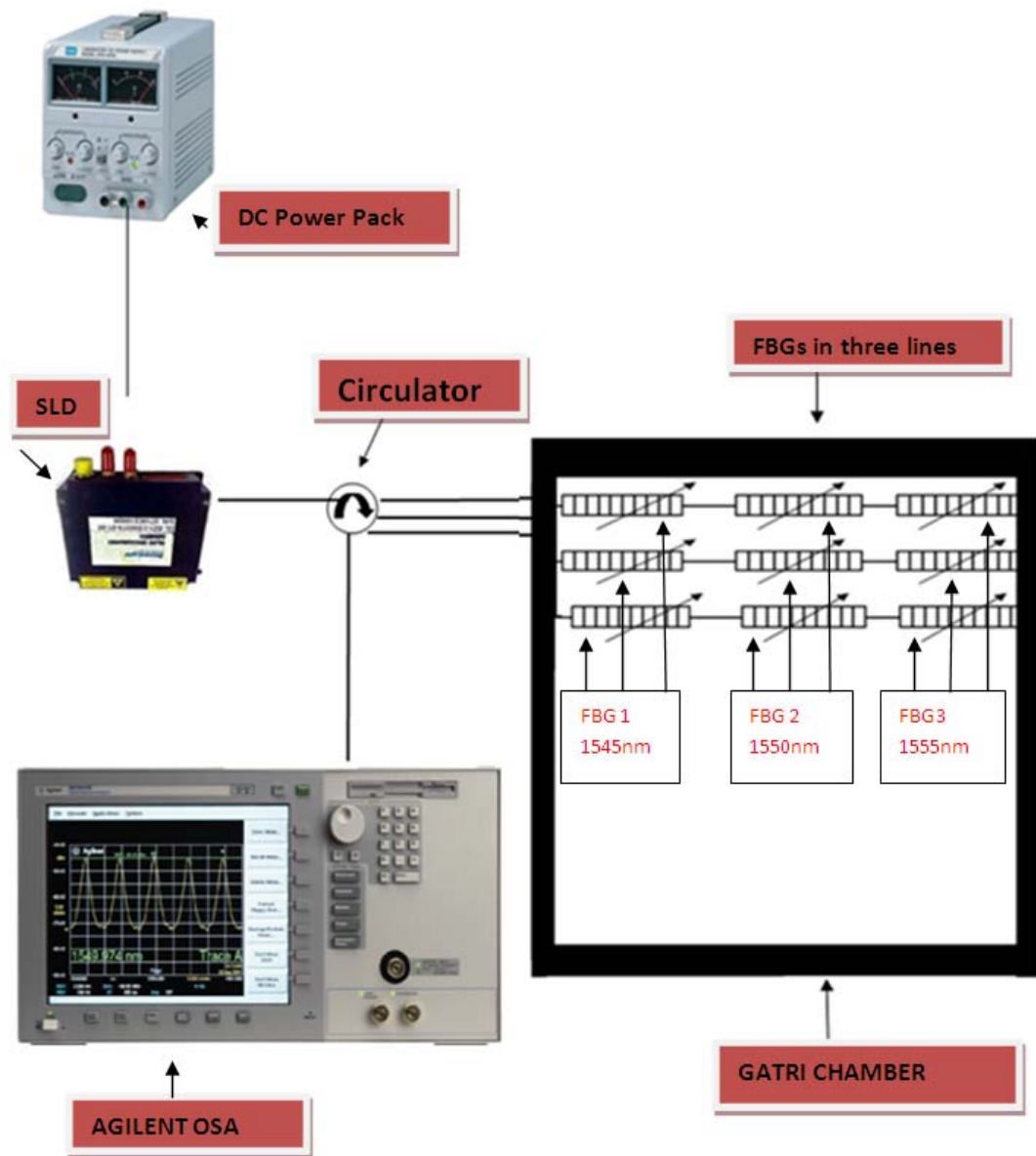


**Figure 4.3** Experimental equipment set up for the optical measurements.

Measurements were performed at a temperature range of 21.5C to 23.7C. The dosimeter type used was Ceric Cerous, which were calibrated in a cobalt-60 radiation field, in which the dose rate was determined from reference dosimeter measurements made under similar conditions. The overall uncertainty associated with an individual dosimeter reading includes both the uncertainty of calibration of the batch of

dosimeters, and the uncertainty due to variation within the batch, and was calculated to be 3.5%. This expanded uncertainty is based on the standard uncertainty multiplied by a coverage factor of two, providing a level of confidence of approximately 95%.

#### **4.4 Gamma Irradiation Protocol**

The data collection was conducted on site inside the GATRI facility. Measurements were performed in the presence of a ANSTO staff member both during daylight hours and at night. For safety and security, two persons had to be present at all times when entering the GATRI facility. Measurement or stop date times were recorded by the ANSTO staff. The exposure period and relative dose were also recorded. The accumulated dose was also noted when a measurement was taken. When the facility was stopped, either for relaxation purposes or for repair, total times were recorded. My hand written records maintained the same format for continuity. My data collection matched the completed printout summary from ANSTO.

There were four periods when the radiation source was lowered. Two were unscheduled due to maintenance and repair whilst two were when the relaxation stages were about to begin. These can be seen in Table 4.2.

On the 28/11/2012 at 11.46am, with an accumulated dose of 111.3 kGy, irradiation stopped, due to a loss in signal from Line3. We lost two of the three peaks. After a period of 0.8 hours we were able to rectify the problem and continue recording as shown in the JPEG images of Line3 in Figure 4.4. The images show that there was a slight problem in Line3, even in the early stages of irradiation at the 16 hour stage. FBG 1 and 2 have lower outputs than FBG 3. Eventually, at the 27 hour mark, we lost the FBG 1 and 2 peaks. When the irradiation source was lowered it was discovered that the tape holding Line3 in position had begun to melt and had become loose. Line3 had to be re-positioned, and the old tape removed and replaced. This eventually seemed to help with the eventual appearance of the two missing peaks, as shown in Figure 4.4 in the 28 hour image, albeit with a lower output compared to the original. For the remainder of the experiment, FBG 1 and FBG 2 were displaying weaker outputs, which was a factor when analysing the data.

**Table 4.2. Measurements schedule from ANSTO Irradiation report.****Results**

Measurement or stop date/time	Exposure period (h)	Dose (kGy)	Accumulated dose (kGy)	Comments
27/11/2012 09:32	2.000	8.1	8.1	first measurement
27/11/2012 10:19	0.783	3.2	11.2	irradiation stop for 37 min
27/11/2012 11:38	0.700	2.8	14.0	measurement
27/11/2012 13:30	1.867	7.5	21.6	measurement
27/11/2012 15:30	2.000	8.1	29.6	measurement
27/11/2012 17:35	2.083	8.4	38.0	measurement
27/11/2012 19:40	2.083	8.4	46.4	measurement
27/11/2012 22:29	2.817	11.4	57.8	measurement
28/11/2012 01:27	2.967	12.0	69.8	measurement
28/11/2012 04:22	2.917	11.8	81.5	measurement
28/11/2012 07:31	3.150	12.7	94.2	measurement
28/11/2012 09:37	2.100	8.5	102.7	measurement
28/11/2012 11:46	2.150	8.7	111.3	measurement
28/11/2012 11:54	0.133	0.5	111.9	irradiation stop for 51 min No. 3 cable has only one peak
28/11/2012 13:30	0.750	3.0	114.9	measurement
28/11/2012 15:34	2.067	8.3	123.2	measurement
28/11/2012 17:36	2.033	8.2	131.4	measurement
28/11/2012 19:30	1.900	7.7	139.1	measurement
28/11/2012 22:24	2.900	11.7	150.8	measurement
29/11/2012 01:24	3.000	12.1	162.9	measurement
29/11/2012 04:22	2.967	12.0	174.8	measurement
29/11/2012 07:33	3.183	12.8	187.7	measurement
29/11/2012 09:39	2.100	8.5	196.1	measurement
29/11/2012 11:34	1.917	7.7	203.8	measurement
29/11/2012 12:18	0.733	3.0	206.8	irradiation stopped for relaxation
30/11/2012 13:30	3.000	12.1	218.9	measurement
30/11/2012 15:32	2.033	8.2	227.1	measurement
30/11/2012 17:29	1.950	7.9	234.9	measurement
30/11/2012 19:25	1.933	7.8	242.7	measurement
30/11/2012 22:17	2.867	11.5	254.3	measurement
1/12/2012 01:30	3.217	13.0	267.2	measurement
1/12/2012 07:30	6.000	24.2	291.4	measurement
1/12/2012 10:30	3.000	12.1	303.5	measurement
1/12/2012 13:27	2.950	11.9	315.3	measurement
1/12/2012 16:26	2.983	12.0	327.4	measurement
1/12/2012 19:25	2.983	12.0	339.4	measurement
1/12/2012 22:27	3.033	12.2	351.6	measurement
2/12/2012 01:19	2.867	11.5	363.1	measurement
2/12/2012 07:21	6.033	24.3	387.4	measurement
2/12/2012 10:38	3.283	13.2	400.6	measurement
2/12/2012 11:17	0.650	2.6	403.2	irradiation stopped for relaxation
3/12/2012 07:21	-	-	403.2	completed relaxation

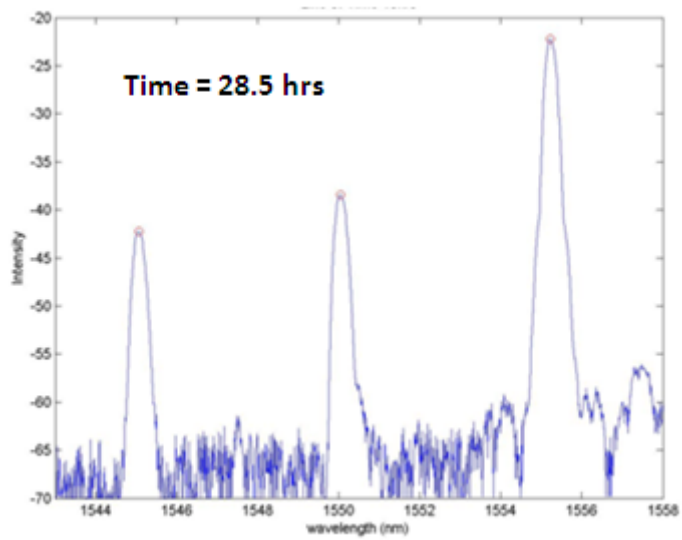
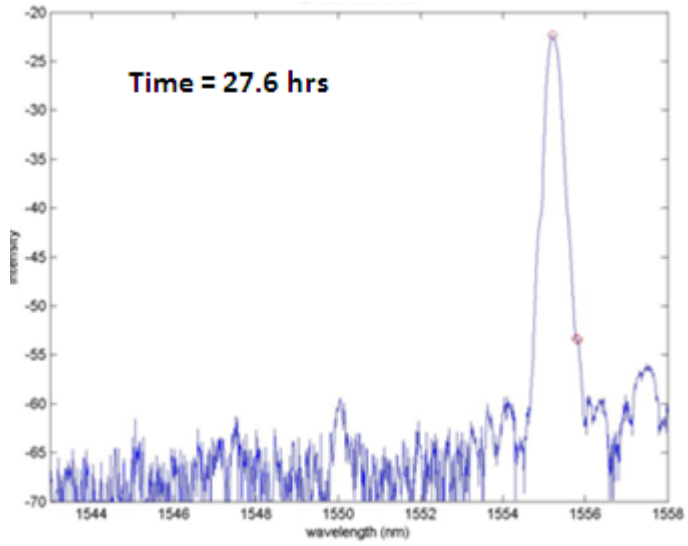
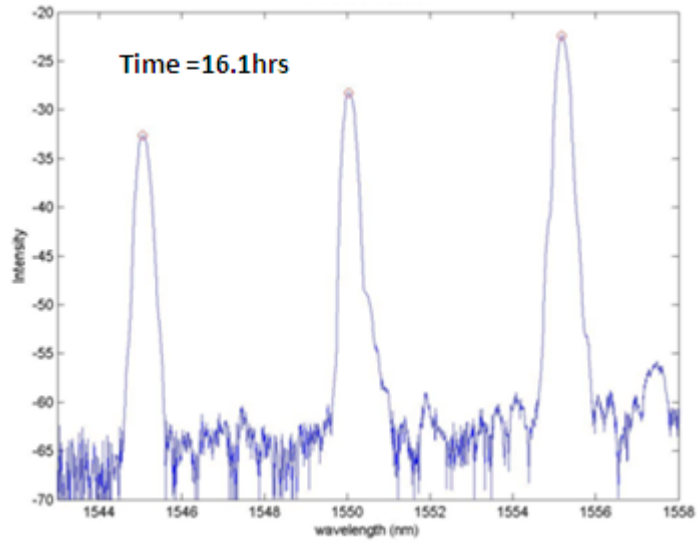


Figure 4.4 Series of images showing loss and eventual recovery of the three peaks in Line3.

## 4.5 Data Analysis

To analyse the data, files had to be converted from DAT files to EXCEL files, as we had recorded the data from the OSA on to a floppy disk. Once the data had been converted, we had to insert the floppy back into the OSA to make a separate readable file, e.g. the three DAT files at the measurement time of 11.38am on 27/11/12 were originally ST00009, ST00010 and ST00011, representing Lines 1, 2 and 3 respectively. The new converted file was entered into the OSA and then re-recorded back as an Excel file with the new prefix of TR00006, TR00007, TR00008. We had to be careful, as you can see they don't quite match numerically. This is due to the fact that the ST files had started ST00000, ST00001, ST00002 the previous day while we were testing the OSA. The actual recording of irradiation started at ST00003, ST00004, ST00005. Thus, the TR files were TR00000, TR00001, TR00002 for the first set of data. Therefore, there is a slight lag effect in the TR files. The process was time consuming, and one had to concentrate when transferring each individual file. Some of the zero points and outlier data points in the graphs may be due to human error in the manual transference.

To show the BWS as a function of accumulated dose, we used a search algorithm. The uncertainty of the mean value of the BWS for the first irradiation period is found by the range/ $n$  method [45]. Range represents lowest BWS to the Highest BWS, where ( $n$ ) is the number of measurements to reach 206.8 kGy, which equated to an uncertainty of 6.3pm for Line1, 7.0pm uncertainty for Line2 and 7.25 pm for Line3. The value of each BWS uncertainty for the three lines averaged 7pm. In combination with the uncertainty of the OSA, which is 0.01nm or 10pm for the specified wavelength range between 1480 to 1570nm, the total uncertainty was 12.2pm. For the second irradiation period, the overall uncertainty for the each BWS reduced to 5.4 pm, due to the reduced number of measurements to achieve the 196.4kGy dose level. This led to an overall uncertainty in combination with the OSA of 11.1pm. The OSA uncertainties were extracted from the Agilent 8641xB Optical Spectrum Analyser user's guide.

## CHAPTER 5

### RESULTS

This chapter gives an overview of the results from all four stages of the experiment. It shows the Bragg wavelength shift in relation to the accumulated dose during the first irradiation and second irradiation stages. The effects of relaxation on the Bragg wavelength are also highlighted after each irradiation stage. Any changes of the peak amplitude and change of FWHM both before and after each irradiation are also recorded.

#### 5.1 First Irradiation Period.

Results shown in Table 5.1 indicate Bragg Wavelength Shifts (BWS) consistent with the fabricating methods used. The only inconsistent measurement is the 90pm shift in Line 1 for the Ge+H fibre (1550nm). This could be due to outgassing of the hydrogen or an error when converting data from DAT files to Excel files. The overall average shift by the 9 FBGs is 151.6 pm. With hydrogen loading plus germanium doping the peak shift should be significantly higher. The average BWS for the Ge fibre over the 3 lines is 155pm. The average BWS for the SMF28+H fibre was 165pm, whilst the average for the Ge+H was 135pm.

**Table 5.1 Bragg wavelength peak shift, accumulated dose of 206.8 kGy**

<b>Line</b>	<b>Fibre Type</b>	<b>Base Wavelength(nm)</b>	<b>Final Wavelength(nm)</b>	<b>Bragg Peak Shift (pm)</b>
<b>1</b>	SMF28+H	1545.220	1545.370	<b>150±12</b>
<b>2</b>	SMF28+H	1549.765	1549.915	<b>150±12</b>
<b>3</b>	SMF28+H	1555.060	1555.255	<b>195±12</b>
<b>1</b>	Ge + H	1550.020	1550.110	<b>90±12</b>
<b>2</b>	Ge + H	1554.805	1554.955	<b>150±12</b>
<b>3</b>	Ge + H	1544.950	1545.115	<b>165±12</b>
<b>1</b>	Ge	1555.030	1555.210	<b>180±12</b>
<b>2</b>	Ge	1544.755	1544.920	<b>165±12</b>
<b>3</b>	Ge	1549.960	1550.080	<b>120±12</b>

## 5.2 Second Irradiation Period.

The overall average BWS for the initial irradiation for the 9 samples amounted to 151.6 pm, whilst after the second irradiation or pre-irradiation shown in Table 5.2 was completed, the BWS reduced to an average of 88.3 pm. These results are consistent with previous studies [26], which indicated that pre-irradiation of the FBGs results in a reduced BWS due to radiation hardening. The data also confirms that gratings written in fibre using medium to high Ge content and Hydrogen loading can increase the radiation sensitivity overall [27]. The lowest BWS of 60pm was obtained for the grating written in Ge-doped fibre without Hydrogen loading after the second irradiation period, which indicates that pre-irradiation may be a prospect for producing radiation hard FBG sensors. An overall perspective of the BWS after the first and second irradiation periods for Lines 1 and 2 are shown in Figures 5.1(a), 5.1(b), 5.2, 5.3, and 5.4. The differences in the shift can be seen clearly in Figure 5.1(b).

**Table 5.2 Bragg wavelength shift, for an additional dose of 196.4 kGy(total 403.2 kGy)**

<b>Line</b>	<b>Fibre Type</b>	<b>Initial Wavelength(nm)</b>	<b>Final Wavelength(nm)</b>	<b>Bragg Peak Shift (pm)</b>
<b>1</b>	SMF28+H	1545.340	1545.430	<b>90±11</b>
<b>2</b>	SMF28+H	1549.885	1549.975	<b>90±11</b>
<b>3</b>	SMF28+H	1555.210	1555.345	<b>135±11</b>
<b>1</b>	Ge + H	1550.080	1550.155	<b>75±11</b>
<b>2</b>	Ge + H	1554.940	1555.015	<b>75±11</b>
<b>3</b>	Ge + H	1545.070	1545.175	<b>105±11</b>
<b>1</b>	Ge	1555.180	1555.255	<b>75±11</b>
<b>2</b>	Ge	1544.890	1544.980	<b>90±11</b>
<b>3</b>	Ge	1550.050	1550.110	<b>60±11</b>

As mentioned in the literature review, the affects of irradiation on FBGs in fibre, loaded with hydrogen at different pressures, have been studied [29]. The most common pressures are 100bar, 200bar and 300bar. Our results for the second irradiation period indicate, FBGs written in fibre loaded with hydrogen at 100bar, seem to show a slight difference in the average BWS, compared with the Ge-doped only fibre. This could be due to the 100bar loading.

Although the BWS has reduced significantly for the second stage, the average of the Ge only fibre (75pm) is less than the Ge+H (85pm) and SMF+H (105pm). The increased sensitivity with the 100bar hydrogen loading may be the cause of the slight increase in the BWS, even with the effects of pre-irradiation at play. As studies have shown [29], FBGs written in fibre with hydrogen loading at 300bar lead to a 14% increase in radiation sensitivity, making them strong candidates to be used for radiation dosimetry. Even with the reduced loading of 100bar, our results do show there is an increased sensitivity, which is in keeping with previous studies [29].

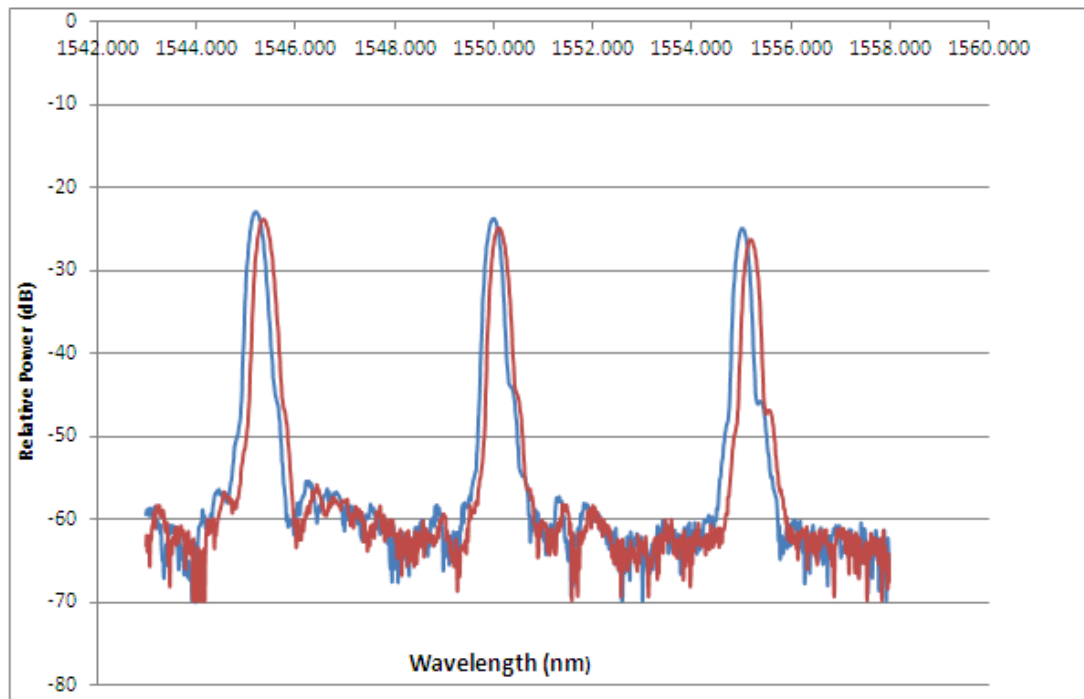


**Figure 5.1(a) First complete irradiation period for Line1 showing Bragg peak shifts at: 1545nm(SMF28+ H), 1550nm(Ge+H), 1555nm (Ge). Blue peaks are initial peaks, whilst the red peaks are the final peak shift.**

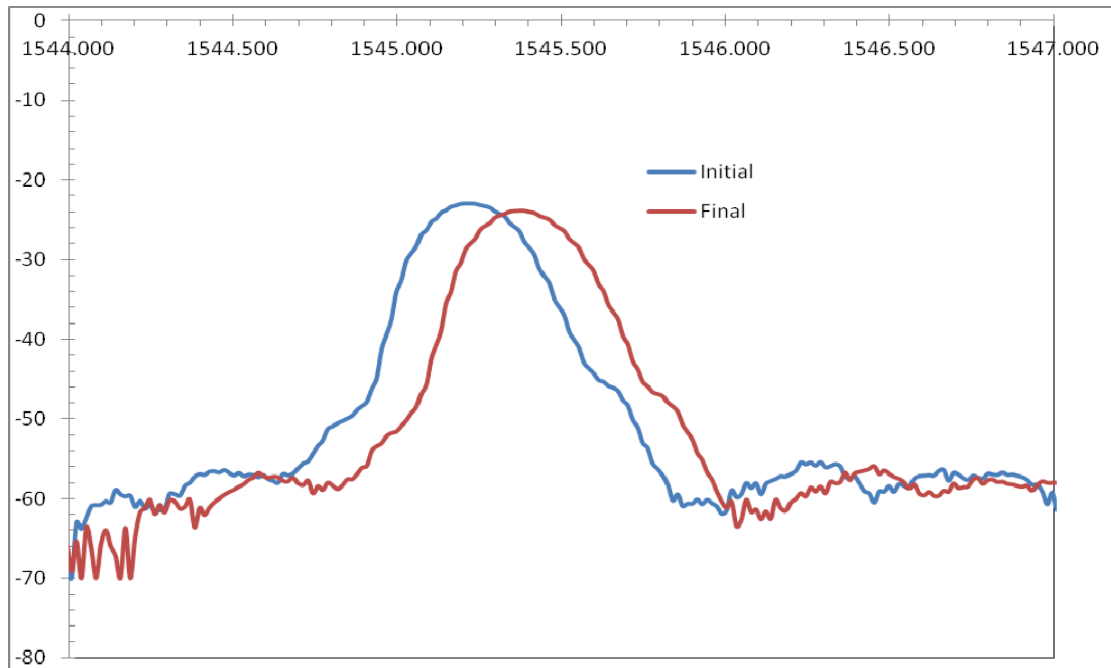


**Figure 5.1(b) Expanded graph highlighting BWS of SMF28+H (1545nm)**

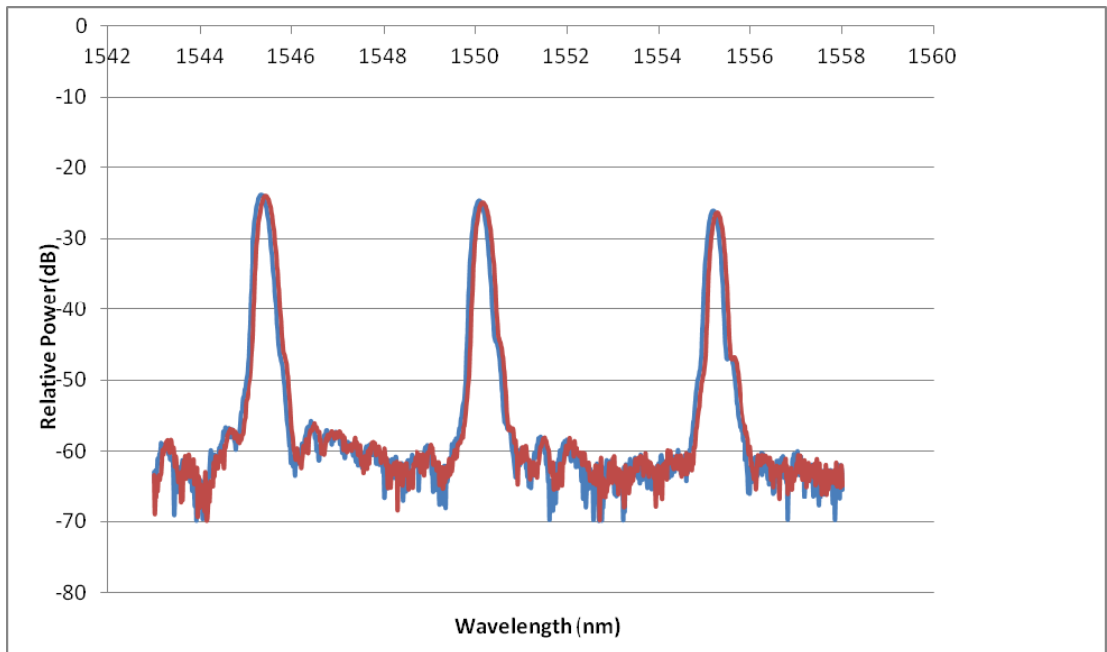


**Figure 5.2 Second complete irradiation period for Line 1, showing reduction in Bragg wavelength peak.**

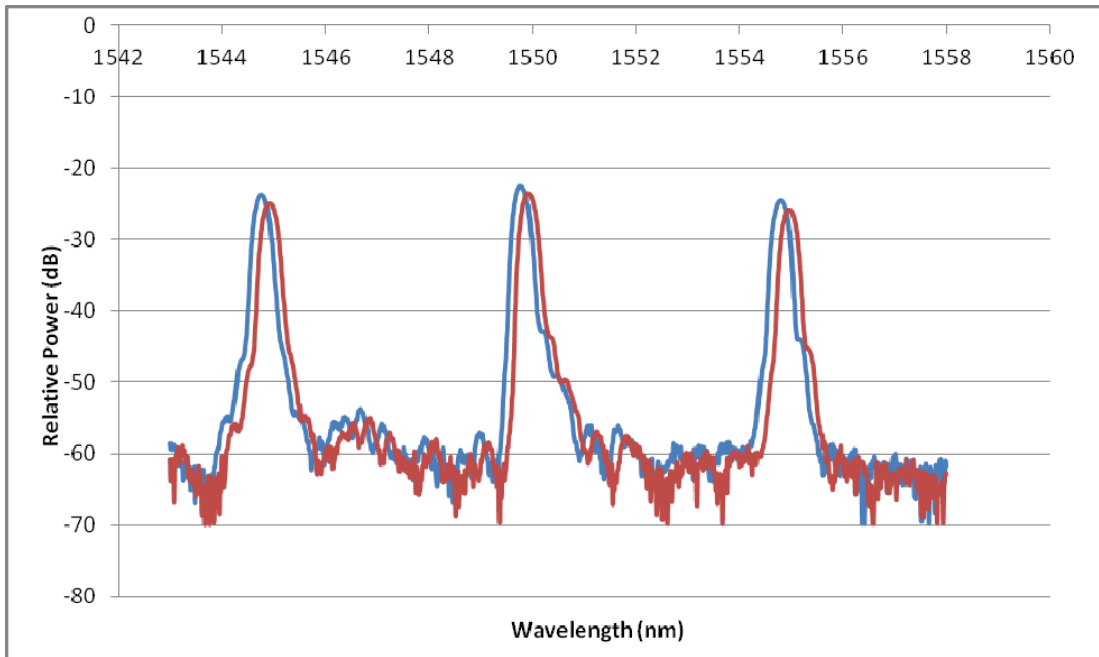


**Figure 5.3 First complete irradiation period for Line 2, showing Bragg peak shifts for 1545nm(Ge), 1550nm(SMG28+H), and 1555(Ge+H).**

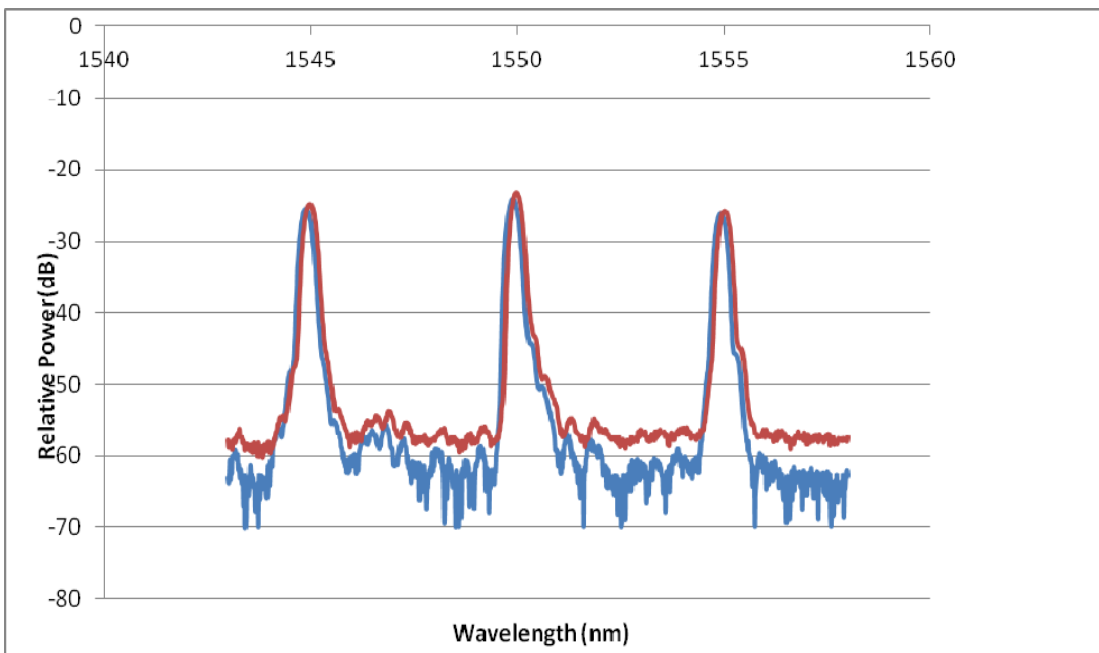


**Figure 5.4 Second complete irradiation for Line2, showing reduction in the Bragg peak shift.**

The performance of an individual sample (FBG) in Lines 1 and 2, as a function of accumulated dose in both the initial irradiation and second irradiation stages, are shown in Figures 5.5, 5.6, 5.7 and 5.8.

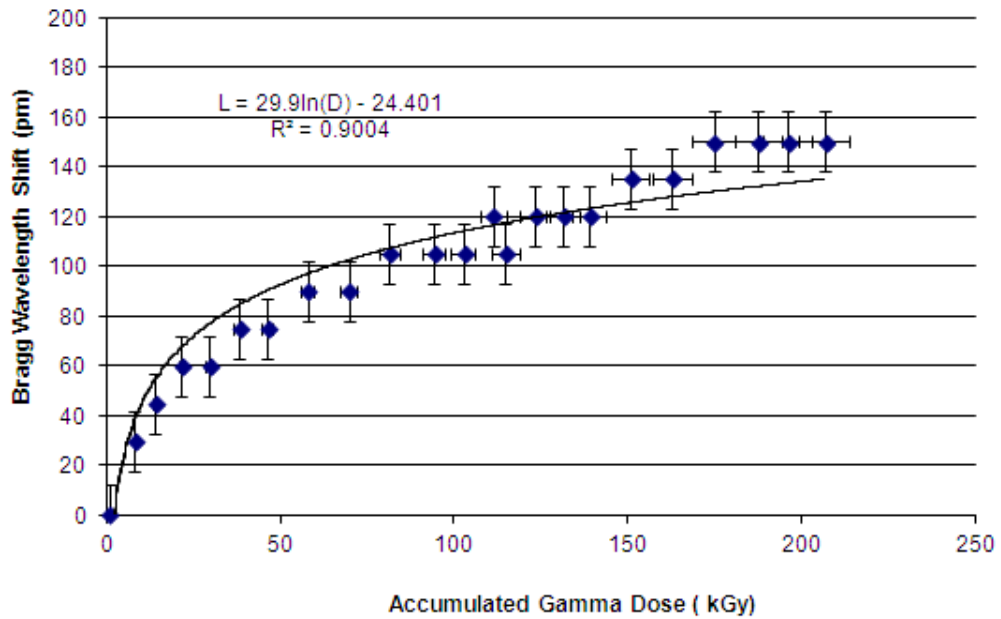


**Figure 5.5 BWS of Line 1 FBG (SMF 28+ H; 1545nm) after the first complete irradiation period, for an accumulated dose of 206.8 kGy.**

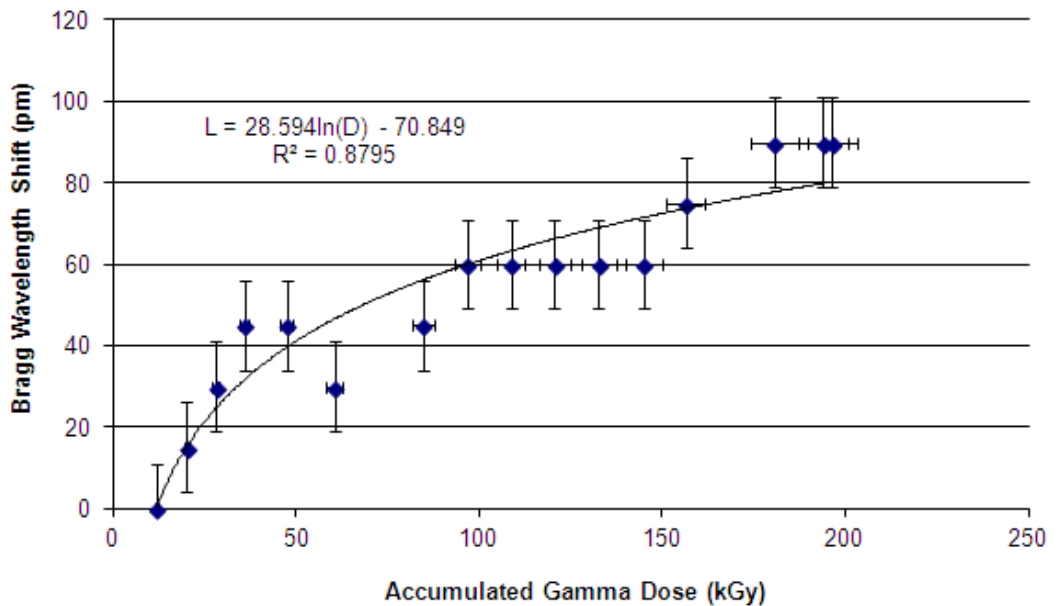


**Figure 5.6 BWS of Line 1 FBG (SMF28+H; 1545 nm) after the second irradiation period, for an accumulated dose of 196.4 kGy.**

The same trend is observed as with the overall BWS. For the first irradiation period, there is a continued increase in the BWS for the first 100 kGy, confirming

radiation sensitivity. Saturation is not observed up to 100kGy, which shows that FBGs with higher wavelengths (>1520nm) are good candidates for high dose sensing [9]. In Line 1 after the second irradiation, the BWS at 100kGy is 60pm compared to 105pm in the first period. Saturation, although not completely observed, may be beginning to commence at the 180kGy dose for both periods, with the second irradiation period saturating at a lower Bragg peak. Both sets of data indicate a logarithmic trend, although the fits of the data points are not ideal ( $R^2 < 0.95$ ) they nevertheless represent a relatively good fit. For the FBG (Ge+H) sample in Line 2, as shown in Figures 5.7 and 5.8, the results are similar for the first period with the BWS at 100kGy being 120pm. The second irradiation period is lower, 30pm at 100kGy. This is significantly lower than the 60pm shift at 100kGy for Line 1 in the second irradiation period.

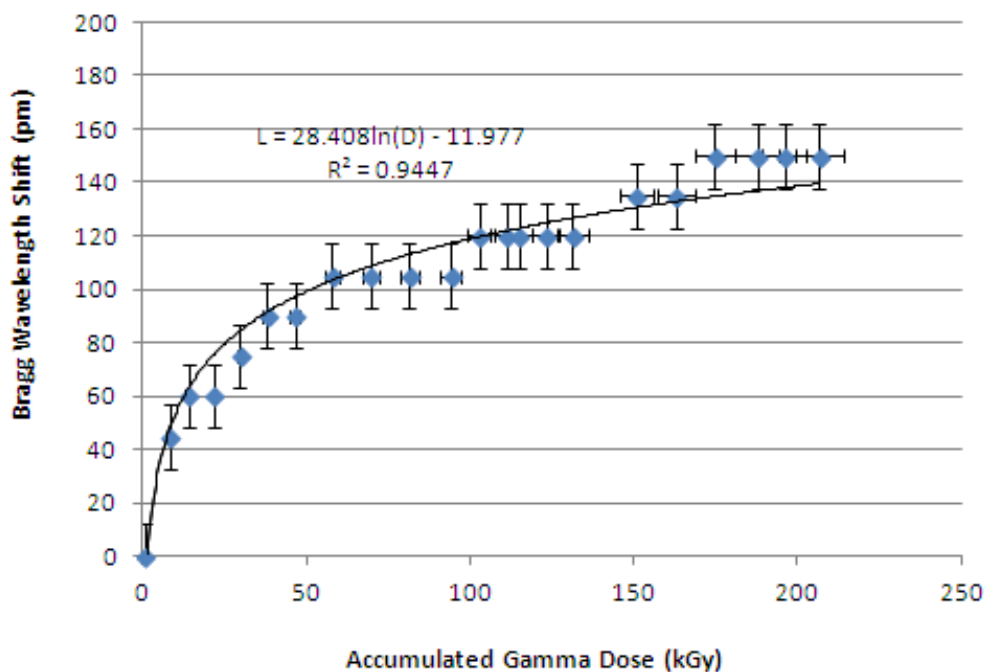


**Figure 5.7. BWS of Line 2 FBG (Ge+H; 1555nm) after the first complete irradiation period.**

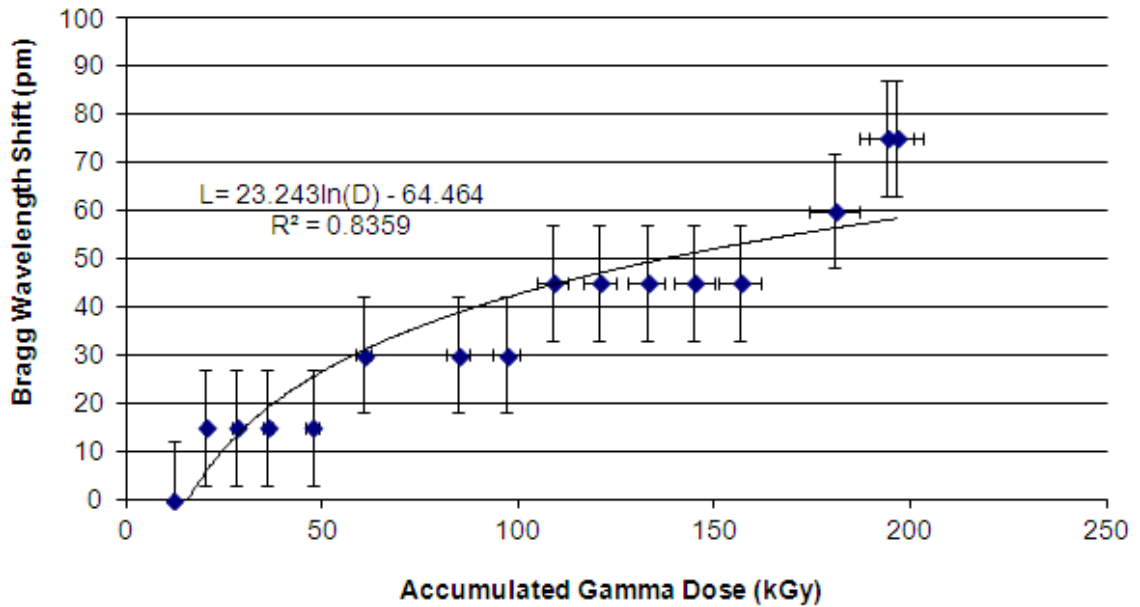


**Figure 5.8. BWS of Line 2 FBG (Ge+H; 1555nm) after the second irradiation period.**

Logarithmic trend lines are good for data that rises quickly and then starts to level off. During the first irradiation period on both graphs, there is a rapid increase up to the first 100kGy of gamma dose. Both graphs indicate a 100pm BWS. Beyond the 100kGy dose there is a slowing or leveling off effect in both graphs. When comparing with the second irradiation dose, the BWS does not rise as rapidly. There is a gradual rise to the 100kGy mark with a reduction or slowing of the BWS. This also coincides with the reduction of the correlation coefficient  $R^2$  values for the second irradiation period. There is, however a relationship between the variables. The stabilizing effect of pre-irradiation seems to be highlighted by these results. All the graphs during the first and second irradiation stages have  $R^2$  values between 0.80 and 1.00. Figures 5.5 and 5.7 indicate higher  $R^2$  values representing relatively good fits, rather than the lower  $R^2$  values in Figures 5.6 and 5.8. The resolution of measurements in Figure 5.8, with the smallest  $R^2$  value of 0.8359, are not high enough to precisely plot the relationship between the change in Bragg wavelength and accumulated dose. Hence, future measurements would need to be performed at a higher wavelength resolution. This would require the use of a higher resolution OSA, as the uncertainty of the wavelength is 10pm, which is the largest source of uncertainty.

### 5.3 Effects of Relaxation

After the completion of each irradiation period, when the GATRI cobalt-60 source was lowered, data was recorded to examine the effects on the Bragg wavelength as a function of time compared to the Bragg wavelength recorded at the end of each irradiation period. This was to see if there was any movement back in the direction of the original base wavelength (i.e. relaxation). In all cases, there was a shift back towards the base wavelength, as shown in Tables 5.3 and 5.4. Good results are shown for the Ge-doped only fibre during the first relaxation period. All achieved a 30pm drop, back towards the original base wavelength. The consistency may be due to the high Ge-only content. This is in keeping with established data, which states that, gratings written in a high Ge doped fibre are more stable [44], thus giving similar results. Even in after the second relaxation period, two out of the three FBGs shifted 30pm back towards the original for the Ge only fibre.

The results show that there is little difference in the relaxation shift between the first and second irradiation, although pre-irradiation and subsequent radiation hardening may affect the fibre types differently. Although the results indicate small shifts, there is a trend back towards the original value. The only factor that I would change in future experiments would be to increase relaxation time to 48-72hrs. The average shift for the Ge+H fibre is 30pm for the first relaxation, and 35pm for the second relaxation period. The average for the SMF28+H is 25pm for the first relaxation, and 30pm for the second relaxation. For the Ge fibre the average is 30pm for the first relaxation and 25pm for the second relaxation. These results show that there is a slight difference in the Hydrogen loaded fibre compared to the non hydrogen loaded Ge fibre. With Hydrogen loading, the shift in wavelength back towards the original value is greater on average, compared to the germanium only doped fibre, during the second relaxation period. This is due to the increased sensitivity from hydrogen and radiation hardening from pre-irradiation.

**Table 5.3 Bragg wavelength shift for the first relaxation after 22hrs and dose of 206.8 kGy.**

<b>Line</b>	<b>Fibre Type</b>	<b>Base Bragg Wavelength(nm)</b>	<b>Bragg Wavelength(nm) After 206.8kGy</b>	<b>Bragg Wavelength(nm) After 22hrs. Relaxation</b>	<b>Relaxation Shift <math>\Delta\lambda_B</math> (pm)</b>
<b>1</b>	SMF28	1545.220	1545.370	1545.355	<b>15</b>
<b>2</b>	SMF28	1549.765	1549.915	1549.900	<b>15</b>
<b>3</b>	SMF28	1555.060	1555.255	1555.210	<b>45</b>
<b>1</b>	Ge+H	1550.020	1550.110	1550.095	<b>15</b>
<b>2</b>	Ge+H	1554.805	1554.955	1554.925	<b>30</b>
<b>3</b>	Ge+H	1544.950	1545.115	1545.070	<b>45</b>
<b>1</b>	Ge	1555.030	1555.210	1555.180	<b>30</b>
<b>2</b>	Ge	1544.755	1544.920	1544.890	<b>30</b>
<b>3</b>	Ge	1549.960	1550.080	1550.050	<b>30</b>

Another factor which may be influencing the reduction of the Bragg wavelength during the relaxation periods could be temperature. Previous studies have shown that when FBGs are exposed to 100kGy of gamma irradiation there is a temperature rise of 0.5<sup>o</sup> C within the FBG [9]. After 200kGy an increase of temperature of 1<sup>o</sup>C or higher is expected. With the cooling associated with relaxation, the Bragg wavelength may reduce back towards the original base by a factor of, 10pm/<sup>o</sup>C at 1550nm for Ge-doped silica fibers [44]. The results indicate that the average shift of the Bragg wavelength overall, inclusive of the second relaxation is 29.2pm. This equates to a temperature change of 2-3<sup>o</sup>C. For future experiments we intend to look at temperature effects to determine if it is a main factor influencing the Bragg wavelength.

**Table 5.4 Bragg wavelength shift for the second relaxation after 20hrs and dose of 196.4 kGy.**

<b>Line</b>	<b>Fibre Type</b>	<b>Base Bragg Wavelength(nm)</b>	<b>Bragg Wavelength(nm) After 196.4kGy</b>	<b>Bragg Wavelength(nm) After 20hrs. Relaxation</b>	<b>Relaxation Shift <math>\Delta\lambda_B</math> (pm)</b>
<b>1</b>	SMF28	1545.220	1545.430	1545.415	<b>15</b>
<b>2</b>	SMF28	1549.765	1549.975	1549.960	<b>15</b>
<b>3</b>	SMF28	1555.060	1555.345	1555.285	<b>60</b>
<b>1</b>	Ge+H	1550.020	1550.155	1550.125	<b>30</b>
<b>2</b>	Ge+H	1554.805	1555.015	1554.985	<b>30</b>
<b>3</b>	Ge+H	1544.950	1545.175	1545.130	<b>45</b>
<b>1</b>	Ge	1555.030	1555.255	1555.225	<b>30</b>
<b>2</b>	Ge	1544.755	1544.980	1544.950	<b>30</b>
<b>3</b>	Ge	1549.960	1550.110	1550.095	<b>15</b>

The Bragg wavelength of an individual sample (FBG) in Line 1 and 2 as a function of time in both the initial relaxation and second relaxation stages, are shown in Figures 5.9, 5.10, 5.11 and 5.12. There are a number of outliers in the data presented which appear to affect the precision of the data fit, as evidenced by the poor correlation coefficients ( $R^2$ ). In Figures 5.9, 5.10 and 5.11, the fifth data point at approximately the 13 hour mark show a slight increase in the wavelength. As they occur at the same time there may be a common cause. It could be due to a connection error or recording error on my behalf when swapping lines and reconnecting them to the circulator for measurement. I removed the outliers to do a comparison of the  $R^2$  values which are shown in Figures 5.13 and 5.14. There is large improvement of the logarithmic fit confirming that the outlier is more than likely an anomaly due to error. Overall, the relaxation results indicate a logarithmic trend and negative correlation by the fact that, as

the relaxation time increases, there is a reduction and movement of the wavelength shift back towards the original base. There is also an indication that saturation is starting to occur at approximately the 6 hour mark. To confirm this trend I would like to extend the relaxation period to approximately 48 hours in future experiments.

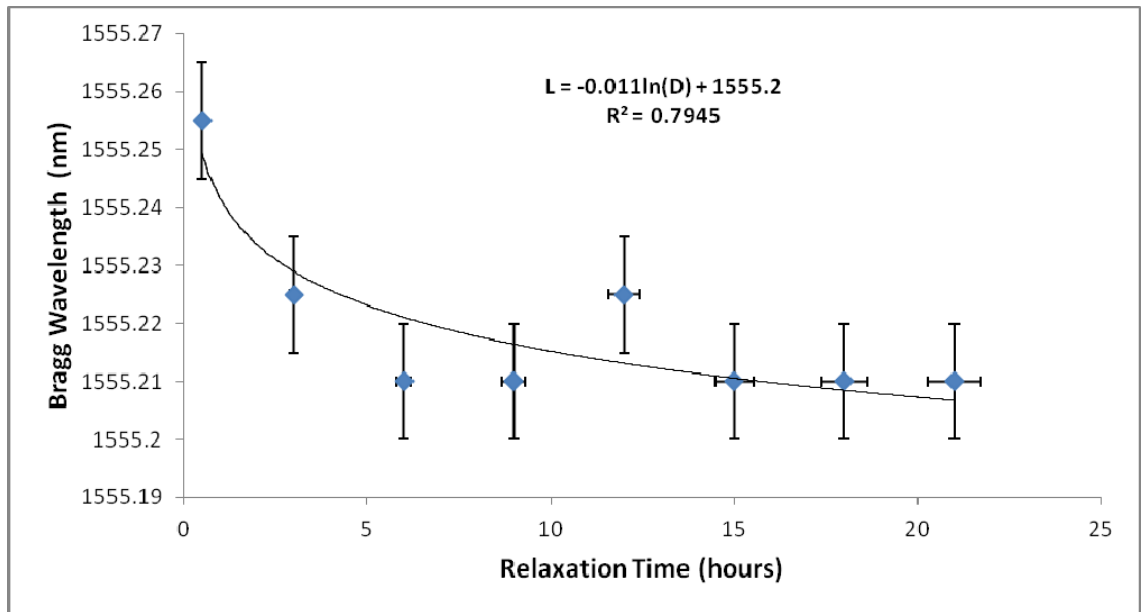


**Figure 5.9** Bragg wavelength of Line three FBG (SMF 28+H; 1555nm) for first the relaxation period of 22hrs.

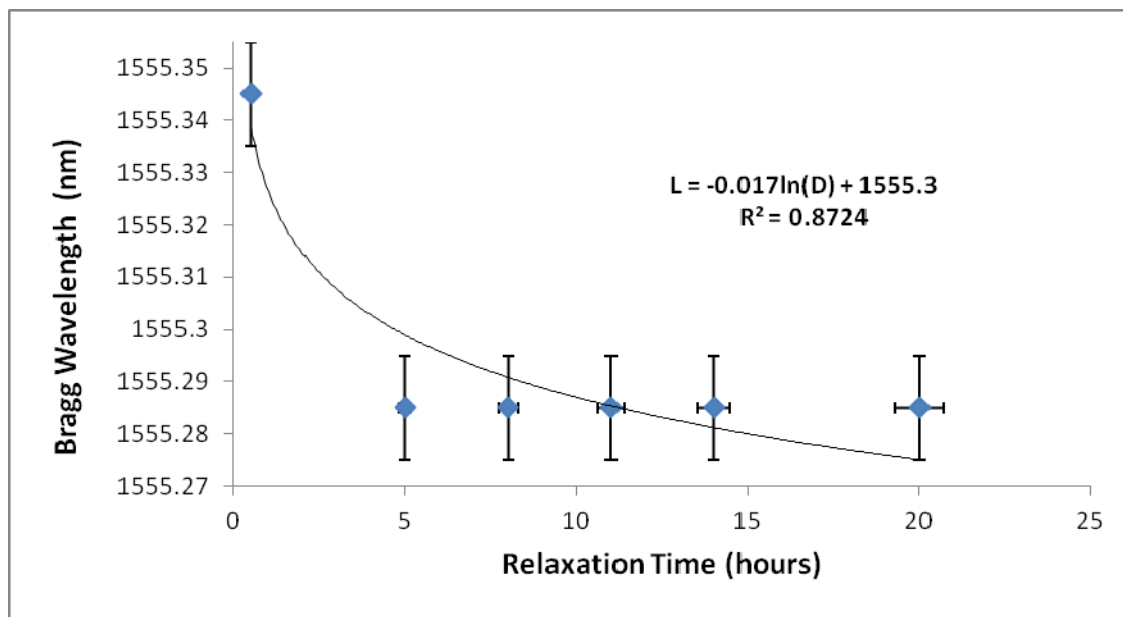


**Figure 5.10** Bragg wavelength of Line 3 FBG (SMF 28+H; 1555nm) after the second relaxation period of 20hrs.

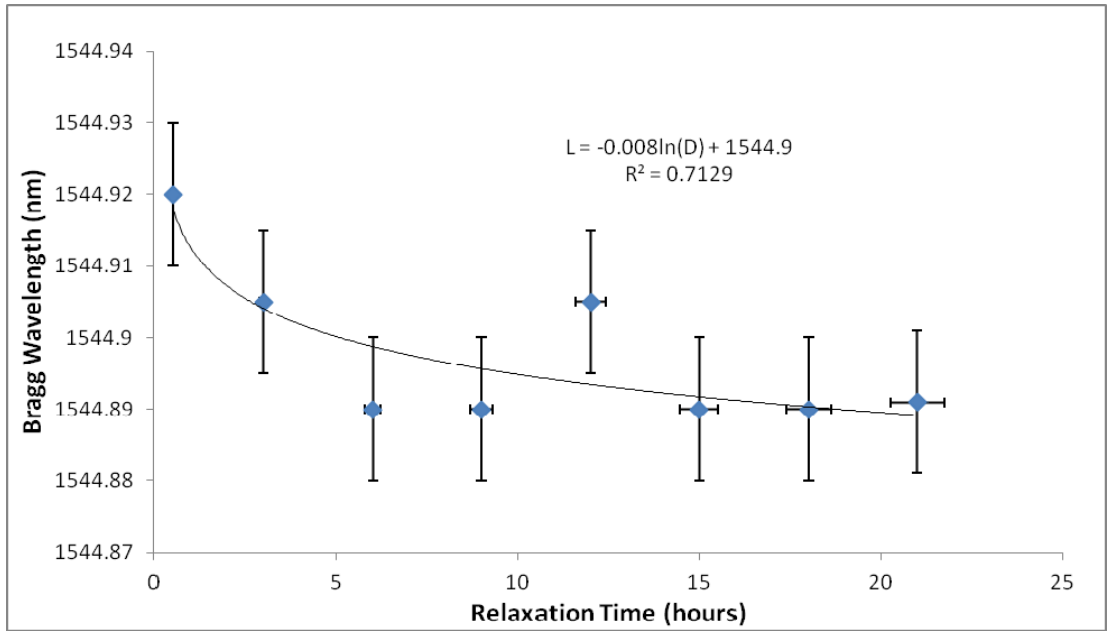


**Figure 5.11** Bragg wavelength of Line 2 FBG (Ge; 1545nm) for the first relaxation period of 22hrs.

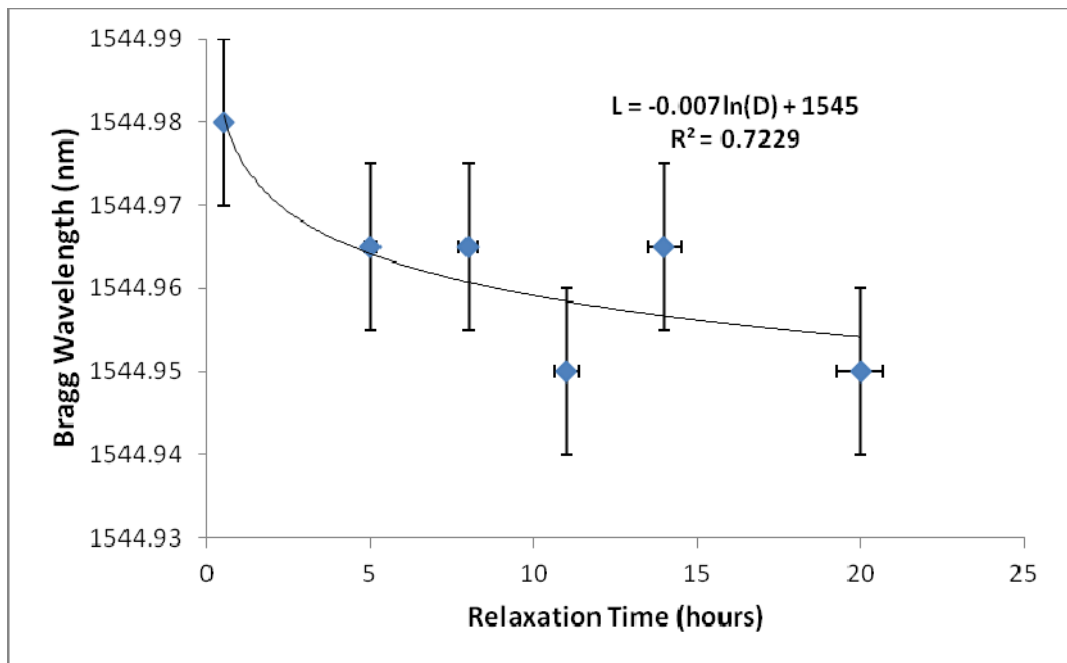


**Figure 5.12** Bragg wavelength for Line 2 FBG (Ge; 1545nm) for the second relaxation period of 20hrs.

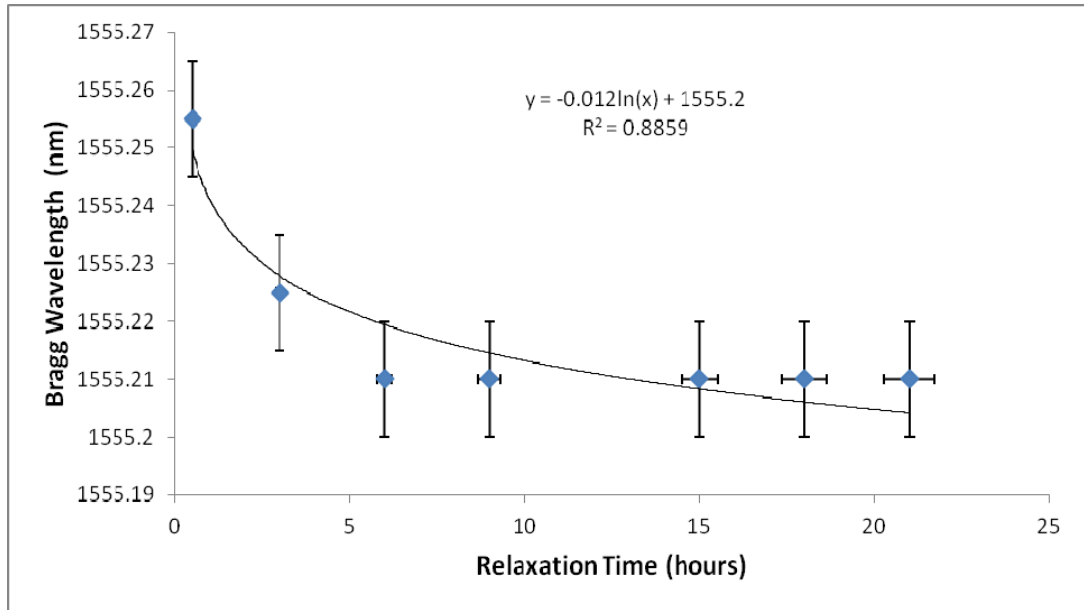


**Figure 5.13** Bragg wavelength of Line three FBG (SMF 28+H; 1555nm) for first the relaxation period of 22hrs with outlier removed, noting improved  $R^2$  value.

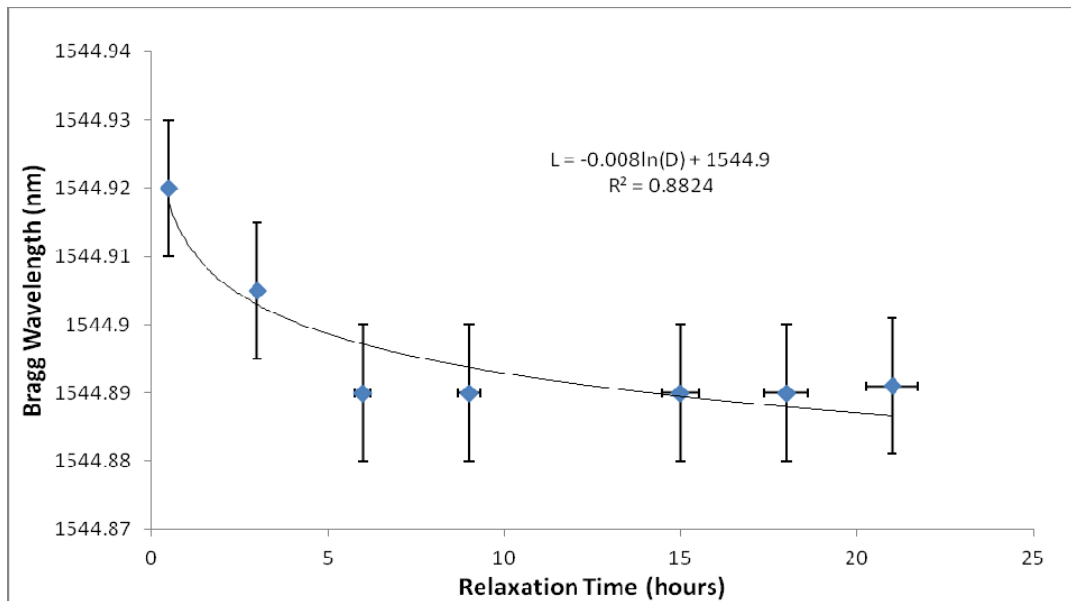


**Figure 5.14** Bragg wavelength of Line 2 FBG (Ge; 1545nm) for the first relaxation period of 22hrs with outlier removed, noting improved  $R^2$  value.

#### 5.4 Amplitude variation during first irradiation.

The amplitude variations of the FBGs are shown in Table 5.5. The maximum amplitude change is very small over the 51.3hour period. This is in keeping with previous data [3] showing that FBG's are able to avoid the broadband radiation induced optical power loss (radiation induced attenuation) because of the narrow wavelength encoding or narrow spectral range of < 5nm [3].

**Table 5.5 Reflection spectra of 1<sup>st</sup> irradiation, for total absorbed dose of 206.8 kGy.**

Line	Fibre Type	Base Wavelength(nm)	Peak Amplitude(dB) Before Irradiation	Peak Amplitude(dB) After Irradiation	Max.Amp. Change(dB)
1	SMF28H	1545.220	-22.994	-23.866	<b>-0.872</b>
2	SMF28H	1549.765	-22.533	-23.623	<b>-1.090</b>
3	SMF28H	1555.060	-22.519	-22.768	<b>-0.249</b>
1	Ge+H	1550.020	-23.799	-24.899	<b>-1.100</b>
2	Ge+H	1554.805	-24.517	-25.889	<b>-1.372</b>
3	Ge+H	1544.950	-32.216	-42.832	<b>-10.616</b>
1	Ge	1555.030	-24.985	-26.300	<b>-1.315</b>
2	Ge	1544.755	-23.711	-25.041	<b>-1.330</b>
3	Ge	1549.960	-28.135	-39.722	<b>-11.587</b>

The only variation of significance is in Line 3 for FBG1 (Ge+H) and FBG2 (Ge), highlighted in red in Table 5.5. Both show amplitude changes of above 10 dB. This can be attributed to the fact that we had trouble with the loss of signals during the irradiation at approximately 112kGy, as previously mentioned. We managed to rectify the transmissions for FBG1 and FBG2, however when we recovered the signal, output was less than the original output. There seemed to be a problem from the start with FBG1 and FBG2 due to connectivity problems, as shown in Figure 5.15.

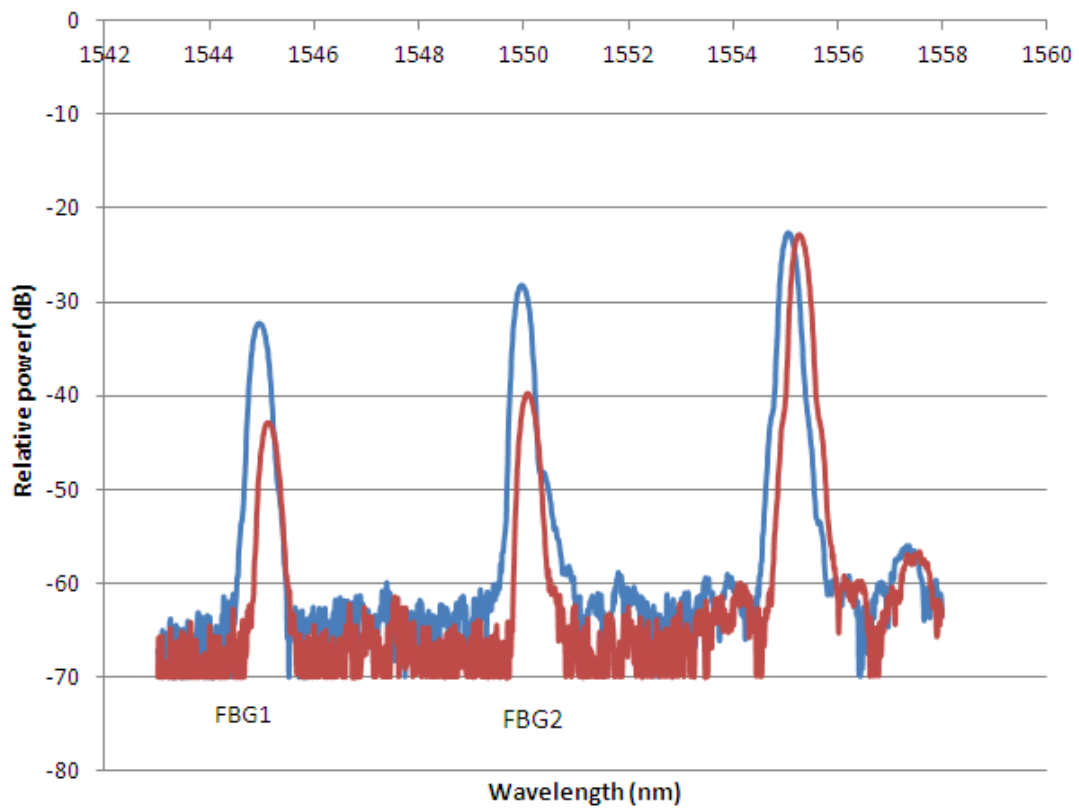


**Figure 5.15. Reflection spectra of Line 3 showing weaker output from FBG1 and FBG2. The blue peaks are the initial peaks, with red peaks being the final shift during the first irradiation stage.**

### **5.5 Amplitude Variation during Second Irradiation.**

For comparison, the results of the pre-irradiation measurements are shown in Table 5.6. Overall, they show that the output is consistent through each line, though the amplitude variation is much smaller than the first irradiation. Again, this can be attributed to the effects of radiation hardening, which makes the FBGs more stable and tolerant overall to the effects of gamma irradiation. To highlight this, the results in Line3, FBG1 and FBG2, show a marked difference in the output signal, which shows there is continuity in the results. The amplitude before irradiation column shows a higher value, due to the fact that the relaxation period was limited to 22 hours.

**Table 5.6 Reflection spectra of second irradiation. Dose 196.4kGy.**

<b>Line</b>	<b>Fibre Type</b>	<b>Base Wavelength(nm)</b>	<b>Peak Amplitude(dB) Before Irradiation</b>	<b>Peak Amplitude(dB) After Irradiation</b>	<b>Max.Amp. Change(dB)</b>
<b>1</b>	SMF28H	1545.220	-23.787	-23.987	<b>-0.200</b>
<b>2</b>	SMF28H	1549.765	-24.100	-23.277	<b>-0.823</b>
<b>3</b>	SMF28H	1555.060	-22.624	-22.831	<b>-0.207</b>
<b>1</b>	Ge+H	1550.020	-24.692	-24.918	<b>-0.226</b>
<b>2</b>	Ge+H	1554.805	-26.212	-25.792	<b>-0.420</b>
<b>3</b>	Ge+H	1544.950	-42.350	-40.959	<b>-1.391</b>
<b>1</b>	Ge	1555.030	-24.097	-26.321	<b>-0.224</b>
<b>2</b>	Ge	1544.755	-25.466	-24.867	<b>-0.599</b>
<b>3</b>	Ge	1549.960	-40.767	-35.592	<b>-5.175</b>

### 5.6 FWHM changes Vs Irradiation dose

The results in Tables 5.7 and 5.8 show the Full Width Half Maximum (FWHM) from the data using MATLAB (7.12.0.635). The table shows the FWHM at the beginning and end of the first irradiation period and second irradiation periods. The FWHM of each peak was determined fitting a theoretical Gaussian peak to each of the experimental peaks. The Gaussian fit is where the signal is at half the maximum, 3dB down from the peak. Considering the total overall dose of 206.8 kGy and 196.4 kGy, the FWHM remained fairly stable except for FBG1 and FBG2 in Line 3, highlighted in red in Table 5.7. The problem we had in the set up of Line 3 is the probable cause of the larger FWHM.

**Table 5.7 FWHM of each FBG at start and end of first irradiation period.**

<b>Line</b>	<b>Fibre Type</b>	<b>Base Wavelength(nm)</b>	<b>FWHM(nm) Before Irradiation</b>	<b>FWHM(nm) After Irradiation</b>	<b>Total FWHM Change(nm)</b>
<b>1</b>	SMF28H	1545.220	0.7480	0.7237	<b>-0.0243</b>
<b>2</b>	SMF28H	1549.765	0.8308	0.8177	<b>-0.0131</b>
<b>3</b>	SMF28H	1555.060	0.8485	0.8376	<b>-0.0110</b>
<b>1</b>	Ge+H	1550.020	0.7340	0.7173	<b>-0.0167</b>
<b>2</b>	Ge+H	1554.805	0.8020	0.7984	<b>-0.0036</b>
<b>3</b>	Ge+H	1544.950	0.6934	0.5591	<b>-0.1343</b>
<b>1</b>	Ge	1555.030	0.7225	0.7088	<b>-0.0137</b>
<b>2</b>	Ge	1544.755	0.8203	0.7943	<b>-0.0260</b>
<b>3</b>	Ge	1549.960	0.7514	0.5734	<b>-0.1780</b>

**Table 5.8 FWHM of each FBG at start and end of second irradiation period.**

<b>Line</b>	<b>Fibre Type</b>	<b>Base Wavelength(nm)</b>	<b>FWHM(nm) Before Irradiation</b>	<b>FWHM(nm) After Irradiation</b>	<b>Total FWHM Change(nm)</b>
<b>1</b>	SMF28H	1545.220	0.7122	0.7373	<b>+0.0251</b>
<b>2</b>	SMF28H	1549.765	0.8164	0.6172	<b>-0.1992</b>
<b>3</b>	SMF28H	1555.060	0.8485	0.8667	<b>+0.0195</b>
<b>1</b>	Ge+H	1550.020	0.7249	0.7303	<b>+0.0126</b>
<b>2</b>	Ge+H	1554.805	0.7761	0.5640	<b>-0.2121</b>
<b>3</b>	Ge+H	1544.950	0.5612	0.5760	<b>+0.0147</b>
<b>1</b>	Ge	1555.030	0.7121	0.7088	<b>-0.0033</b>
<b>2</b>	Ge	1544.755	0.7750	0.6107	<b>-0.1643</b>
<b>3</b>	Ge	1549.960	0.5573	0.6257	<b>+0.0684</b>

Two results for Line2 are highlighted in red in Table 5.8, to show that there is a large difference between the start FWHM and final FWHM compared to Lines1 and 3 during the second irradiation period. I have gone back through my data and extracted GIF image files to see if there was a probable cause. The increase in the FWHM seemed to occur at the same time there was a change in the output of the three peaks as shown in Figures 5.16, 5.17. The normal three peaks are shown in Figure 5.16, whilst Figures 5.17 show the change in the images when there was spike in the FWHM result.

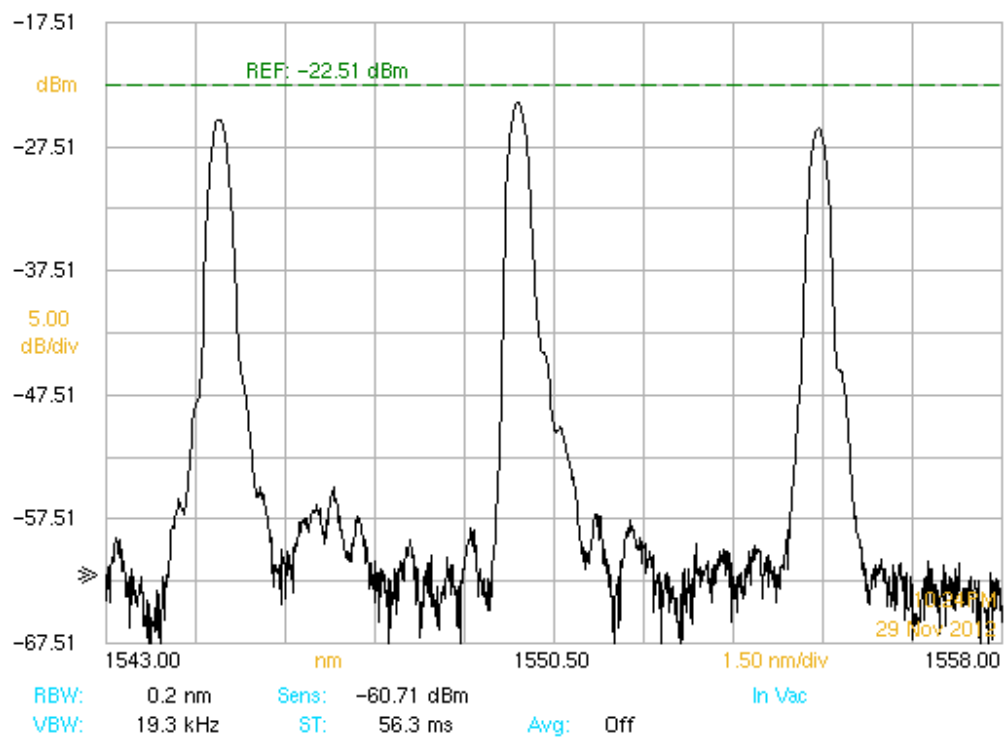


**Figure 5.16 . Normal GIF image of Line 2 during the early stages of irradiation.**

Overall, the FWHM shape was not affected by the radiation in FBGs written in Ge doped and/or Hydrogen loaded fibre both in the initial and second irradiation stages. The results agree with previous data [3], that while the Bragg peak shift is dependent on accumulated dose, gamma irradiation has no influence on the shape of the FWHM.

The Gaussian fit is shown in Figures 5.18(a), 5.18(b), 5.19(a), 5.19(b), 5.20(a), and 5.20(b). However, after the first full irradiation period and second irradiation periods, a small drop in relative power can be seen, therefore a small drop in peak wavelength. FBG1 and FBG2 of Line 3 show the largest change in the reduction of the Half-maximum

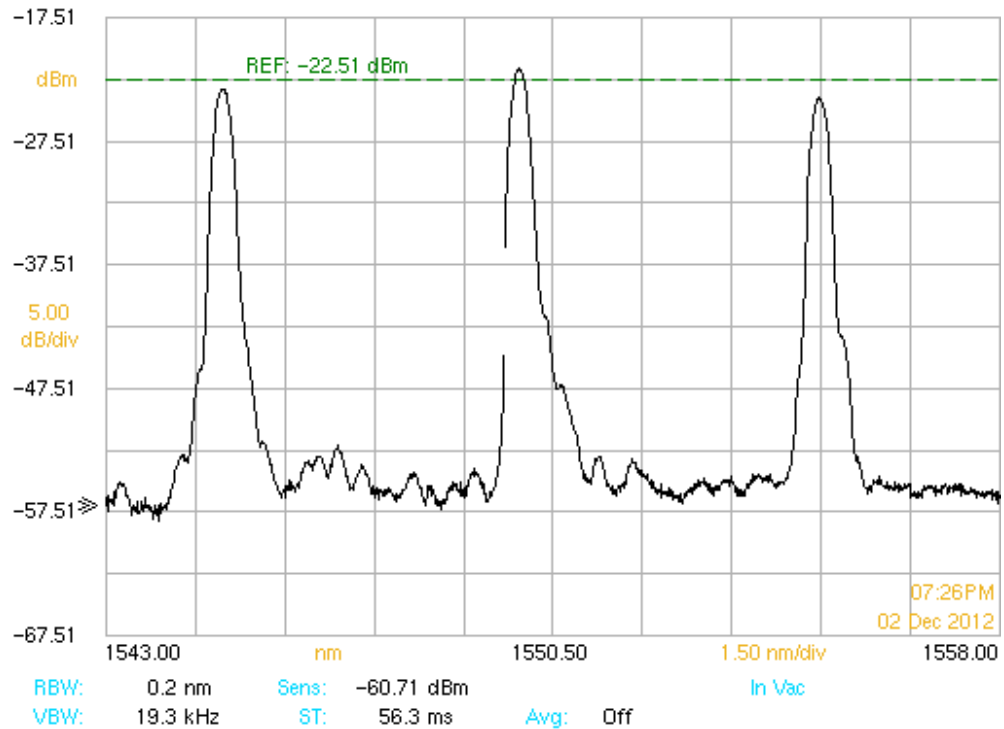


**Figure 5.17 Change in GIF image of Line 2 in the final stages of the second irradiation period.**

The relative stability of the FWHM during irradiation indicates FBGs could be used in the nuclear environment for detection of stress and temperature with confidence. These types of measurements require radiation tolerant and more stable FBGs.

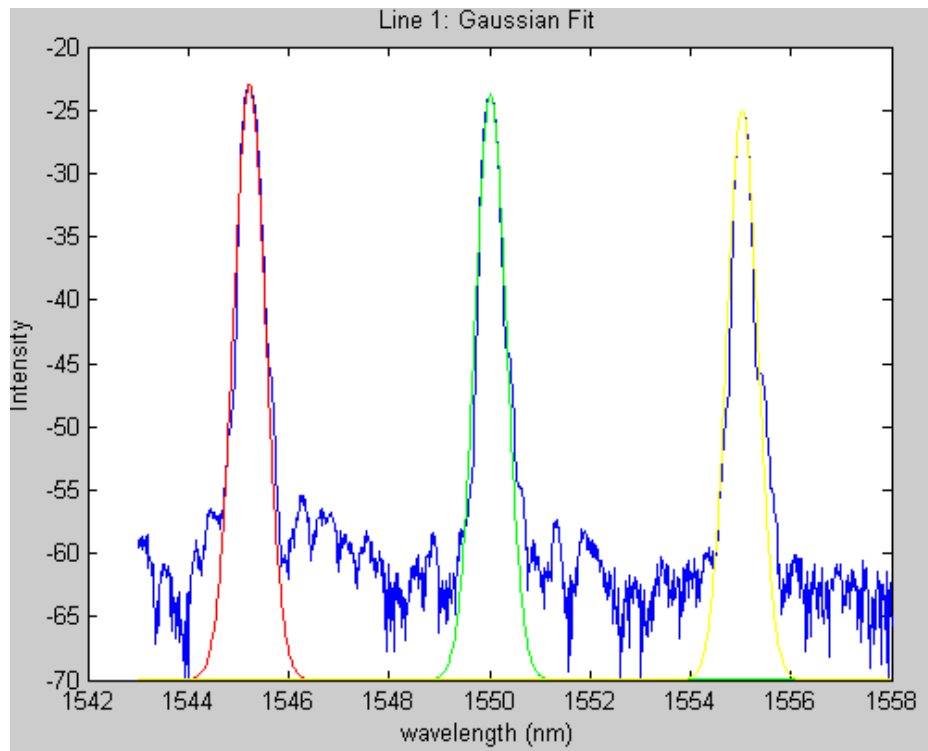


**Figure 5.18 (a) Line 1 Gaussian fit of reflection intensity at start of first irradiation.**

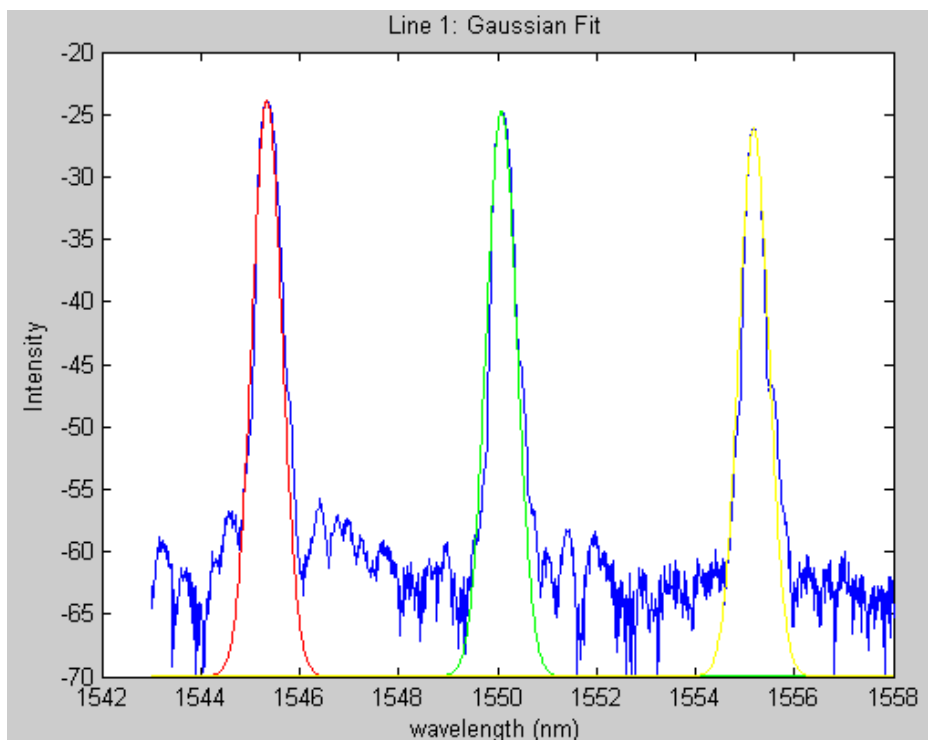


**Figure 5.18 (b) Line 1 Gaussian fit of reflection intensity at start of second irradiation.**

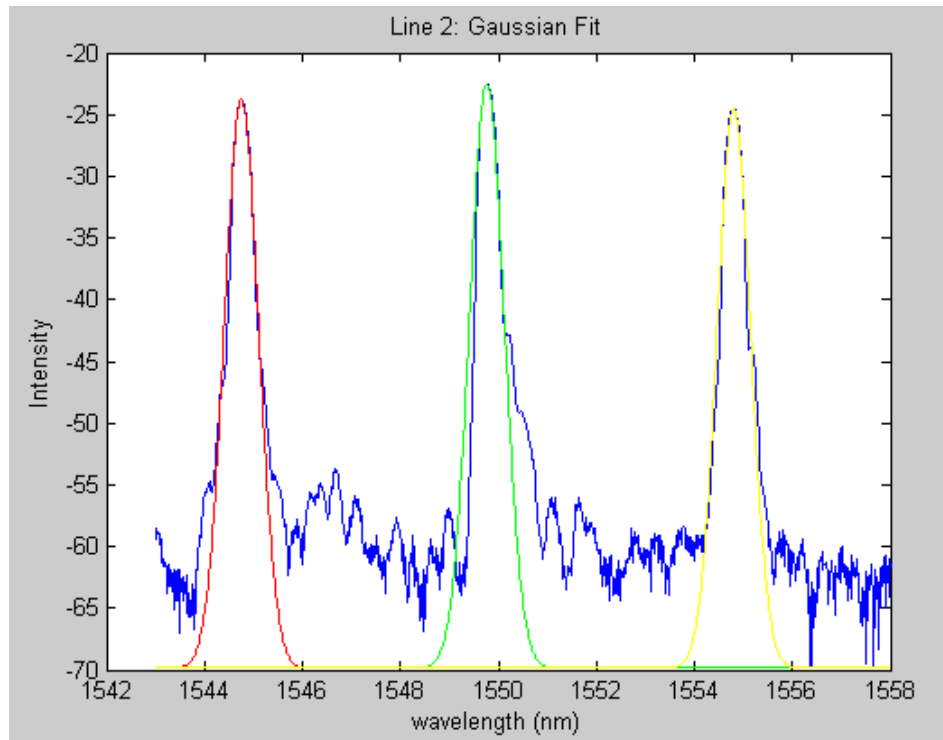


**Figure 5.19 (a) Line 2 Gaussian fit of reflection intensity at start of first irradiation.**

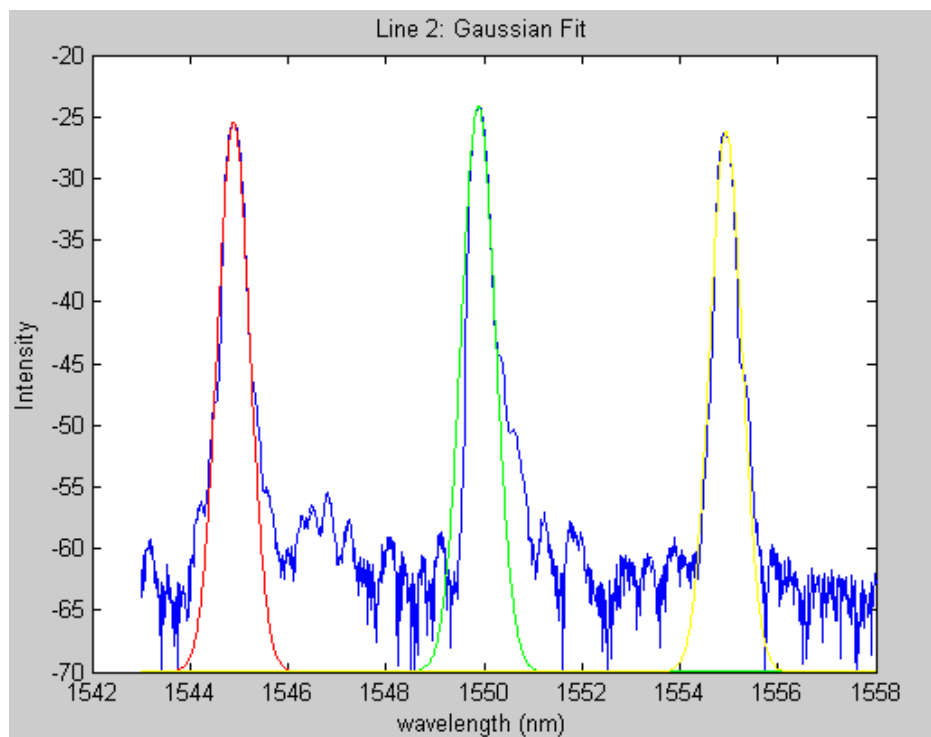


**Figure 5.19 (b) Line 2 Gaussian fit of reflection intensity at start of second irradiation.**

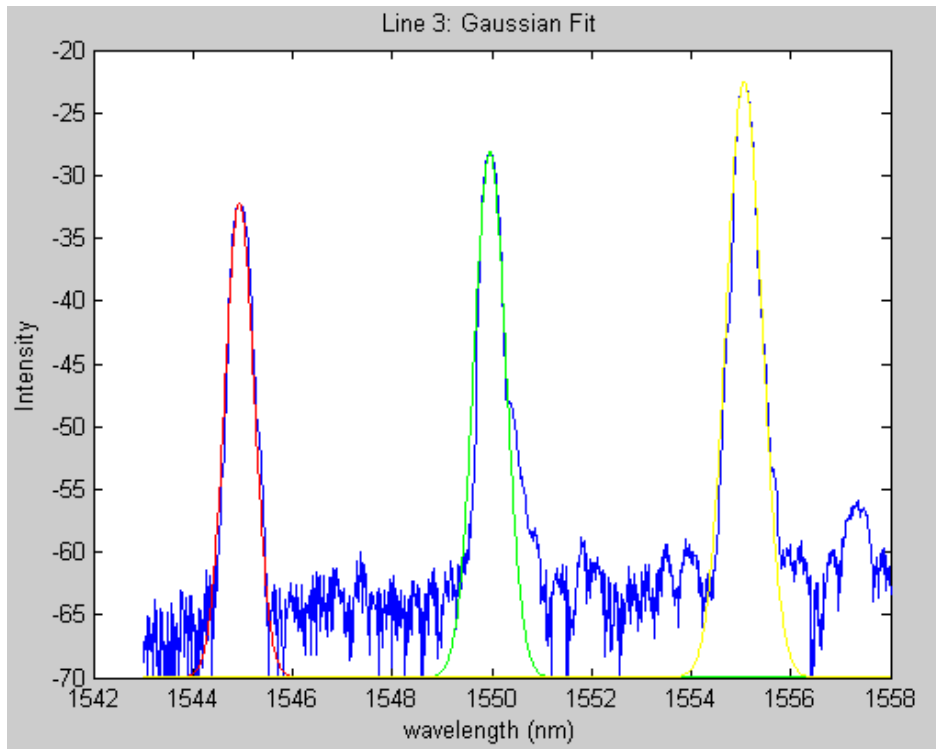


**Figure 5.20 (a) Line 3 Gaussian fit of reflection intensity at start of first irradiation.**

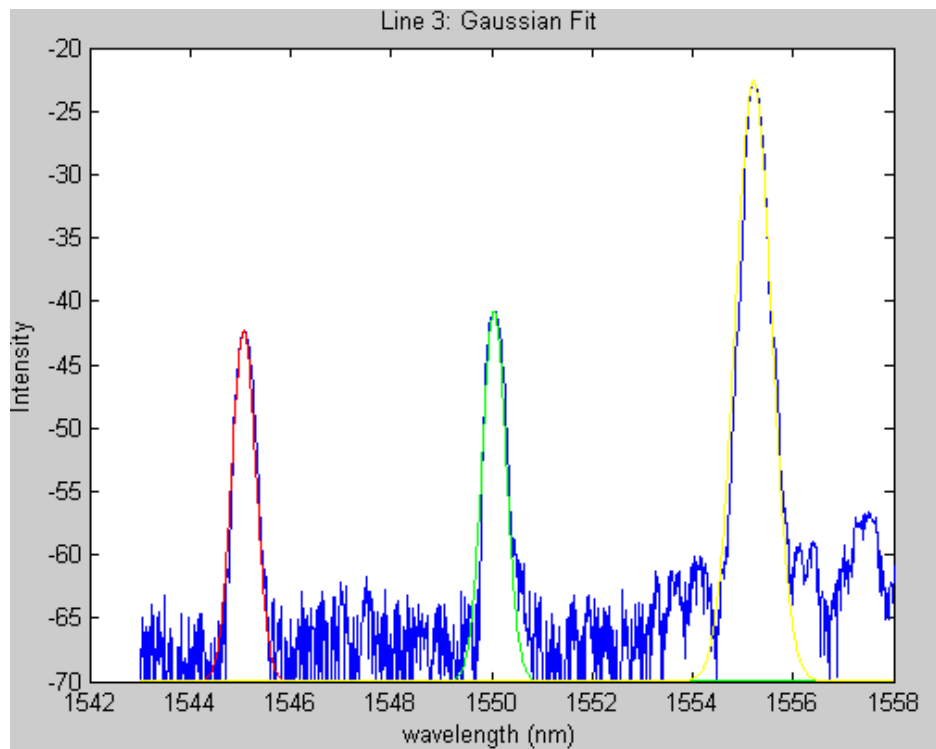


**Figure 5.20 (b) Line 3 Gaussian fit of reflection intensity at start of second irradiation.**

## CHAPTER 6

### DISCUSSION & FUTURE WORK

#### 6.1 Discussion

The results obtained for the 9 FBGs over the 6 day period, seem to show consistency in all aspects whilst under gamma irradiation. The Bragg wavelength shift (BWS) as a function of the accumulated dose show an increase in the peak shift as the dose increases in all FBGs during the initial irradiation and second irradiation stage. The highest BWS shift occurred after 206.8kGy of 195pm with the FBG written in SMF28 fibre loaded with Hydrogen. The overall average radiation induced BWS was shown experimentally to be 151.6pm for the first irradiation stage. An example of the total Bragg wavelength shift over the full duration of the experiment, inclusive of the first and second irradiation stages and first and second relaxation stages by FBG3 in Line 2 (Ge+H,1555nm) is shown in Figure 6.1. The fact that the BWS seems to be restarted after the first relaxation period when re-irradiated, indicates that the effects are cumulative, which is what is needed in a dosimeter.

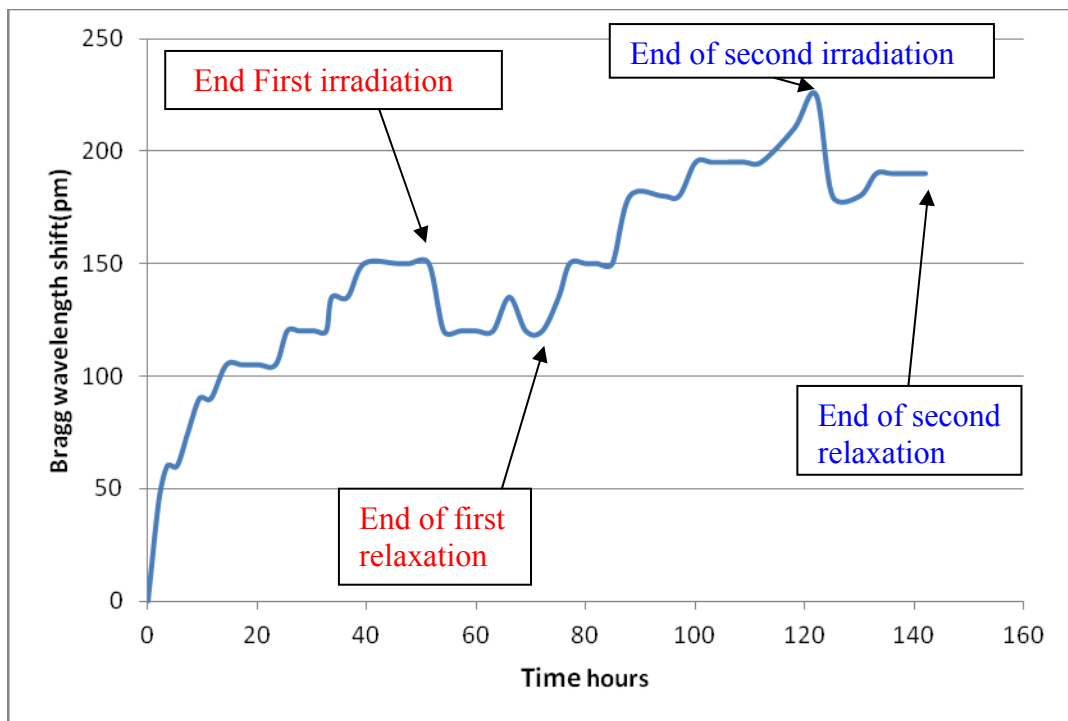


**Figure 6.1 Bragg Wavelength Shift over complete experiment inclusive of both relaxation periods and both irradiation periods for Line 2 (Ge+H, 1555nm).**

The individual averages for the FBGs created in Germanium with Hydrogen(Ge+H) fibre is 135pm; Germanium only, 155pm; and SMF28 + Hydrogen, 165pm. All results indicate that FBGs created in Ge doped fibre and Hydrogen loaded result in greater sensitivity to high dose gamma radiation, when compared to results from a previous study [9], which showed that Ge free fibre produced a low BWS of only 50pm at 100kGy. This bodes well for FBGs being suitable for use as high dose radiation sensors. When the samples were irradiated for the second time, we were able to establish the effects of pre-irradiation on the BWS. There was a marked reduction in the overall average, dropping to 88.3pm, with the lowest recording of 60pm occurring in the Ge doped fibre. Therefore, we can conclude that FBGs exposed to pre-irradiation have a lower Bragg wavelength shift compared to no pre-irradiation exposure. Pre-irradiation is a possibility for producing radiation hard FBG sensors.

When examining the relaxation effects on the first and second irradiation periods, the overall trend was a wavelength shift back towards the base wavelength. The shifts were all consistent, with the average relaxation shift for the first period being 28pm and for the second 30pm. Although they were only small shifts the trend was always back towards the base wavelength. For future studies, it will be necessary to increase the relaxation period to establish an accurate trend, with regards to saturation, which seemed to be occurring from the 6 hour mark in this study.

The results concerning amplitude variation seem to indicate that the increased sensitivity of the fibres affects the amplitude change. During the first stage of irradiation, when sensitivity is highest, the amplitude changes were overall markedly higher. After the second irradiation stage, pre-irradiation effects from radiation hardening seem to take hold. There is less sensitivity, resulting in smaller amplitude changes. Radiation hard sensors due to pre-irradiation seem to be less sensitive but more stable. To determine the cause or major trigger for the BWS is difficult without further investigations in the form of e.g. composition analysis and/or electron microscopy imaging. However, data from previous research [40] show that the concentrations of colour defect centres in silica glass when exposed to irradiation vary, which affects attenuation loss [33]. The study found that the presence of defect centres can be reduced by pre-irradiation and/or thermal annealing [40], which in turn reduces radiation induced attenuation. This seems to be linked to our data regarding the amplitude reduction after pre-irradiation.

## 6.2 Future Work

Future irradiation studies should involve the use of new generation optical fibres such as Photonic Crystal Fibre (PCF) and, in particular, Random Hole Optical Fibre (RHOF). Results have been promising, showing a possible minimisation of the effects of defect colour centres [40]. Through the development also of co-doped fibres using Germanium and Boron or Phosphorous, the FBG performance should be investigated for a comparison. Further investigation of relaxation and the effects of pre-irradiation should also be investigated with the new generation of optical fibres. In future we would also like to vary the total dose and dose rates for a comparison.

We also hope to pursue further irradiation studies to note the effect of gamma irradiation on the new generation of FBGs, manufactured by high energy femtosecond (fs) laser with increased hydrogen loading of 300 bar. The results of the increase in hydrogen loading would be of interest, as the data suggests [29] there should be a 14% increase in the BWS due to the increase of sensitivity. A good comparison could be made as we used the lowest hydrogen loading of 100bar.

## **CHAPTER 7**

### **CONCLUSION**

#### **7.1 Conclusion**

To conclude, the primary objectives and most of my secondary objectives have been met. We achieved a radiation induced BWS in FBGs created by UV light, in fibre with and without hydrogen loading and germanium doping. The results indicate that FBGs written in the H<sub>2</sub>-loaded fibres with Ge-doping show a higher sensitivity to high dose irradiation. This makes them good candidates as possible replacements for current radiation dosimeters in use for radiation processing in nuclear environments. The effects of pre-irradiation has also been shown to reduce the FBGs sensitivity resulting in an increased stability and improved radiation tolerance overall. This increased stability will help in temperature and stress sensing or structural monitoring of space structures. By continuing to improve radiation tolerances of FBGs through pre-irradiation techniques, the applications of FBGs in the space environment may eventuate. Overall, the data seems to be consistent with previous research, however with regards to relaxation effects, longer relaxation times are needed to fully establish the saturation of the Bragg wavelength. As mentioned previously, for future experiments, the relaxation period should be extended to at least 48-72 hours.

A footnote to my conclusion; I would just like to emphasise the importance of the experimental set up. For the FBG sensor to perform at the optimum level, it was found that it should be in a highly stable and stress free environment, and at constant temperature for the best results. This can be seen in our data when Line 3 lost two peak outputs when the setup became unstable due to the tape holding the gratings in position becoming loose.

## REFERENCES

- [1] R.Sharma, R.Rohilla, M.Sharma, Dr.T.Manjunath, “Design & simulation of optical fibre Bragg grating pressure sensor for minimum attenuation criteria,” Journal of Theoretical and Applied Information Technology, Vol.5, No.5, pp.515-530, 2009
- [2] S.O’Keeffe, C.Fitzpatrick,E.Lewis, A.I. Al-Shamma, “A review of optical fibre radiation dosimeters,” Sensor Review, Vol.28, No.2, pp.136-142, 2008.
- [3] A.Fernandez, B.Brichard, F.Berghnans and M.Decreton, “Dose rate dependencies in gamma-irradiated fiber Bragg grating filters,” IEEE Transactions on Nuclear Science, Vol.49, No.6, pp.2874-2878, December, 2002.
- [4] ARPANSA-Australian Radiation Protection and Nuclear Safety Agency, “Gamma Radiation”, Available from the ARPANSA website: <http://www.arpansa.gov.au/radiationprotection/basics/gamma.cfm>, 2012.
- [5] BOTDA, “Fibre Bragg Grating”, Available from the BOTDA website: [http://www.botda.com/index.php?option=com\\_content](http://www.botda.com/index.php?option=com_content), 2012
- [6] J.Dakin and B.Culshaw, “ Optical Fibre Sensors. Applications, Analysis and Future Trend,” Artech House, ISBN-13, 978-0890069400, Norwood,MA,1997.
- [7] G.Allwood, G.Wild and S.Hinckley, “In-Ground Optical Fibre Grating Pressure Switch for Security Applications,” SPIE proceedings, Vol.8351, January,2012.
- [8] F.Urban, J.Kadler, R.Vlack & R.Kuchta, “Design of a Pressure Sensor based on Optical Fibre Bragg Grating Lateral Deformation,” Sensors, 10, 11212-11225,2010.
- [9] Karerina Krebber,Henning Henschel and Udo Weinand, “Fibre Bragg gratings as high dose radiation sensors,” Measurement Science and Technology, 17, pp.1095-1102, 2006.

- [10] Robert J. Fielder, Roger G. Duncan, Matthew L. Palmer, "Recent Advancements in Harsh Environment Fiber Optic Sensors: An Enabling Technology of Emerging Nuclear Power Application," IAEA Meeting, Knoxville, June 27-28, 2005.
- [11] The Industrial Physicist, "Tunable Lasers and Fibre Bragg Sensors," Retrieved from The Industrial Physicist website: <http://www.aip.org>, 2012.
- [12] "Fibre Bragg Gratings", Available from Smartfibre website: <http://www.smartfibres.com>, 2012.
- [13] Raman Kashyap, "Fibre Bragg Gratings, Second Edition", Academic Press, Burlington, MA., USA, 2010.
- [14] A. Gusarov, B. Brichard and D. N. Nikogosyan, "Gamma- radiation effects on Bragg gratings written by femtosecond UV laser in Ge-doped fibers," IEEE Transactions on Nuclear Science, Vol.57, No.4, pp.2024-2028, August, 2010.
- [15] B.E.A. Saleh, and M.C. Teich, "Fundamental of Photonics", Second Edition, John Wiley & Sons, Inc., Hoboken, New Jersey, 2007.
- [16] IPHT, "Applications of Fibre Bragg Grating Sensors", Available from the Institute of Photonic Technology website: <http://www.Ipht-jena-de>, 2012.
- [17] NASA Dryden Flight Research Centre, 2011, "Lightweight Fiber Optic Sensors for Real Time Strain Monitoring," Available from the NASA website : <http://www.nasa.gov>
- [18] T. Shikama, K. Toh, S. Nagata and B. Tsuchiya, "Optical Dosimetry for ionizing radiation fields by infrared radio luminescence," SPIE, Vol.5855, pp.507-510, 2005.

- [19] A.I.Gusarov, F.Berghmans, A.Fernandez Fernandez, O.Deparis, Y. Defosse, D.Starodubov, M.Decreton, P.Megret and M.Blondel, "Behavior of Fibre Bragg Gratings Under High Total Dose Gamma Irradiation," IEEE Transactions on Nuclear Science, Vol.47, No.3, pp. 688-692, June,2000.
- [20] Stefan K.Hoeffgen, Henning Henschel, Jochen Kuhnenn, Udo Weinand, Christophe Caucheteur, Dan Grobnc and Steven J. Mihailov, "Comparison of the Radiation Sensitivity of Fiber Bragg Gratings Made by Four Different Manufacturers," IEEE Transactions on Nuclear Science, Vol.58, No.3, pp.906-909, June 2010.
- [21] Stephen A. Slattery and David N. Nikogosyan and Gilberto Brambilla, "Fiber Bragg grating inscription by high intensity femtosecond UV laser light: comparison with other existing methods of fabrication," J. Opt. Soc. Am.B, Vol.22, No.2, pp.354-361, February 2005.
- [22] Henning Henschel, Dan Grobnc, Stefan K. Hoeffgen, Jochen Kuhnenn, Stephen J.Mihailov and Udo Weinand, "Development of Highly Radiation Resistant Fiber Bragg gratings," IEEE Transactions on Nuclear Science, Vol.58, No.4, pp.2103-2110, August 2011.
- [23] Dan Grobnc, Henning Henschel, Stefan K. Hoegggen, Jochen Kuhnenn, Stephen J.Mihailov, Udo Weinand, "Radiation sensitivity of Bragg gratings written with femtosecond IR lasers," SPIE, Vol.7316, p.73160C, 2009
- [24] Stephen J. Mihailov, "Fibre Bragg grating sensors for harsh environments," Sensors, Vol.12, No.2, pp.1898-1918, 2012.
- [25] A. Fernandez Fernandez, A. Gusarov, F. Berghmans, M. Decreton, P. Megret, M. Blondel and A. Delchambre, "Long term irradiation of fibre Bragg gratings in a low dose rate gamma neutron radiation field," SPIE, Vol.4823, pp.205-212, September, 2002.

- [26] Song Lin, Ningfang Song, Jing Jin, Xueqin Wang, and Gongliu Yang, “ Effect of Grating Fabrication on Radiation Sensitivity of Fibre Bragg Gratings in Gamma Radiation Field,” IEEE Transactions on Nuclear Science, Vol. 58, No. 4, pp.2111-2117, August,2011.
- [27] Henning Henschel, Stefan K. Hoeffgen, Katerina Krebber, Jochen Kuhnenn and Udo Weinand, “Influence of Fiber Composition and Grating Fabrication on the Radiation Sensitivity of Fiber Bragg Gratings,” IEEE Transactions on Nuclear Science, Vol.55, No. 4, pp. 2235-2242, August 2008.
- [28] Photograph of ANSTO facility and GATRI cobalt-60 source, available from the ANSTO website: [http:// www.ansto.gov.au](http://www.ansto.gov.au),2012
- [29] Henning Henschel, Stefan K. Hoeffgen, Jochen Kuhnenn, Udo Weinand, “Influence of Manufacturing Parameters and Temperature Sensitivity of Fibre Bragg Gratings,” IEEE Transactions on Nuclear Science, Vol.57, No.4, pp.2029-2034, August,2010.
- [30] A.Gusarov, “ Long –Term Exposure of Fiber Bragg Gratings in the BR1 Low-Flux Nuclear Reactor,” IEEE Transactions on Nuclear Science, Vol.57, No.4, pp. 2044-2048, August, 2010.
- [31] A.Fernandez Fernandez. A.Gusarov, B.Prichard, M.Decreton, F.Berghmans, P.Megret, A. Delchambre, “Long-term radiation effects on fibre Bragg grating temperature sensors on a low flux nuclear reactor,” Measurement Science and Technology, Vol. 15, pp.1506-1511, 2004.
- [32] S.O’Keefe, C. Fitzpatrick,E.Lewis, A.I. Al-Shamma, “A Review of Optical Fibre Radiation Dosimeters,” Sensor Review, Vol.28, No.2, pp.136-142, 2008.
- [33] Wenyun Luo, Zhongyin Xiao, Jianxiang Wen, Jianchong Yin, Zhenyi Chen, Zihua Wang and Tingyun Wang, “Defect center characteristics of silica optical fiber material by gamma ray radiation,” SPIE, Vol.8307, 83072H, 2011.

- [34] Fuhua Liu, Yuying An, Ping Wang, Bibo Shao and Shaowu Chen. Effects of Radiation on Optical Fibers, Recent Progress in Optical Fiber Research, Moh. Yasin, Sulaiman W. Harun and Hamzah Arof (Ed.), ISBN: 978-953-307-823-6, InTech, Available from: <http://www.intechopen.com/books/recent-progress-in-optical-fiber-research/effects-of-radiation-on-optical-fibers,2012>.
- [35] Sylain Girard, Youcef Ouerdane, Giusy Origlio, Claude Marcandella, Aziz Boukenter, Nicolas Richard, Jacques Baggio, Phillippe Paillet, Marco Cannas, Jean Bisutti, Jean-Pierre, Meunier, and Roberto Boscaino, "Radiation effects on silica based preforms-I: Experimental study with canonical samples," IEEE Transactions on Nuclear Science, Vol.55, No.6, pp.3473-3482, December, 2008.
- [36] S.Girard, N.Richard, Y.Ouerdane, G.Origlio. A. Boukenter, L.Martin-Samos, P.Paillet, J.-P.Meunier, J.Baggio, M.Cannos and R.Boscaino, "Radiation effects on silica based preforms and optical fibers-II: Coupling ab-initio simulations and experiments," IEEE Transactions on Nuclear Science, Vol. 55, No.6, pp.3508-3514, December 2008.
- [37] Evgeny M.Dianov and Valery M. Mashinsky, "Germania-Based Core Optical Fibers," Journal of Lightwave Technology, Vol.23, No.11, pp.3500-3508, November, 2005.
- [38] Andreas Othonos, "Fiber Bragg Gratings," Review of Scientific Instruments, (0034-6748), Vol. 68, issue 12, pp.4309-4341, 1997.
- [39] Jan Troska, Jeremy Batten, Karl Gill, Francois Vasey, "Radiation effects in commercial off the shelf single mode optical fibres," "Photonics for Space Environments VI," San Diego, SPIE proceedings, Vol. 3440, pp.112-129, July, 1998

- [40] Tingyun Wang, Zhongyin Xiao and Wenyun Luo, "Influences of Thermal Annealing Temperatures on Irradiation Induced E Centers in Silica Glass," IEEE Transactions on Nuclear Science, Vol.55, No.5, pp.2685-2688, October, 2008.
- [41] Philip St. J. Russell, "Photonic Crystal Fibers," Journal of Lightwave Technology, Vol.24, Issue 12, pp. 4729-4749, 2006.
- [42] Tomasz Nasilowski, Francis Berghmans, Thomas Geernaert, Karima Chah, Jurgen Van Erps, Gabriela Statkiewicz, Marcin Szpulak Jacek Olszewski, Grzegorz Golojuch, Tadeusz Martynkien, Waclaw Urbanczyk, Pawel Mergo, Mariusz Makara, Jan Wojeik, Christoph Chojeczki and Hugo Thienpont, "Sensing with Photonic Crystal Fibres," Intelligent Signal Processing Symposium, WISP, IEEE, 2007.
- [43] Bassam Alfeeli, Gary Pickrell, Marc A. Garland and Anbo Wang, "Behavior of random hole optical fibers under gamma ray irradiation and its potential use in radiation sensing applications," Sensors, Vol. 7, pp. 676-688, May, 2007.
- [44] A.Gusarov,S.Vasiliev, O.Medvedkov, I.Mckenzie and F.Berghmans, "Stabilization of Fibre Bragg Gratings against Gamma Radiation," IEEE Trans.Nucl. Sci. Vol.55, No.4, pp. 2205-2212, Aug., 2008.
- [45] Les Kirkup, "Experimental Methods, an introduction to the analysis and presentation of data," John Wiley & Sons, Milton, Queensland, 1994.

# APPENDICES

## APPENDIX 1

### EXPERIMENTAL RESEARCH PAPER

Presented at the 20<sup>th</sup> AIP National Congress, University of NSW, Sydney,  
December, 2012.

## Gamma Irradiation in Fibre Bragg Gratings

Desmond Baccini<sup>1</sup>, Steven Hinckley<sup>1</sup>, Graham Wild<sup>1,2</sup>, Connie Banos<sup>3</sup>, and Justin B. Davies<sup>3,4</sup>

<sup>1</sup>Centre for Communications Engineering Research, Edith Cowan University, Joondalup WA 6027, Australia.

<sup>2</sup>School of Aerospace, Mechanical, and Manufacturing Engineering, RMIT University, Melbourne VIC 3000, Australia.

<sup>3</sup>Australian Nuclear Science and Technology Organisation, Lucas Heights NSW 2234, Australia.

<sup>4</sup>Institute of Medical Physics, School of Physics, University of Sydney, NSW 2006, Australia.

#### Abstract Summary

We report a preliminary study of gamma radiation effects on the current generation of optical fibre Bragg grating sensors, and the effects of relaxation after gamma irradiation, as a function of dose.

**Keywords-** fibre Bragg gratings (FBGs), gamma irradiation, sensors.

#### I. INTRODUCTION

Optical fibre sensing systems have been used as sensors for temperature, strain, pressure and other important measurement systems. In the past decade, there has been increased interest in extending the application of these sensors to ionizing radiation environments, including their use in monitoring various parameters in space environments (low dose rate and level) and hazardous nuclear areas (high dose rate and levels) [1]. There has even been some development in the area of using these types of sensing systems (and in particular, the damage caused to the fibres) for ionizing radiation dosimetry [2].

Results obtained to-date indicate that gamma irradiation causes attenuation degradation in various optical fibre types, through the generation of defects such as color centers [1-3], causing refractive index changes in the fibre. Studies so far have limited the determination of the effects of gamma radiation on the optical properties of fibres to the visible wavelength range of 400 nm to 700 nm. It has also been found that the specific type of fibre (for example, fibres made with different dopant types) have different responses to ionizing radiation [3].

The FBG is a fundamental building block of any optical fibre-based sensing system [4]. Recently, a number of studies have examined the changes in the Bragg wavelength of FBGs under gamma irradiation [4,5,6]. These studies have reported conflicting results, and the mechanism responsible for the proposed shift in the Bragg wavelength is still unknown.

Previous work [3] examined the influence of fibre composition and the effect this has on the Bragg wavelength under irradiation. Irradiation dose rates of 0.90Gy/s up to a dose of 100kGy were used, which is compatible to our accumulated dose of about 86kGy. The highest Bragg wavelength shift (BWS) recorded was 160pm for Ge-doped fibres, and the lowest BWS was 50pm with Ge-free fibre. Gamma-induced attenuation loss was also examined [6] in Ge-doped fibres and pure silica core fibres, when exposed at a dose rate of 720Gy/hr up to a total dose of 100kGy. The optical loss of all fibres was in the range 0.04-0.06dB/m at 100kGy.

In this study, we performed a preliminary study of gamma radiation effects on a selection of optical fibres and FBGs. This study was needed to examine the feasibility of performing these types of measurements on different samples using the facilities at ANSTO, and to determine the most appropriate procedures to complete our proposed study. The three day project generated some interesting data, which demonstrated some interesting, although not totally conclusive, results on the effects of gamma radiation on our sample set. Our eventual aim is to investigate the use of FBG sensors as gamma dosimeters for high dose applications.

#### II. FIBRE BRAGG GRATINGS

##### A. General Theory of FBGs

Fibre Bragg gratings (FBGs) are passive devices utilized extensively in optical fiber communications and sensing. A FBG is a short section of optical fibre that is manufactured to reflect a particular wavelength of light and to transmit all other wavelengths. This is achieved by having a periodic variation to the refractive index in the core of the optical fibre, as shown in Fig. 1. Since some light will be reflected at a change in refractive index, a specific wavelength will be reflected, while all others will be transmitted. Hence, the FBG acts as an optical filter, reflecting a narrow wavelength range, centred about a peak wavelength. This wavelength, known as the Bragg wavelength ( $\lambda_B$ ), is given by [7]

$$\lambda_B = 2n\Lambda, \quad (1)$$

where  $n$  is the average refractive index of the grating (average of  $n_2$  and  $n_3$  in Fig. 1), and  $\Lambda$  is the grating period (as shown in Fig. 1).

Any measurand that has the ability to affect either the refractive index or the grating period will result in a change in the Bragg wavelength. This allows FBGs to be used in sensing applications. For example, if there is a change in the length of the FBG due to strain, the spacing between the dielectric mirrors changes, so the wavelength that the FBG reflects changes. In this instance, the change in length will decrease the optical density of the fibre, which would decrease the refractive index.

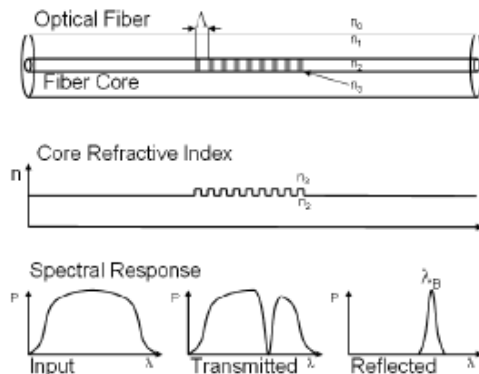


Figure 1. FBG structure and operation.

### B. Gamma Irradiation of FBGs

When FBGs have been exposed to gamma irradiation, a Bragg wavelength shift (BWS) occurs. A recent study examined the relationship between the total dose and BWS up to a dose of 100kGy [8]. Results indicate that the BWS and FBGs sensitivity increase as the radiation dose increases with FBGs of varying Bragg wavelengths (820nm, 1285nm and 1516nm). The BWS was about 40-50pm for a total dose of 100kGy for all FBG wavelengths.

The effect of the variation in fabricating methods of FBGs has shown that fibres with medium to high germanium (Ge) content (10-21mol%) and loaded with hydrogen result in a high BWS (approximately 160pm after a dose of 100kGy) [3]. Fibres without Ge resulted in a 50pm BWS.

Further study has revealed the influence of hydrogen loading pressure on the radiation sensitivity of FBGs. The Bragg wavelength as a function of dose rate was measured, with FBGs that were made after loading the fibre at various pressures of 100, 200 and 300bar [9]. When increased to 300bar, the radiation sensitivity increased by 14% compared to the 100 and 200bar. The BWS for a dose of 100kGy was in the range 130-150pm for 100-300bar hydrogen.

Hence, there is a range of structural, compositional and manufacturing parameters that influence the FBGs sensitivity and wavelength shift. There is a need to study the properties of FBG sensors, and their manufacturing methods and fibre types, under the influence of ionising radiation.

## III. EXPERIMENTAL METHOD

In this study, we measured the transmission characteristics of optical fibres and incorporated FBGs as a function of the accumulated gamma dose over a three day period. All measurements were performed at approximately 22°C.

### A. Gamma Irradiation

Gamma irradiation was performed using a wet storage cobalt-60 irradiation facility at ANSTO. FBGs were irradiated for various times at dose rates of 50-64 Gy/minute to

accumulated doses of between 1 and 100 kGy. For example, for Sample 3 was subjected to consecutive irradiation times of 1, 5, 30, 30, 240, 600 and 600 minutes. After each irradiation period, the samples were removed from the gamma irradiation facility, and optical measurements performed. The samples were then returned for further irradiation. Unfortunately, the time between when the sample was removed and then subsequently returned to the irradiator was random due to the short and rushed timetable involved.

Dose rates were determined using Fricke [10] and Ceric Cerous [11] dosimeters. These dosimeters were calibrated in a cobalt-60 radiation field, in which the dose rate was determined from reference dosimeter measurements made under similar conditions. The overall expanded uncertainty ( $k=2$ ) [12] associated with an individual dosimeter reading included both the uncertainty of calibration of the batch of dosimeters and the uncertainty due to variation within the batch, and was calculated to be 2.0% (Fricke) and 3.5% (Ceric Cerous).

### B. FBG Samples

The FBG samples were purchased from Photonix Technologies (Malaysia). FBGs were manufactured in standard SMF-28 and SMF-28e optical fibres, with no H2 loading. They have a reflectivity of 80-98% and a 3dB spectral width of 0.2 to 1.0nm. All gratings were used without coatings.

### C. Optical Measurements

Optical measurements were performed in the wavelength range from 1520 nm to 1600 nm using a superluminescent laser diode (DenseLight DL-BZ1-SC5403A) and an optical spectrum analyzer (Agilent 86142A). The transmittance spectrum was measured, and used to determine the shift in the Bragg wavelength as a function of absorbed dose, and as a function of relaxation time post-irradiation.

### D. Relaxation Effects

At the completion of the irradiation studies, a relaxation experiment was performed. After final removal from the gamma irradiation cell, the Bragg wavelength of the FBG was determined as a function of relaxation time, and compared to the initial (base) Bragg wavelength.

## IV. RESULTS AND DISCUSSION

The results of two basic experiments are reported in this section: the transmittance of an FBG (Sample 3) as a function of accumulated gamma dose, and relaxation of Sample 1 post-irradiation.

### A. FBG Bragg Wavelength Shift vs Dose

In general, our results show an increase in the Bragg wavelength with dose, although this effect did not saturate as observed in previous work, as the accumulated dose of < 86kGy was too low. Fig. 2 shows the transmittance curves versus light wavelength as a function of gamma dose. The data has been normalized to a baseline of 0 dB for comparison.

Fig. 3 shows the Bragg wavelength shift (BWS) as a function of accumulated gamma dose (in kGy) obtained from the data shown in Fig. 2 for sample 3. To obtain the BWS, we need to determine the transmittance minimum of each curve in Fig. 2. This was obtained by first smoothing the data using a 4-point smoothing algorithm, normalizing each curve to 0 dB, and then implementing a search algorithm to find the minimum transmitted optical power. The uncertainty in each Bragg wavelength was estimated to be 5 pm based on a combination of the resolution of the OSA and the uncertainty in determining position of the minimum for each curve.

The results for low dose (< 3 kGy) seem inconsistent, and there are negative shifts in the Bragg wavelength compared to the pre-irradiation value. This small negative BWS could be due to two possible sources: temperature sensitivity during the optical measurements, and the limited resolution and repeatability of the OSA. Since these values are of the same magnitude as the resolution and repeatability of the OSA, then these will be affected by "noise" related issues.

Temperature cross-sensitivity is a major issue in the application of FBGs to the measurement of parameters other than temperature. Typical temperature sensitivity coefficients for FBGs are of the order of 10pm/°C at 1300nm [13], depending on fibre type. Therefore, there may be an expectation that, after removal from the irradiation apparatus, the fibre may not cool down to room temperature in the time before the optical measurements were performed, if the gamma irradiation caused the temperature of the fibre to increase. Previous work indicates that a maximum temperature rise of 0.5°C occurs in FBGs subjected to 100kGy gamma irradiation [6], so the uncertainty in the BWS due to temperature would be 6pm at most for a 1550nm FBG if the fibre temperature remained 0.5°C above room temperature. The wavelength resolution of the OSA was 10pm, so the total BWS uncertainty was about 12pm, which allows for any uncertainty in the BWS measurement.

The remaining data points (for dose > 3kGy) are reasonably consistent, except for the data point at 51.6kGy, where the BWS appears to have decreased compared to the other data points. This occurred since, after removal from the gamma irradiator, the optical measurements were not performed for at least 12 hours, so that this data point is affected by the relaxation of the Bragg wavelength post-irradiation. Hence, we have re-plotted a restricted data set showing the BWS versus Accumulated Dose in Fig. 4. This data set indicates a logarithmic dependence of the BWS on gamma dose for accumulated dose in the range of about 3 to 87 kGy. This behaviour is consistent with previously observed results [3,9].

#### B. FBG Relaxation After Removal of Gamma Source

Fig. 5 shows the effect of post-irradiation relaxation for sample 1 after a total irradiated dose of 100.8kGy (accumulated 30 hours at 56Gy/minute). That is, the effect of removal of the radiation source and the subsequent relaxation of the shifted Bragg wavelength back towards the pre-irradiation (base) value. The initial Bragg wavelength was 1540.787nm. Post-irradiation, the Bragg wavelength relaxed to 1540.866nm after 9 hours and 1540.840nm after 13 hours.

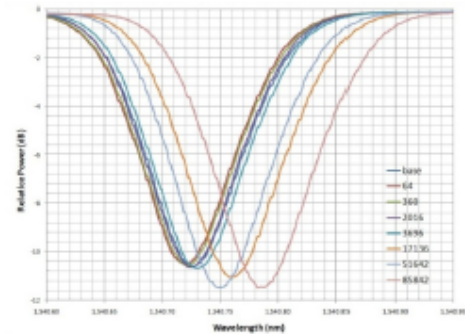


Figure 2. Transmittance spectra versus wavelength of FBG Sample 3, as a function of accumulated gamma dose (in Gy). All curves are normalised to a transmitted optical power of 0 dB.

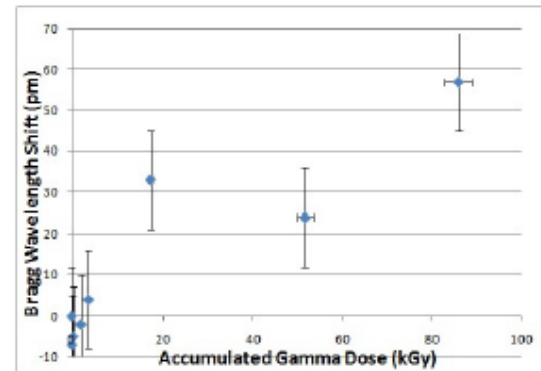


Figure 3. Plot of complete data set of the Bragg wavelength shift as a function of accumulated dose (in kGy) for FBG Sample 3.

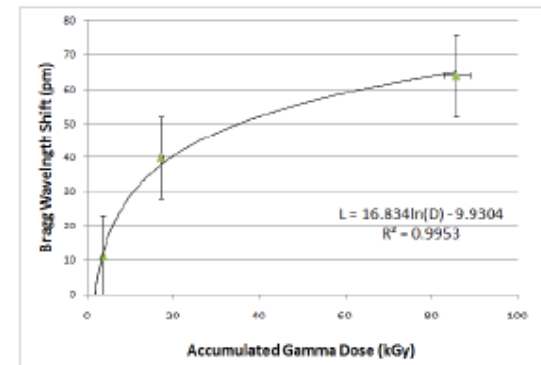


Figure 4. Plot of modified data set of the Bragg wavelength shift as a function of accumulated dose (in kGy) for FBG Sample 3.

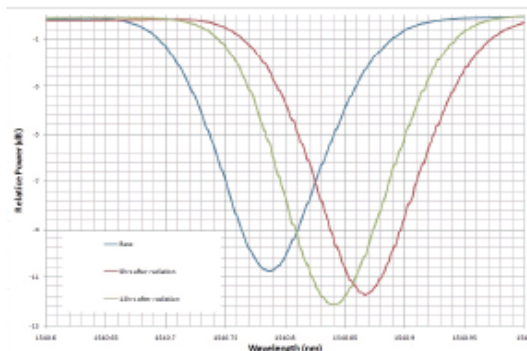


Figure 5. Bragg wavelength shift after removal from irradiation source, for Sample 1. The base curve corresponds to the pre-irradiation FBG properties.

### V. FUTURE WORK

Unfortunately, the limited nature of the previous study does not allow us to report a definitive quantitative behavior and subsequent explanation of gamma radiation-optical fibre-FBG interaction. Future measurements are planned that will eliminate some of the uncertainty occurring in the current results. This will involve (i) performing optical measurements in-situ (which will increase the uncertainty in the dose measurements, but considerably reduce any uncertainty in the optical measurements), (ii) quantification of the relaxation phenomenon, (iii) explicit quantification of the BWS for different types of fibre-FBG combinations, and (iv) examination of the affect of temperature cross-sensitivity (which will be an issue for in-situ optical measurements) on the performance of FBGs as potential gamma dosimeters. We also intend to automate the optical measurements, to allow us to obtain continuous measurements of the BWS as a function of accumulated dose.

### VI. CONCLUSION

We have made some interesting observations in this preliminary study of gamma irradiation effects in SMF FBG sensors, especially the relaxation behaviour in Fig. 5, which needs further examination and quantification. However, the results do show important trends that indicate that FBGs may be useful as gamma dosimeters, especially for high accumulated doses (of the order of 100's of kGy). The Bragg wavelength shift followed a logarithmic dependence on gamma absolute dose, and a significant relaxation in the Bragg shift was observed post-irradiation. This experiment has also given us the opportunity to explore the capabilities of the ANSTO irradiation facility, and we intend to use this information to modify future experiments to obtain greater efficiency and reduced experimental time.

### ACKNOWLEDGMENTS

The authors would like to thank the staff at ANSTO for their technical assistance throughout. This work was supported by an AINSE research grant (ALNGRA1035). The Optical

Spectrum Analyzer was provided on loan by Dr Peter Reece of the Optoelectronics Laboratory, School of Physics, The University of New South Wales, Australia.

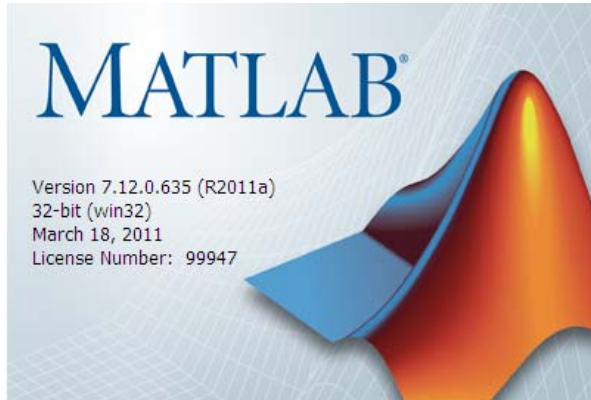
### REFERENCES

- [1] Lu X. Bao, N. Kulkarni, and K. Brown, "Gamma ray induced visible light absorption in P-doped silica fibers at low dose levels," *Radiation Measurements*, vol. 30, no. 6, pp. 725-733, 2009.
- [2] D. Sporea and A. Sporea, "Radiation effects in sapphire optical fibres," *Physica Status Solidi C*, vol. 4, pp. 1356-1359, 2007.
- [3] H. Henschel, S. K. Hoeffgen, K. Krebber, J. Kuhnemann, and U. Weinand, "Influence of fiber composition and grating fabrication on the radiation sensitivity of fiber Bragg gratings," *IEEE Transactions on Nuclear Science*, vol. 55, no. 4, pp. 2235-2242, August 2008.
- [4] A. Fernandez Fernandez, B. Pritchard, F. Berghmans, and M. Decretion, "Dose-rate dependencies in gamma-irradiated fiber Bragg grating filters," *IEEE Trans. Nuclear Science*, vol. 49, no. 6, pp. 2874-2878, December 2002.
- [5] A. Fernandez-Fernandez, A. Gusarov, B. Pritchard, M. Decretion, F. Berghmans, P. Megret, & A. Delchambre, "Long-term radiation effects on fibre Bragg grating temperature sensors in a low flux nuclear reactor," *Meas. Sci. Technol.*, vol. 15, no. 8, pp. 1506-1511, 2004.
- [6] K. Krebber, H. Henschel, and U. Weinand, "Fibre Bragg gratings as high dose radiation sensors," *Measurement Science and Technology*, vol. 17, pp. 1095-1102, 2006.
- [7] G. Wild & S. Hinckley, "Acousto-ultrasonic optical fiber sensors: Overview and state-of-the-art," *IEEE Sensors Journal*, vol. 8., no. 7, pp. 1184-1193, July 2008.
- [8] H. Henschel, S. K. Hoeffgen, J. Kuhnemann, and U. Weinand, "Influence of manufacturing parameters and temperature sensitivity of fibre Bragg gratings," *IEEE Transactions on Nuclear Science*, vol.57, no.4, pp. 2029-2034, August 2010.
- [9] J. Troska, J. Brien, K. Gill, and F. Vasey, "Radiation effects in commercial off-the shelf single mode optical fibres," *Proc. SPIE*, vol. 3440, pp. 112-119, "Photonics for Space Environments VI", San Diego, 22 July 1998.
- [10] American Society for Testing and Materials (ASTM) International, "Standard practice for using the Fricke reference-standard dosimetry system. E1026-04," in *Annual Book of ASTM Standards*, Vol. 12.02, 2004.
- [11] American Society for Testing and Materials (ASTM) International, "Standard practice for use of a Ceric-Cerous sulfate dosimetry system. ISOASTM 51205," in *Annual Book of ASTM Standards*, Vol. 12.02, 2009.
- [12] International Organization for Standardization, "Uncertainty of measurement - Part 3: Guide to the expression of uncertainty in measurement," *ISO/IEC Guide 98-3*, 2008.
- [13] Lin Zhang, W. Zhang, I. Bennion, "In-fiber grating optics sensors," Chapter 4 in *Fiber Optic Sensors*, Francis T. S. Yu and Shizhuo Yin (ed), CRC Press 2002.

## APPENDIX 2

### MATLAB 7.12.0.635

To extract the FWHM Gaussian fit for each line of FBGs, we used MATLAB (7.12.0.635). Book 2 and Book 3 contained the data for the first and second irradiation periods.



```
% Load the data from the Excel files.
```

```
[num1,txt1,row1]=xlsread('book3.xlsx',1);
```

```
[num2,txt2,row2]=xlsread('book3.xlsx',2);
```

```
[num3,txt3,row3]=xlsread('book3.xlsx',3);
```

```
% 2. Equation for the Gaussian Approximation for each FBG response. The  
% parameter selection will be made to match the peak and FWHM.
```

```

%%% Determine Gaussian Parameters.

%%% Line 1

HM1=(Q1(1,1)/2+min(num1(:,3))/2 Q1(2,1)/2+min(num1(:,3))/2 Q1(3,1)/2+min(num1(:,3))/2);

count=0;
HMt1=zeros(6,1);
for i=1:size(num1,1)-1
    if ((num1(i,3)-HM1(1))*(num1(i+1,3)-HM1(1))<=0) && ((count==0 && num1(i,3)<num1(i+1,3)) || (count==1 && num1(i,3)>num1(i+1,3)))
        count=count+1;
        alpha=(HM1(1)-num1(i,3))/(num1(i+1,3)-num1(i,3));
        HMt1(count)=alpha*num1(i+1,2)+(1-alpha)*num1(i,2);
    end
    if (num1(i,3)-HM1(2))*(num1(i+1,3)-HM1(2))<=0 && ((count==2 && num1(i,3)<num1(i+1,3)) || (count==3 && num1(i,3)>num1(i+1,3)))
        count=count+1;
        alpha=(HM1(2)-num1(i,3))/(num1(i+1,3)-num1(i,3));
        HMt1(count)=alpha*num1(i+1,2)+(1-alpha)*num1(i,2);
    end
    if (num1(i,3)-HM1(3))*(num1(i+1,3)-HM1(3))<=0 && ((count==4 && num1(i,3)<num1(i+1,3)) || (count==5 && num1(i,3)>num1(i+1,3)))
        count=count+1;
        alpha=(HM1(3)-num1(i,3))/(num1(i+1,3)-num1(i,3));
        HMt1(count)=alpha*num1(i+1,2)+(1-alpha)*num1(i,2);
    end
end
FWHM1=[HMt1(2)-HMt1(1) HMt1(4)-HMt1(3) HMt1(6)-HMt1(5)];

```

Results from MATLAB showing FWHM at beginning of second irradiation.

Workspace			
Name	Value	Min	Max
A	<10x17 cell>		
B	<10x4 cell>		
F	<1x1 struct>		
FWHM1	[0.7122,0.7249,0.7121]	0.7121	0.7249
FWHM2	[0.7750,0.8164,0.7761]	0.7750	0.8164
FWHM3	[0.5612,0.5573,0.8468]	0.5573	0.8468
G1	<3x1001 double>	-69.9360	-23.8760
G2	<3x1001 double>	-69.9590	-24.1000
G3	<3x1001 double>	-69.9620	-22.6240
HM1	[-46.9060,-47.3140,-4...	-48.0165	-46.9060
HM2	[-47.7125,-47.0295,-4...	-48.0855	-47.0295
HM3	[-56.1560,-55.3645,-4...	-56.1560	-46.2930
HMt1	[1.5451e+03;1.5458e...	1.5451e+03	1.5556e+03
HMt2	[1.5446e+03;1.5453e...	1.5446e+03	1.5554e+03
HMt3	[1.5448e+03;1.5454e...	1.5448e+03	1.5557e+03
P1	<3x16 double>	1.5453e+03	1.5553e+03

```

% Load the data from the Excel files.
[num1,txt1,row1]=xlsread('book2.xlsx',1);
[num2,txt2,row2]=xlsread('book2.xlsx',2);
[num3,txt3,row3]=xlsread('book2.xlsx',3);

% 2. Equation for the Gaussian Approximation for each FBG response. The
% parameter selection will be made to match the peak and FWHM.

```

Results from MATLAB showing FWHM at beginning of first irradiation

```

FWHM1          [0.7480,0.7340,0.7225]  0.7225  0.7480
FWHM2          [0.8203,0.8308,0.8020]  0.8020  0.8308
FWHM3          [0.6934,0.7514,0.8485]  0.6934  0.8485
G1             <3x1001 double>         -69.9... -22.9...
G2             <3x1001 double>         -69.8... -22.5...
G3             <3x1001 double>         -69.9... -22.5...
HM1            [-46.4750,-46.8775,-4... -47.4... -46.4...
HM2            [-46.7815,-46.1925,-4... -47.1... -46.1...
HM3            [-51.0885,-49.0480,-4... -51.0... -46.2...

```

Output data from MATLAB showing FWHM change over the first irradiation period  
 For line one, FBG 1,2,3.

	1	2	3	4
1	0.7480	0.7340	0.7225	
2	0.7272	0.7324	0.7261	
3	0.7303	0.7361	0.7286	
4	0.7312	0.7287	0.7289	
5	0.7254	0.7302	0.7224	
6	0.7351	0.7223	0.7270	
7	0.7229	0.7207	0.7321	
8	0.7226	0.7201	0.7240	
9	0.7305	0.7170	0.7279	
10	0.7376	0.7180	0.7229	
11	0.7219	0.7170	0.7192	
12	0.7336	0.7142	0.7189	
13	0.7194	0.7207	0.7096	
14	0.7202	0.7277	0.7184	
15	0.7245	0.7228	0.7215	
16	0.7224	0.7209	0.7240	
17	0.7319	0.7272	0.7165	
18	0.7280	0.7184	0.7217	
19	0.7229	0.7157	0.7108	
20	0.7225	0.7240	0.7125	
21	0.7175	0.7166	0.7114	
22	0.7131	0.7148	0.7097	
23	0.7237	0.7173	0.7088	
24				
25				

Output data from MATLAB showing FWHM change over the second irradiation period for Line two noting the change in particular at the 14, 15, 16 data entries. This coincides with the GIF image in my thesis.

FWHM2 <16x3 double>			
	1	2	3
1	0.7750	0.8164	0.7761
2	0.7346	0.8003	0.7601
3	0.6973	0.7855	0.7258
4	0.7843	0.8193	0.7873
5	0.7779	0.8101	0.7902
6	0.7695	0.8014	0.7751
7	0.7891	0.8130	0.8003
8	0.7489	0.7954	0.7721
9	0.7948	0.8204	0.7986
10	0.7874	0.8177	0.7955
11	0.7888	0.8271	0.7936
12	0.7900	0.8216	0.7893
13	0.7981	0.8167	0.7962
14	0.6802	0.7721	0.7116
15	0.6256	0.6491	0.5844
16	0.6107	0.6172	0.5640
17			
18			
19			

## APPENDIX 3



Nuclear-based science benefiting all Australians

ANSTO – Radiation Technology  
Building 23, New Illawarra Road, Lucas Heights NSW 2234, Australia  
T +61-2-9717 3441  
F +61-2-9717 9325  
E [radtech@ansto.gov.au](mailto:radtech@ansto.gov.au)  
<http://www.ansto.gov.au>

21 December 2012

### Irradiation Report

**ANSTO Reference** 12-2241

**Customer** Edith Cowan University

**Address** School of Engineering & Mathematics  
270 Joondalup Drive  
Joondalup WA 6027

**Contact** Steven Hinckley  
Desmond Baccini  
Graham Wild

**Customer Reference** AINSE Award No. ALNGRA12029P

ANSTO Ref: 12-2241

SRT F 004

Prepared



Authorised



Date 21.12.12

Page 1 of 5

Connie Banos

Justin Davies

## Product Details

<b>Product / Quantity</b>	Fibre Bragg Grating Optical Sensors (FBG) / 9 samples plus 1 spare
<b>Product Type</b>	Samples 1, 2 & - 3 Ge + H Samples 4, 5 & - 6 Ge Samples 8, 9 & - 10 SMF 28

## Irradiation Conditions

<b>Irradiation Facility</b>	Gamma Technology Research Irradiator (GATRI)
<b>Radiation type</b>	Gamma radiation (cobalt-60)
<b>Irradiation Date</b>	27 November to 3 December 2010
<b>Required Dose</b>	Time exposure readings until saturation, relaxation period, re-start time exposure until saturation again and relaxation period. Refer to results for doses
<b>Dosimeter Type</b>	Ceric Cerous
<b>Dosimeter Batch</b>	CCAD (low dose)
<b>Irradiation Temperature</b>	21.5 to 23.7 °C

ANSTO Ref: 12-2241

SRT F 004

Prepared



Connie Banos

Authorised



Justin Davics

Date

21.12.12

Page 2 of 5

The spare FBG was set up in a polystyrene box and placed on a rig in a predetermined position, as close as possible to the irradiation source. Dosimeters were sited on the FBG. The sample was exposed to radiation for 2 hours. The dosimeters were measured and a dose rate was established.

The remaining FBGs were set up in a polystyrene box on three lines, as in Photo1. Line 1 had FBG no.s 8, 6 & 2 in sequence, Line 2 had FBG no.s 9, 4 & 3 in sequence and Line 3 had FBG no.s 10, 5 & 1 in sequence. The lines were each attached to cables that were threaded through an access port in the irradiation facility shield. The box was placed on a rig in the predetermined position. The cables were attached one at a time to an Optical Spectrum Analyzer to establish a baseline (no irradiation) for each. Once the baseline was measured the irradiation process commenced.

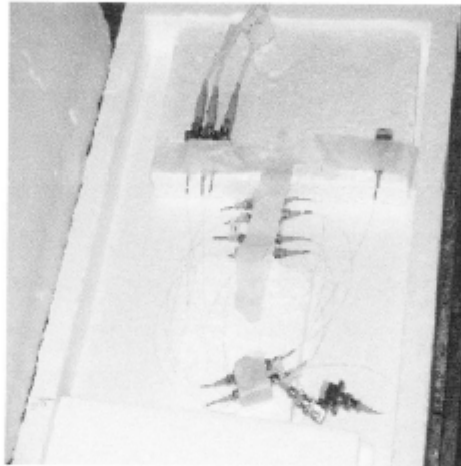


Figure 1. The FBGs arranged in the polystyrene box.

During the irradiation process at regular intervals measurements from each of the 3 lines were taken. The irradiation process continued until the measurements showed the FBGs to be “saturated”. Measurements from the 3 lines continued until they showed no further “relaxation”. The irradiation process recommenced and the whole process repeated. Once the second relaxation period was reached the experiment was terminated.

Refer to Table1 for dose results.



## Results

Measurement or stop date/time	Exposure period (h)	Dose (kGy)	Accumulated dose (kGy)	Comments
27/11/2012 09:32	2.000	8.1	8.1	first measurement
27/11/2012 10:19	0.783	3.2	11.2	irradiation stop for 37 min
27/11/2012 11:38	0.700	2.8	14.0	measurement
27/11/2012 13:30	1.867	7.5	21.6	measurement
27/11/2012 15:30	2.000	8.1	29.6	measurement
27/11/2012 17:35	2.083	8.4	38.0	measurement
27/11/2012 19:40	2.083	8.4	46.4	measurement
27/11/2012 22:29	2.817	11.4	57.8	measurement
28/11/2012 01:27	2.967	12.0	69.8	measurement
28/11/2012 04:22	2.917	11.8	81.5	measurement
28/11/2012 07:31	3.150	12.7	94.2	measurement
28/11/2012 09:37	2.100	8.5	102.7	measurement
28/11/2012 11:46	2.150	8.7	111.3	measurement
28/11/2012 11:54	0.133	0.5	111.9	irradiation stop for 51 min No. 3 cable has only one peak
28/11/2012 13:30	0.750	3.0	114.9	measurement
28/11/2012 15:34	2.067	8.3	123.2	measurement
28/11/2012 17:36	2.033	8.2	131.4	measurement
28/11/2012 19:30	1.900	7.7	139.1	measurement
28/11/2012 22:24	2.900	11.7	150.8	measurement
29/11/2012 01:24	3.000	12.1	162.9	measurement
29/11/2012 04:22	2.967	12.0	174.8	measurement
29/11/2012 07:33	3.183	12.8	187.7	measurement
29/11/2012 09:39	2.100	8.5	196.1	measurement
29/11/2012 11:34	1.917	7.7	203.8	measurement
29/11/2012 12:18	0.733	3.0	206.8	irradiation stopped for relaxation
30/11/2012 13:30	3.000	12.1	218.9	measurement
30/11/2012 15:32	2.033	8.2	227.1	measurement
30/11/2012 17:29	1.950	7.9	234.9	measurement
30/11/2012 19:25	1.933	7.8	242.7	measurement
30/11/2012 22:17	2.867	11.5	254.3	measurement
1/12/2012 01:30	3.217	13.0	267.2	measurement
1/12/2012 07:30	6.000	24.2	291.4	measurement

ANSTO Ref. 12-2241

SRT F 004

Prepared [REDACTED] Authorised [REDACTED] Date 29.12.12 Page 4 of 5

Connie Banos

Justin Davies

Measurement or stop date/time	Exposure period (h)	Dose (kGy)	Accumulated dose (kGy)	Comments
1/12/2012 10:30	3.000	12.1	303.5	measurement
1/12/2012 13:27	2.950	11.9	315.3	measurement
1/12/2012 16:26	2.983	12.0	327.4	measurement
1/12/2012 19:25	2.983	12.0	339.4	measurement
1/12/2012 22:27	3.033	12.2	351.6	measurement
2/12/2012 01:19	2.867	11.5	363.1	measurement
2/12/2012 07:21	6.033	24.3	387.4	measurement
2/12/2012 10:38	3.283	13.2	400.6	measurement
2/12/2012 11:17	0.650	2.6	403.2	irradiation stopped for relaxation
3/12/2012 07:21	-	-	403.2	completed relaxation

### Measurement Traceability & Uncertainty

ANSTO's dosimeters are calibrated in a cobalt-60 radiation field, in which the dose rate has been determined from reference dosimeter measurements made under similar conditions. The reference dosimeter measurements are traceable to the Australian standard for absorbed dose.

The overall uncertainty associated with an individual dosimeter reading includes both the uncertainty of calibration of the batch of dosimeters and the uncertainty due to variation within the batch and was calculated to be 3.5 %. This expanded uncertainty is based on the standard uncertainty multiplied by a coverage factor of two, providing a level of confidence of approximately 95%. The uncertainty evaluation has been carried out in accordance with the *ISO Guide to the Expression of Uncertainty in Measurement*.

### Conclusion

The dose absorbed by the product complies with the required specifications.

Radiation Technology maintains a quality management system that complies with ISO 9001:2008 and adheres to the principles of international best practice for dosimetry (ISO 17025 and ISO/ASTM standards for dosimetry for radiation processing).

This report shall not be reproduced except in full without the written approval of Radiation Technology, ANSTO.

ANSTO Ref: 12-2241

SRT F 004

Prepared

Authorised



Date 21.12.12

Page 5 of 5

Connie Banos

Justin Davies

